Arch Comput Methods Eng (2009) 16: 31–75
DOI 10.1007/s11831-008-9028-8

ORIGINAL PAPER

Multiscale Methods for Composites: A Review

P. Kanouté · D.P. Boso · J.L. Chaboche · B.A. Schrefler

Received: 15 March 2008 / Accepted: 15 March 2008 / Published online: 22 January 2009

Abstract Various multiscale methods are reviewed in the context of modelling mechanical and thermomechanical responses of composites. They are developed both at the material level and at the structural analysis level, considering sequential or integrated kinds of approaches. More specifically, such schemes like periodic homogenization or mean field approaches are compared and discussed, especially in the context of non linear behaviour. Some recent developments are considered, both in terms of numerical methods (like FE^2) and for more analytical approaches based on Transformation Field Analysis, considering both the homogenization and relocalisation steps in the multiscale methodology. Several examples are shown.

1 Introduction

Composite materials are commonly applied in engineering practice. They allow to take advantage of the different properties of the component materials, of the geometric structure and of the interaction between the constituents to obtain a tailored behaviour as a final result. Such composite materials may present both high stiffness and high damping, improved strength and toughness, improved thermal conductivity and electrical permittivity, improved permeability, unusual physical properties such as negative Poisson ratio, negative stiffness inclusions, etc.

Most composite materials are multiscale in nature, i.e. the scale of the constituents is of lower order than the scale of the resulting material and structure. To fix the ideas, we speak of the *macroscopic* scale as the particular scale in which we are interested in (e.g. at structural level), while the lower scales are referred to as *microscopic* scales (sometimes an intermediate scale is called *mesoscopic* scale). We exclude here scales at atomic level, which would require a separate paper.

For most of the analyses of composite structures, effective or homogenized material properties are used, instead of taking into account the individual component properties and geometrical arrangements. These effective properties are usually difficult or expensive to measure and in the design stage the composition may vary substantially, making frequent measurements prohibitive. Hence a lot of effort went into the development of mathematical and numerical models to derive homogenized material properties directly from those of the constituents and from their microstructure. Many engineering problems are solved at macroscopic scale with such homogenized properties. However, sometimes such analyses are not accurate enough.

In principle it would be possible to refer directly to the microscopic scale, but such microscopic models are often far too complex to handle for the analysis of a large structure. Further, the data obtained would be redundant and complicated procedures would be required to extract information of interest.

P. Kanouté · J.L. Chaboche
The French Aerospace Lab, 29 avenue de la Division Leclerc, 92322 Châtillon, France

P. Kanouté
e-mail: pascale.kanoute@onera.fr

J.L. Chaboche
e-mail: Jean-Louis.Chaboche@onera.fr

D.P. Boso (✉) · B.A. Schrefler
Department of Structural and Transportation Engineering, University of Padua, Via Marzolo 9, 35131 Padua, Italy
e-mail: boso@dic.unipd.it

B.A. Schrefler
e-mail: bas@dic.unipd.it

A way out is what is now commonly known as *multi-scale* modelling, where macroscopic and microscopic models are coupled to take advantage of the efficiency of macroscopic models and the accuracy of the microscopic models. The scope of such multiscale modelling is to design combined macroscopic-microscopic computational methods that are more efficient than solving the full microscopic model and at the same time give the information that we need to the desired accuracy [56].

In the case of material multiscale modelling and in homogenization in general, one usually proceeds from the lower scales upward, in order to obtain equivalent material properties. Alternatively, in the case of structural modelling it is important to be able to step down through the scales until the desired scale of the real, not homogenized, material is reached. This technique is often known as *unsmearing*, *localization* or *recovering* method. Usually in a global analysis both aspects need to be pursued, think for instance of a damage or fracture analysis. The procedure just described is that of a *serial* coupling and represents some sort of data passing up and down the scales. An alternative is the *concurrent* coupling where both microscale and macroscale models are strongly interwoven and have to be addressed continuously as the computation goes on. This is particularly the case in nonlinear situations.

In this paper we will briefly review the most common methods applied to obtain equivalent properties and then consider full multiscale modelling. Both linear and nonlinear aspects will be covered. Unsmearing is then dealt with in some detail because it is often neglected while in many cases it is of fundamental importance.

In Sect. 2 usual bounds and other estimates are presented, starting from the Voigt and Reuss bounds. Section 3 illustrates asymptotic homogenisation and its numerical implementation. In Sect. 4 mean field approaches are dealt with, while in Sect. 5 semi-analytical methods are described. In Sect. 6 sequential multiscale procedures are addressed and computational techniques are shown in some details in Sect. 7. Recovery methods are presented in the final section. Examples of applications of the discussed methods can be found throughout the paper.

2 Bounds and Other Estimates

Over the last decades a large body of literature was developed, which deals with the micromechanical modelling techniques for heterogeneous materials. As far as the effective properties are concerned, the various approaches may be divided into two main categories, depending upon the microstructure characteristics.

In case of composites with linear constitutive behaviour, if the microstructure is sufficiently regular to be considered periodic, the effective properties may be determined in terms of unit cell problems with appropriate boundary conditions. This case is presented in Sect. 3. If the microstructure is not regular the effective properties cannot be determined exactly. Thus the goal consists instead in the definition of the range of the possible effective behaviour in terms of bounds, which depend on some parameters characterizing the microstructure, such as for instance the volume ratio of the inclusions in a matrix. To this purpose many homogenisation methods have been developed. We mention the pioneering studies by Voigt [175] and Reuss [151], who formulated rigorous bounds for the effective moduli of composites with prescribed volume fraction. Some decades later Hashin and Shtrikman [88–90] presented an extension of the method, based on variational formulations. If the microstructure is composed of a matrix and spheric or spheroidal inclusions, the effective behaviour of composite can be obtained by means of the self-consistent method [24, 26, 91, 93, 102], for which an example will be shown in Sect. 7.6.

If the composite materials have non linear constitutive behaviour, for periodic microstructure the effective properties can still be obtained in terms of unit cell problems with appropriate boundary conditions. For composites with random microstructures the first bounds are obtained by Bishop and Hill [12, 13] for rigid perfectly plastic polycrystals. Some extensions of the self-consistent method are also available in literature, for example in Hill [94], Hutchinson [99] and Berveiller and Zaoui [11].

In the framework of non linear bounds we mention also the work by Willis and Talbot [166, 181], which provides extensions of the Hashin-Shtrikman variational principles for non linear composites. Their work is followed by the introduction of several new variational principles making use of appropriately chosen "linear comparison composites", which allow the determination of Hashin-Shtrikman and more general bounds and estimates, directly from corresponding estimates for linear composites. These include the variational principles of Ponte Castañeda [141, 142] and Talbot and Willis [167] for general classes of nonlinear composites, of Suquet [163] for power-law composites and Olson [138] for perfectly plastic composites.

2.1 The Voigt and Reuss Bounds

Consider an N-phase composite occupying the domain Ω, with each phase occupying sub-domains $\Omega^{(r)}$ $(r = 1, \ldots, N)$, and let the energy-density function $w(\mathbf{x}, \boldsymbol{\varepsilon})$ and the complementary energy function $u(\mathbf{x}, \boldsymbol{\sigma})$ be expressed in terms of the homogeneous phase potentials $w^{(r)}(\boldsymbol{\varepsilon})$ and $u^{(r)}(\boldsymbol{\sigma})$ as

$$w(\mathbf{x}, \boldsymbol{\varepsilon}) = \sum_{r=1}^{N} \chi^{(r)}(\mathbf{x}) w^{(r)}(\boldsymbol{\varepsilon}), \tag{1}$$

$$u(\mathbf{x},\boldsymbol{\sigma}) = \sum_{r=1}^{N} \chi^{(r)}(\mathbf{x}) u^{(r)}(\boldsymbol{\sigma}), \tag{2}$$

where $\chi^{(r)}(\mathbf{x}) = 1$ if $\mathbf{x} \in \Omega^{(r)}$ or 0 otherwise, is the characteristic function of phase r. These functions define the microstructure.

The characterization of the effective behaviour of a composite can be obtained from the principle of minimum potential energy. An effective potential $\tilde{W}$ is defined for the composite from the average minimum potential energy defined as

$$\tilde{W}(\bar{\boldsymbol{\varepsilon}}) = \min_{\boldsymbol{\varepsilon}(\mathbf{x}) \in K} \langle w(\mathbf{x},\boldsymbol{\varepsilon}) \rangle, \tag{3}$$

where the McCauley brackets denote volume average on the domain, $\bar{\boldsymbol{\varepsilon}} = \langle \boldsymbol{\varepsilon} \rangle$ is the average of the actual strain field $\boldsymbol{\varepsilon}$ and K is the set of kinematically admissible strains. A similar formulation defines the stress potential $\tilde{U}$

$$\tilde{U}(\bar{\boldsymbol{\sigma}}) = \min_{\boldsymbol{\sigma}(\mathbf{x}) \in S} \langle u(\mathbf{x},\boldsymbol{\sigma}) \rangle, \tag{4}$$

where $\bar{\boldsymbol{\sigma}} = \langle \boldsymbol{\sigma} \rangle$ is the average of the actual stress field $\boldsymbol{\sigma}$, and S is the set of statically admissible stresses satisfying an average stress boundary condition.

For linear elastic composites, the effective strain and stress potentials may be written in terms of the effective elasticity tensor $\tilde{\mathbf{L}}$ and compliance tensor $\tilde{\mathbf{M}}$ in the following way

$$\tilde{W}(\bar{\boldsymbol{\varepsilon}}) = \frac{1}{2} \bar{\boldsymbol{\varepsilon}} : \tilde{\mathbf{L}} : \bar{\boldsymbol{\varepsilon}}, \tag{5}$$

$$\tilde{U}(\bar{\boldsymbol{\sigma}}) = \frac{1}{2} \bar{\boldsymbol{\sigma}} : \tilde{\mathbf{M}} : \bar{\boldsymbol{\sigma}}. \tag{6}$$

Usually Voigt's analysis [175] is indicated as the first study of the effective mechanical properties of composite solids, with a complementary contribution given later by Reuss [151]. Voigt assumes that the strain field within an aggregate sample of heterogeneous material is uniform, arriving to the estimate

$$\bar{\mathbf{L}} = \sum_{r=1}^{N} c^{(r)} \mathbf{L}^{(r)}, \tag{7}$$

where $c^{(r)}$ and $\mathbf{L}^{(r)}$ are respectively the volume fraction and the elasticity tensors of the r phase.

The dual assumption is made by Reuss, who approximates the stress fields within the aggregate of a polycrystalline material as uniform, obtaining

$$(\bar{\mathbf{L}}^{-1})^{-1} = \left[\sum_{r=1}^{N} c^{(r)} (\mathbf{L}^{(r)})^{-1} \right]^{-1}. \tag{8}$$

In the context of linear composites, Hill [92] and Paul [140] made the observation that the choice of a uniform strain field in the variational statement (3) for $\tilde{W}$ leads to the rigorous upper bound

$$\tilde{W}(\bar{\boldsymbol{\varepsilon}}) < \frac{1}{2} \bar{\boldsymbol{\varepsilon}} : \bar{\mathbf{L}} : \bar{\boldsymbol{\varepsilon}}. \tag{9}$$

This relation implies that the Voigt estimate is a rigorous upper bound for $\tilde{\mathbf{L}}$.

Similarly the choice of a uniform stress field for $\tilde{U}$ leads to the upper bound

$$\tilde{U}(\bar{\boldsymbol{\sigma}}) \leq \frac{1}{2} \bar{\boldsymbol{\sigma}} : \bar{\mathbf{M}} : \bar{\boldsymbol{\sigma}}. \tag{10}$$

This relation implies that the Reuss estimate is a rigorous lower bound for $\tilde{\mathbf{L}} = \tilde{\mathbf{M}}^{-1}$.

Therefore, one can interpret the Voigt and Reuss fields as providing two microfields extremes, since the Voigt stress field is one where the tractions at the phase boundaries cannot be in equilibrium, that is, statically inadmissible, while the implied Reuss strains are such that the heterogeneities and the matrix could not be perfectly bonded, that is, kinematically inadmissible.

The bounds provide a rough and quick way of determining approximate aggregate responses of micro-heterogeneous materials. However, the wideness of the bounds grows with the volume fractions of inhomogeneities and the degree of relative phase contrast in the properties.

2.2 More Refined Estimates

After the early work of Voigt, Reuss, Hill and Paul, improved estimates have been pursued. Considering a composite made of particles dispersed in a matrix, one can assume that there is no particle interaction, so that the problem is transformed into the analysis of a single inclusion immersed in an infinite domain made of the matrix material [57]. However, the assumption of non-interacting particles can lead to unreliable results, especially for randomly dispersed particulate microstructure.

An improvement of this approach is given by the Self Consistent method [26, 93]. The main idea is still to replace the problem of the interaction among many particles by the problem of interaction of one particle and an infinite matrix: but now the unbounded domain is made of the effective medium. Unfortunately, the self-consistent method can produce negative effective bulk and shear responses, for voids, for volume fractions of 50% and higher. For rigid inclusions, it produces infinite effective bulk responses for any volume fraction and infinite effective shear responses above 40% [3, 185]. To avoid this problem, the generalized self consistent methods encase the particle in a shell of matrix material, surrounded by the effective medium (see Christensen [43]).

However, such methods also exhibit problems, which are discussed e.g. in Hashin [87].

On the basis of variational principles, Hashin and Shtrikman [88–90] developed their approximations, which can also be regarded as bounds for the effective properties of a composite. These bounds are sensitive to sample size and are strictly valid only when the body is assumed to be infinite, the microstructure isotropic and the effective responses are isotropic.

One can arrive—for the bulk and shear modulus respectively—to the following relations

$$\kappa_1 + \frac{\nu_2}{\frac{1}{\kappa_2-\kappa_1} + \frac{3(1-\nu_2)}{3\kappa_1+4\mu_1}} \leq \kappa^* \leq \kappa_2 + \frac{1-\nu_2}{\frac{1}{\kappa_1-\kappa_2} + \frac{3\nu_2}{3\kappa_2+4\mu_2}} \tag{11}$$

$$\mu_1 + \frac{\nu_2}{\frac{1}{\mu_2-\mu_1} + \frac{6(1-\nu_2)(\kappa_1+2\mu_1)}{5\mu_1(3\kappa_1+4\mu_1)}} \leq \mu^* \leq \mu_2 + \frac{(1-\nu_2)}{\frac{1}{\mu_1-\mu_2} + \frac{6\nu_2(\kappa_2+2\mu_2)}{5\mu_2(3\kappa_2+4\mu_2)}} \tag{12}$$

for a two-phase microstructure, where κ_1, μ_1 and κ_2, μ_2 are the bulk and shear moduli for the phases, while ν_2 is the phase 2 volume fraction. It is also assumed that $\kappa_2 \geq \kappa_1$ and $\mu_2 \geq \mu_1$.

There exist a lot of other approaches investigating the effective properties and the responses of micro-heterogeneous materials. For detailed reviews, we refer the reader to the works of Hashin [87], Mura [133], Aboudi [3], Nemat-Nasser and Hori [136] and recently Torquato [172] and Zohdi [185]. Also, for analyses of the nonlinear behaviour, we cite the extensive works of Llorca and co-workers [80–82, 114–116, 149, 156, 157].

3 Asymptotic Homogenisation

In this section, composites with a regular or nearly regular structure are considered. In this case it is possible to assume a periodic structure for the composite made up of many repetitive unit cells and make use of periodic homogenisation. Provided that the scale associated with the repetitive unit cell is well separated from that of the overall structure, the linear effective properties of the composite can be determined by solving a finite number of unit-cell problems. The nonlinear case will be addressed separately in Sect. 7.

3.1 Statement of the Problem and Assumptions

Asymptotic analysis not only permits one to obtain equivalent material properties, but also allows one to solve the full structural problem down to stresses in the constituent materials at a micro (or local) scale. It is mostly applied to linear two-scale problems, but it can be extended to non-linear analysis [18, 70, 71, 117, 154, 161, 162] and to several scales [68]. We do not intend to give a full account of the underlying theory in this work. In references [10, 45, 137, 153] the interested reader will find a rigorous formulation of the method, its application in many fields and further references. We present here the main points of the method.

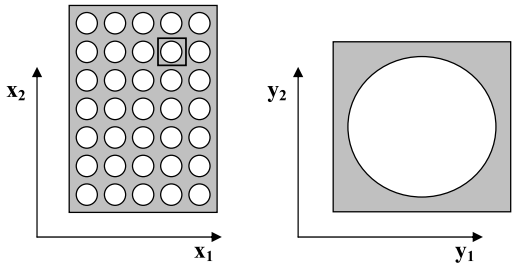

Fig. 1 Example of a periodic structure with two levels: global on the *left* and local on the *right*

Let us consider a structure with just two levels, the micro (or local) level and the macro (or global) level. These levels are shown in Fig. 1 for a structure assumed to be periodic and, thus, asymptotic analysis can be successfully applied.

In a composite body Ω having a periodic structure any function Φ denoting some physical quantity has the following property:

$$\text{if } \mathbf{x} \in \Omega \text{ and } (\mathbf{x}+\mathbf{Y}) \in \Omega \rightarrow \Phi(\mathbf{x}+\mathbf{Y}) = \Phi(\mathbf{x}), \tag{13}$$

where $\mathbf{x}$ is the position vector and $\mathbf{Y}$ is a constant vector which determines the period of the structure.

One important assumption for asymptotic analysis is that it must be possible to distinguish two length scales associated with the macroscopic and microscopic phenomena. The ratio of these scales defines the small parameter ε. Two sets of coordinates related by the following equation (14) formally express this separation of scales between macro and micro phenomena. The global coordinate vector $\mathbf{x}$ refers to the whole body and the stretched local coordinate vector $\mathbf{y}$ is related to the single, repetitive cell of periodicity

$$\mathbf{y} = \frac{\mathbf{x}}{\varepsilon}. \tag{14}$$

In the asymptotic analysis the normalized cell of periodicity is mapped onto a sequence of finer and finer structures as ε tends to 0. If the equivalent material properties as defined below are employed, the considered fields (e.g. temperature, displacement) converge towards the homogeneous macroscopic solution as the micro-structural parameter ε tends to 0. In this sense problems for a heterogeneous body and a homogenized one are equivalent. (For more details concerning the mathematical meaning see [10] and [153]).

We consider now a problem of thermo-elasticity in a heterogeneous body such as that depicted in Fig. 1, defined by the following equations

balance equations

$$\sigma^{\varepsilon}_{ij,j}(\mathbf{x}) + f_i(\mathbf{x}) = 0, \tag{15}$$

$$q^{\varepsilon}_{i,i} - r = 0; \tag{16}$$

constitutive equations

$$\sigma^{\varepsilon}_{ij}(\mathbf{x}) = a^{\varepsilon}_{ijkl}(\mathbf{x}) e_{kl}(\mathbf{u}^{\varepsilon}(\mathbf{x})) - \alpha^{\varepsilon}_{ij}\theta, \tag{17}$$

$$q^{\varepsilon}_i = -K^{\varepsilon}_{ij}\theta_{,j}; \tag{18}$$

strain definition

$$e_{ij}(\mathbf{u}^{\varepsilon}(\mathbf{x})) = \frac{1}{2}(u^{\varepsilon}_{i,j}(\mathbf{x}) + u^{\varepsilon}_{j,i}(\mathbf{x})); \tag{19}$$

boundary and discontinuity conditions

$$\begin{aligned} &\sigma^{\varepsilon}_{ij}(\mathbf{x}) n_j = 0 \quad \text{on } \partial\Omega_1 \quad \text{and} \quad u^{\varepsilon}_i(\mathbf{x}) = 0 \quad \text{on } \partial\Omega_2, \\ &q^{\varepsilon}_i(\mathbf{x}) n_i = 0 \quad \text{on } \partial\Omega_q \quad \text{and} \quad \theta^{\varepsilon}(\mathbf{x}) = 0 \quad \text{on } \partial\Omega_\theta, \end{aligned} \tag{20}$$

$$\begin{aligned} &[u^{\varepsilon}_i(\mathbf{x})] = 0, \qquad [\sigma^{\varepsilon}_{ij}(\mathbf{x}) n_j] = 0 \quad \text{on } S_J, \\ &[\theta^{\varepsilon}(\mathbf{x})] = 0, \qquad [q^{\varepsilon}_i(\mathbf{x}) n_i] = 0 \quad \text{on } S_J. \end{aligned} \tag{21}$$

The superscript ε is used to indicate that the variables of the problem depend on the cell dimensions related to the global length. Square parentheses denote the jump of the enclosed value. The other symbols have the usual meaning: $\mathbf{u}$ is the displacement vector, $e_{ij}(\mathbf{u}(\mathbf{x}))$ denotes the linearized strain tensor, $\sigma_{ij}(\mathbf{x})$ the stress tensor, $a_{ijkl}(\mathbf{x})$ the tensor of elasticity, $K_{ij}(\mathbf{x})$ the tensor of thermal conductivity, $\alpha_{ij}(\mathbf{x})$ the tensor of thermal expansion coefficients, $\theta(\mathbf{x})$, $q_i(\mathbf{x})$ temperature and heat flux respectively, and $r(\mathbf{x})$, $f_i(\mathbf{x})$ stand for thermal sources and volume forces.

Since the components of the elasticity and thermal conductivity tensors are discontinuous, differentiation (in the above equations and in (28)–(33) below) should be understood in the weak sense. This is the main reason why most of the problems posed in the sequel will be presented in a variational formulation.

We introduce now the second assumption of homogenisation theory: we assume that the periodicity of the material characteristics imposes an analogous periodical perturbation on quantities describing the mechanical behaviour of the body; hence we will use the following representation for displacements and temperatures

$$\mathbf{u}^{\varepsilon}(\mathbf{x}) \equiv \mathbf{u}^0(\mathbf{x}) + \varepsilon\mathbf{u}^1(\mathbf{x}, \mathbf{y}) + \varepsilon^2\mathbf{u}^2(\mathbf{x}, \mathbf{y}) + \cdots + \varepsilon^k\mathbf{u}^k(\mathbf{x}, \mathbf{y}), \tag{22}$$

$$\theta^{\varepsilon}(\mathbf{x}) \equiv \theta^0(\mathbf{x}) + \varepsilon\theta^1(\mathbf{x}, \mathbf{y}) + \varepsilon^2\theta^2(\mathbf{x}, \mathbf{y}) + \cdots + \varepsilon^k\theta^k(\mathbf{x}, \mathbf{y}). \tag{23}$$

Similar expansion with respect to powers of ε results from (22), (23) for stresses, strains and heat fluxes

$$\boldsymbol{\sigma}^{\varepsilon}(\mathbf{x}) \equiv \boldsymbol{\sigma}^0(\mathbf{x}, \mathbf{y}) + \varepsilon\boldsymbol{\sigma}^1(\mathbf{x}, \mathbf{y}) + \varepsilon^2\boldsymbol{\sigma}^2(\mathbf{x}, \mathbf{y}) + \cdots + \varepsilon^k\boldsymbol{\sigma}^k(\mathbf{x}, \mathbf{y}), \tag{24}$$

$$\mathbf{e}^{\varepsilon}(\mathbf{x}) \equiv \mathbf{e}^0(\mathbf{x}, \mathbf{y}) + \varepsilon\mathbf{e}^1(\mathbf{x}, \mathbf{y}) + \varepsilon^2\mathbf{e}^2(\mathbf{x}, \mathbf{y}) + \cdots + \varepsilon^k\mathbf{e}^k(\mathbf{x}, \mathbf{y}), \tag{25}$$

$$\mathbf{q}^{\varepsilon}(\mathbf{x}) \equiv \mathbf{q}^0(\mathbf{x}, \mathbf{y}) + \varepsilon\mathbf{q}^1(\mathbf{x}, \mathbf{y}) + \varepsilon^2\mathbf{q}^2(\mathbf{x}, \mathbf{y}) + \cdots + \varepsilon^k\mathbf{q}^k(\mathbf{x}, \mathbf{y}), \tag{26}$$

where $\mathbf{u}^k, \boldsymbol{\sigma}^k, \mathbf{e}^k, \theta^k, \mathbf{q}^k$ for $k > 0$ are $\mathbf{Y}$-periodic i.e. take the same values on the opposite sides of the cell of periodicity. The term scaled with the n-th power of ε in (22)–(26) is called term of order n.

3.2 Formalism of the Homogenisation Procedure

The necessary mathematical tools are the chain rule of differentiation with respect to the micro variable and averaging over a cell of periodicity.

We introduce the assumption (22)–(26) into equations of the heterogeneous problem (15)–(21) and make use of the chain rule and of the following notation (see also [153])

$$\frac{\mathrm{d}}{\mathrm{d}x_i} f = \left(\frac{\partial}{\partial x_i} + \frac{1}{\varepsilon}\frac{\partial}{\partial y_i}\right) f = f_{,i(x)} + \frac{1}{\varepsilon} f_{,i(y)}. \tag{27}$$

This equation explains also the notation used in the sequel for differentiation with respect to local and global independent variables.

Because of (27) the balance equations split into terms of different orders (the terms of the same power of ε are equated to zero separately: e.g. (28) and (31) are of order $1/\varepsilon$).

For the equilibrium equation we have

$$\sigma^0_{ij,j(y)}(\mathbf{x}, \mathbf{y}) = 0, \tag{28}$$

$$\sigma^0_{ij,j(x)}(\mathbf{x}, \mathbf{y}) + \sigma^1_{ij,j(y)}(\mathbf{x}, \mathbf{y}) + f_i(\mathbf{x}) = 0, \tag{29}$$

$$\sigma^1_{ij,j(x)}(\mathbf{x}, \mathbf{y}) + \sigma^2_{ij,j(y)}(\mathbf{x}, \mathbf{y}) = 0, \tag{30}$$

$\cdots$

We have similar expressions for the heat balance equation

$$q^0_{i,i(y)}(\mathbf{x}, \mathbf{y}) = 0, \tag{31}$$

$$q^0_{i,i(x)}(\mathbf{x}, \mathbf{y}) + q^1_{i,i(y)}(\mathbf{x}, \mathbf{y}) - r(\mathbf{x}) = 0, \tag{32}$$

$$q^1_{i,i(x)}(\mathbf{x}, \mathbf{y}) + q^2_{i,i(y)}(\mathbf{x}, \mathbf{y}) = 0, \tag{33}$$

$\cdots$.

From (19) and (27) it follows that the main term of $\mathbf{e}$ in expansions (25) depends not only on $\mathbf{u}^0$, but also on $\mathbf{u}^1$

$$e^0_{ij}(x, y) = u^0_{(i,j)(x)} + u^1_{(i,j)(y)} \equiv e_{ij(x)}(\mathbf{u}^0) + e_{ij(y)}(\mathbf{u}^1). \tag{34}$$

The constitutive relationships (17) and (18) assume now the form

$$\sigma^0_{ij}(\mathbf{x},\mathbf{y}) = a_{ijkl}(\mathbf{y})(e_{kl(x)}(\mathbf{u}^0) + e_{kl(y)}(\mathbf{u}^1)) - \alpha_{ij}(\mathbf{y})\theta^0, \tag{35}$$

$$\sigma^1_{ij}(\mathbf{x},\mathbf{y}) = a_{ijkl}(\mathbf{y})(e_{kl(x)}(\mathbf{u}^1) + e_{kl(y)}(\mathbf{u}^2)) - \alpha_{ij}(\mathbf{y})\theta^1, \tag{36}$$

...

$$q^0_k(\mathbf{x},\mathbf{y}) = K_{kl}(\mathbf{y})(\theta^0_{,l(x)} + \theta^1_{,l(y)}), \tag{37}$$

$$q^1_k(\mathbf{x},\mathbf{y}) = K_{kl}(\mathbf{y})(\theta^1_{,l(x)} + \theta^2_{,l(y)}), \tag{38}$$

...

It can be seen that the terms of order n in the asymptotic expansions for stresses (35), (36) and heat flux (37), (38) depend respectively on the displacement and temperature terms of order n and $n+1$. In this way the influence of the local perturbation on the global quantities is accounted for. This is the reason why for instance we need $\mathbf{u}^1(\mathbf{x},\mathbf{y})$ to define via the constitutive relationship the main term in expansion (24) for stresses.

3.3 Global Solution

Referring separately to the terms of the same powers of ε leads to the following variational formulations for unknowns of successive order of the problem. Starting with the first order, it can be formally shown [73, 153] that $\mathbf{u}^1(\mathbf{x},\mathbf{y})$ and similarly $\theta^1(\mathbf{x},\mathbf{y})$ may be represented in the following form with separated variables

$$u^1_i(\mathbf{x},\mathbf{y}) = e_{pq(x)}(\mathbf{u}^0(\mathbf{x}))\chi^{pq}_i(\mathbf{y}) + C_i(\mathbf{x}), \tag{39}$$

$$\theta^1(\mathbf{x},\mathbf{y}) = \theta^0_{,p(x)}(\mathbf{x})\vartheta^p(\mathbf{y}) + C(\mathbf{x}). \tag{40}$$

We will call the $\chi^{pq}_i(\mathbf{y})$ and $\vartheta^p(\mathbf{y})$ the "homogenisation functions" for displacements and temperature respectively.

The zero order component of the equation of equilibrium (28) and of heat balance (31) in the light of (39) and (40) yields the following boundary value problems for functions of homogenisation

find $\chi^{pq}_i \in V_Y$ such that: $\forall v_i \in V_Y$

$$\int_Y a_{ijkl}(\mathbf{y})(\delta_{ip}\delta_{jq} + \chi^{pq}_{i,j(y)}(\mathbf{y}))v_{k,l(y)}(\mathbf{y})d\Omega = 0; \tag{41}$$

find $\vartheta^p \in V_Y$ such that: $\forall \varphi \in V_Y$

$$\int_Y K_{ij}(\mathbf{y})(\delta_{ip} + \vartheta^p_{,i(y)}(\mathbf{y}))\varphi_{,j(y)}(\mathbf{y})d\Omega = 0, \tag{42}$$

where V_Y is the subset of the space of kinematically admissible functions that contains the functions with equal values on the opposite sides of the cell of periodicity Y. The six vectors $\boldsymbol{\chi}^{pq}$ and the three scalar functions ϑ^p depend only on the geometry of the cell of periodicity and on the values of the jumps of material coefficients across S_J. Functions $v(y)$ and $\varphi(y)$ are usual test functions having the meaning of Y-periodic displacements and temperature fields respectively. They are used here to write explicitly the counterparts of the expressions (28) and (31), in which the prescribed differentiations are understood in a weak sense.

The solutions $\boldsymbol{\chi}^{pq}$ and ϑ^p of the "local" (i.e. defined for a single cell of periodicity) boundary value problems (41) and (42) with periodic boundary condition can be interpreted as obtained for the cell subject to a unitary average strain e^{pq} and, respectively, unitary average temperature gradient $\vartheta_{,p(y)}$. The true value of perturbations are obtained after by scaling $\boldsymbol{\chi}^{pq}$ and ϑ^p with true global strains (gradient of global temperature), as it is prescribed by (39) and (40).

In the asymptotic expansion for displacements (22) and for temperature (23) the dependence on $\mathbf{x}$ alone occurs only in the first term. The independence on $\mathbf{y}$ of these functions can be proved (see for example [153]). The functions depending only on $\mathbf{x}$ define the macro-behaviour of the structure and we will call them *global terms*. To obtain the global behaviour of stresses and of heat flux the following mean values over the cell of periodicity are defined [153]

$$\tilde{\sigma}^0_{ij}(\mathbf{x}) = |Y|^{-1}\int_Y \sigma^0_{ij}(\mathbf{x},\mathbf{y})dY,$$
$$\tilde{\mathbf{q}}^0(\mathbf{x}) = |Y|^{-1}\int_Y \mathbf{q}^0(\mathbf{x},\mathbf{y})dY. \tag{43}$$

Averaging of (35) and (37) results in the following, effective constitutive relationships

$$\tilde{\sigma}^0_{ij}(\mathbf{x}) = a^h_{ijkl}e_{kl}(\mathbf{u}^0) - \alpha^h_{ij}\theta^0, \qquad \tilde{q}^0_i = -k^h_{ij}\theta^0_{,j}. \tag{44}$$

In the above equations the effective material coefficients appear. They are computed according to

$$a^h_{ijkl} = |Y|^{-1}\int_Y a_{ijpq}(y)(\delta_{kp}\delta_{lq} + \chi^{pq}_{k,l(y)}(y))dY, \tag{45}$$

$$k^h_{ij} = |Y|^{-1}\int_Y k_{ip}(\mathbf{y})(\delta_{jp} + \vartheta^j_{,p}(\mathbf{y}))dY, \tag{46}$$

$$\alpha^h_{ij} = |Y|^{-1}\int_Y \alpha_{ij}(\mathbf{y})dY. \tag{47}$$

The macro-behaviour can be defined now by averaging first order terms in the equilibrium and flux balance equations (29), (32) and boundary conditions (20) and substituting then the averaged counterparts of stress and heat flux (43) (first order perturbations vanish in averaging of (29), (32) because of periodicity). Equations (17) and (18) should be replaced by (44), while (21) has no more sense since we deal now with homogeneous uncoupled thermo-elasticity.

The heterogeneous structure can now be studied as a homogeneous one with effective material coefficients given by (45)–(47) and global displacements, strains and average stresses and heat fluxes can be computed. Then we go back to (35) for the local approximation of stresses. This last step is the above mentioned *unsmearing* or *localization*.

3.4 Local Approximation of the Stress Vector

We note that the homogenisation approach results in two different kinds of stress tensors. The first one is the average stress field defined by (44). It represents the stress tensor for the homogenized, equivalent but "unreal" body. Once the effective material coefficients are known, the stress field and the heat flux may be obtained from a standard F.E. structural and heat transfer code.

The other stress field is associated with a family of uniform states of strains $e_{pq(x)}(\mathbf{u}^0)$ over each cell of periodicity $\mathbf{Y}$. This local stress is obtained by introducing (34) into (35) and results in

$$\sigma^0_{ij}(\mathbf{x},\mathbf{y}) = a_{ijkl}(\mathbf{y})(\delta_{kp}\delta_{lq} - \chi^{pq}_{k,l(y)})e_{pq(x)}(\mathbf{u}^0) - \alpha_{ij}(\mathbf{y})\theta^0. \tag{48}$$

Because of (28) and (41) this tensor fulfils the equations of equilibrium everywhere in $\mathbf{Y}$. If needed, the stress description can be completed with a higher order term in (24). This approach will be dealt in Sect. 8.2.

Finally the local approximation of heat flux is as follows

$$q^0_j(\mathbf{y}) = k_{ij}(\mathbf{y})(\delta_{ip} + \vartheta^{\,p}_{,i(y)}(\mathbf{y}))\theta^0_{,p(x)}. \tag{49}$$

3.5 Numerical Implementation

It is now shown how the asymptotic homogenization can be implemented in any finite element program [184]. The problem to be solved refers to a unit cell shown for instance on the right hand side of Fig. 1. For the purpose of a finite element solution it is convenient to use matrix notation for the above introduced quantities. Accordingly the homogenisation functions are ordered as defined by (50) and (51) respectively (the numbers in the superscripts in (50) and subscripts in (51) refer to the reference axes 1, 2, 3).

$$\begin{aligned}&\mathbf{X}^T(\mathbf{y})[\{\boldsymbol{\chi}^{11}(\mathbf{y})\}\{\boldsymbol{\chi}^{22}(\mathbf{y})\}\{\boldsymbol{\chi}^{33}(\mathbf{y})\}\{\boldsymbol{\chi}^{12}(\mathbf{y})\}\{\boldsymbol{\chi}^{23}(\mathbf{y})\}\\ &\qquad\{\boldsymbol{\chi}^{13}(\mathbf{y})\}]_{3\times 6},\\ &T^T(y) = \{\theta^1(y)\theta^2(y)\theta^3(y)\}_{1\times 3}.\end{aligned} \tag{50}$$

This is in accordance with the ordering of strains and temperatures

$$\begin{aligned}&\mathbf{e} = \{\mathbf{e}_{11}\,\mathbf{e}_{22}\,\mathbf{e}_{33}\,\mathbf{e}_{12}\,\mathbf{e}_{23}\,\mathbf{e}_{13}\}^T_6 = \{\mathbf{e}_{pq}\}^T_6,\\ &\theta = \{\theta_1,\theta_2,\theta_3\}^T_3 = \{\theta_p\}^T_3.\end{aligned} \tag{51}$$

In the following the superscript e denotes the nodal value in a finite element mesh of the unit cell. We have the usual representations for each element

$$\mathbf{X}(\mathbf{y}) = \mathbf{N}(\mathbf{y})\mathbf{X}^e, \qquad T(\mathbf{y}) = \mathbf{N}(\mathbf{y})\mathbf{T}^e, \tag{52}$$

where $\mathbf{N}$ contains the values of standard shape functions.

It is easy to show that the variational formulation (41) can be rewritten as follows

$$\text{find} \quad \mathbf{X} \in V_Y \quad \text{such that:} \quad \forall \mathbf{v} \in V_Y$$
$$\int_Y \mathbf{e}^T(\mathbf{v}(\mathbf{y}))\mathbf{D}(\mathbf{y})(\mathbf{1} + \mathbf{L}\mathbf{X}(\mathbf{y}))dY = 0. \tag{53}$$

In the above $\mathbf{L}$ denotes the matrix of differential operators, $\mathbf{D}$ contains the material coefficients a_{ijkl} in the repetitive domain. Matrix $\mathbf{X}^e$ which contains the values of homogenization functions at the nodes of the mesh is obtained as a finite element solution of (53). The equation to solve is the following

$$\mathbf{K}\mathbf{X}^e - \mathbf{F} = \mathbf{0}; \tag{54}$$

where $\mathbf{X}$ is Y-periodic, with zero mean value over the cell, and

$$\mathbf{F} = \int_Y \mathbf{B}^T\mathbf{D}(\mathbf{y}), \qquad \mathbf{K} = \int_Y \mathbf{B}^T\mathbf{D}(\mathbf{y})\mathbf{B}, \quad \mathbf{B} = \mathbf{L}\mathbf{N}(\mathbf{y}), \tag{55}$$

$\mathbf{D}$ contains the material coefficients a_{ijkl}.

It can be shown that $\mathbf{X}$ in (53) and thus (54) is a solution of a boundary value problem, for which the loading consists of unitary average strains over the cell. This is seen in the form of the first of (55), which forms a matrix. We solve thus six equations for six functions of homogenisation.

The variational formulation (42) can be represented in a form similar to (54), $\mathbf{T}^e$ being Y-periodic, with given mean zero value over the cell

$$\mathbf{K}\mathbf{T}^e + \mathbf{F} = \mathbf{0}; \tag{56}$$

where

$$\begin{aligned}&F = \int_Y \mathbf{B}^T_\theta \mathbf{K}_\theta(y)dY; \qquad \mathbf{K_T} = \int_Y \mathbf{B}^T_\theta \mathbf{K}_\theta(\mathbf{y})\mathbf{B}_\theta dY;\\ &\mathbf{B}_\theta = \mathbf{L}_\theta\mathbf{N}(y).\end{aligned} \tag{57}$$

$\mathbf{K}_\theta$ contains the conductivities k_{ij} of materials in the repetitive domain. Differential operators in $\mathbf{L}_\theta$ are ordered suitably for the thermal problem.

The periodicity conditions can be taken into account using Lagrange multipliers in the construction of a finite element code. Also the requirements of the zero mean value has to be included in the program.

Having computed $\mathbf{X}^e$, $\mathbf{T}^e$ and by consequence $\mathbf{u}^1$ and θ^1 one can derive the effective material coefficients, according to

$$\begin{aligned}\mathbf{D}^h &= |Y|^{-1}\int_Y \mathbf{D}(\mathbf{y})(\mathbf{1}+\mathbf{B}\mathbf{X}^e)dY\\ \mathbf{K}^h &= |Y|^{-1}\int_Y \mathbf{K}_\theta(\mathbf{y})(1+\mathbf{B}_\theta T^e)dY\\ \alpha^h &= |Y|^{-1}\int_Y \alpha(\mathbf{y})dY.\end{aligned} \tag{58}$$

As already pointed out, any thermoelastic finite element program can be used to obtain global displacements and temperatures. In a linear case the unit cell problem has to be solved only once. The structural or thermo-mechanical problem can then be performed separately, using these effective properties: it is hence a two step procedure on different scales, a homogenization step on the unit cell and a standard thermo-mechanical problem on the structural level. However the method permits one to obtain also local strains and stresses as shown above and dealt with more extensively in Sects. 7 and 8. For this unsmearing procedure the gradients of temperatures and strains are needed in the regions of interest, see (48) and (49). Strains and temperature gradients are directly obtained from the finite element interpolation. To present the graphs of stresses and heat fluxes over the single cell nodal projection can be used. To assure continuity of tangential stresses, this projection should be extended to patches of cells, see Sect. 8.1.

3.6 Boundary Effects and Time Dependent Problems

The periodicity condition used to find the local perturbation is strictly applicable only inside the body. We have hence the solution of a (thermo-)elasticity problem based on an assumed stress or displacement field which is valid nearly everywhere in the region occupied by the body under investigation, except on the boundary. The use of material coefficients based on the assumption of periodicity in the global solution (where the real boundary conditions are imposed) may implicitly impose some unrealistic constraints close to the boundary. This problem can be solved by some corrections which change the solution in the domain close to the boundary while away from the boundary the correction field should asymptotically decrease. Such a correction can be obtained by replacing the expansion (22) by

$$\mathbf{u}^\varepsilon(\mathbf{x}) \equiv \mathbf{u}^0(\mathbf{x}) + \varepsilon(\mathbf{u}^1(\mathbf{x},\mathbf{y}) + \mathbf{b}^1(\mathbf{x},\mathbf{z})) + \cdots, \tag{59}$$

where $\mathbf{z}$ represents the coordinates of an additional system with the origin on the external surface, the axis z_3 directed normal to the boundary surface with the other two axes oriented tangential to the surface and $\mathbf{b}$ is the boundary layer correction. Vector $\mathbf{b}$ should vanish exponentially when z_3 goes to infinity. The procedure is described in detail in [110] and has been implemented by making use of one cell of periodicity and infinite elements with homogenized material properties around it. The use of infinite elements assures the desired exponential decay. Although the procedure is theoretically necessary near free edges, it is seldom applied in practical engineering problems.

An alternative is the window method, where the microstructure with effective properties is embedded in a material with constant properties, subjected at the outer side to the boundary conditions wanted. In case of an applied constant strain field mixed b.c. at the real boundary are obtained [85].

Asymptotic theory of homogenization may involve also the time scale. This is the case in thermo-mechanical problems with non stationary heat conduction or in presence of impulsive heat loads or in problems with impact loads. In the first case correctors for the initial conditions are useful while in the other two cases spatial and temporal multiscale methods should be applied. The interested reader is referred to [21, 42, 111, 183] and references therein.

4 Mean Field Approaches and the Non Linear Case

The development of homogenisation procedures allowing to compute the non-linear effective behaviour of heterogeneous materials depending on the properties of their constituents or microstructure is a field of research in constant evolution. The focus here is on mean field methods which are based on the Eshelby inclusion solution. In these approaches, well adapted for heterogeneous materials with a random microstructure distribution, average fields are considered for each phase in the material.

The first incursions into the non-linear homogenisation dealt with crystal plasticity. The estimate of the elastic limit of polycrystals from one of a single crystal was started by Sachs [152] in 1928 and developed a short time after by Taylor [169]. Later, Lin [113] extended the model of Taylor by imposing the rate of total strain to be uniform in the polycristal. These first approaches are thus specific to crystal plasticity and formulated in the context of the physical metallurgy. In the beginning of the sixties an important change took place when Eshelby [58] gave the solution to the problem of the inclusion through the concept of eigenstrains.

4.1 The Model of Kröner

Budiansky et al. [27] used in 1960 the solution of the problem of inclusion provided by Eshelby to model the initial stages of elasto-plasticity of polycrystals. The authors assumed that only the most favourably oriented grains developed plasticity whereas the matrix remained elastic. This

situation is then assimilated to the inclusion problem. Moreover, by assuming that only a small quantity of grains tend to yield, the authors used the approximation of the dilute medium. Later, Kröner [102], initiator of the self-consistent model in elasticity, proposed to apply it to elasto-plasticity. Contrary to its predecessors who designed the matrix of the Eshelby problem as the whole of non plasticized grains, he assimilated it to the effective equivalent medium itself, that is, to the overall polycristal. The localisation rule obtained is written in the following form:

$$\boldsymbol{\sigma} = \boldsymbol{\Sigma} + 2\mu(1-\beta)(\mathbf{E}^p - \boldsymbol{\varepsilon}^p). \tag{60}$$

In this expression $\boldsymbol{\sigma}$ and $\boldsymbol{\Sigma}$ are respectively the local and overall stress tensors, $\mathbf{E}^p$ and $\boldsymbol{\varepsilon}^p$ the overall and the local plastic strain tensors, μ the overall shear modulus, and β is a parameter depending on the spatial distribution of the grains and their elastic properties. When all inclusions are assumed to be unit spheres (i.e. arising from an isotropic spatial distribution) with isotropic elasticity, we have:

$$\beta = \frac{2}{15}\frac{7-5v}{1-v}. \tag{61}$$

This localisation rule can easily be extended to more general situations. The model of Kröner suffers from the same insufficiencies as the models of Taylor or Lin providing an estimate that is generally too stiff.

4.2 Hill's Incremental Model

The alternative formulation suggested by Hill [94, 95] a few years later is based on a linearization of the local constitutive law. His idea is to bring back the non-linear problem of homogenisation in the scale transition from the single crystal to the polycristal to what he knows well, the linear homogenisation. For that, he linearizes the local constitutive law by bringing it back in an incremental form:

$$\dot{\boldsymbol{\sigma}}(\mathbf{x}) = \boldsymbol{L}(\mathbf{x}) : \dot{\boldsymbol{\varepsilon}}(\mathbf{x}), \tag{62}$$

where $\boldsymbol{L}$ is the tangent modulus.

In this linearized expression, the instantaneous modulus is of elasto-plastic nature and not only elastic. For the same reasons as Kröner, he made the choice of the self-consistent estimate to obtain the macroscopic behaviour of the polycristal. The effective moduli $\bar{\boldsymbol{L}}$ assigned to the reference homogeneous medium is then given by the following expression:

$$\bar{\boldsymbol{L}} = \langle \boldsymbol{L} : \boldsymbol{A} \rangle = \sum_r c_r \boldsymbol{L}_r : \boldsymbol{A}_r,$$

where $\boldsymbol{A}_r$ is the strain localisation tensor, and c_r the volume fraction of the phase r of the composite material. Therefore, the localisation rule is written as:

$$\dot{\boldsymbol{\sigma}}_s = \boldsymbol{B}_s(\boldsymbol{L}_s) : \dot{\boldsymbol{\Sigma}}, \qquad \dot{\boldsymbol{\varepsilon}}_s = \boldsymbol{A}_s(\boldsymbol{L}_s) : \dot{\mathbf{E}}. \tag{63}$$

The strain and stress localisation tensors are given from the solution of a dilute problem for a single inclusion of phase s, embedded in a large volume of a homogeneous medium $\bar{\boldsymbol{L}}$:

$$\boldsymbol{A}_s = [\mathbf{I} + \boldsymbol{P} : (\boldsymbol{L}_s - \bar{\boldsymbol{L}})]^{-1}, \qquad \boldsymbol{B}_s : \bar{\boldsymbol{L}} = \boldsymbol{L}_s : \boldsymbol{A}_s, \tag{64}$$

where the polarisation tensor $\boldsymbol{P}$ is defined by:

$$\boldsymbol{P} = \frac{1}{4\pi|\zeta|}\int_{\|\mathbf{x}\|=1} \mathbf{H}(\mathbf{x})\|\zeta^{-1}.\mathbf{x}\|^{-3} dS_x \tag{65}$$

with $\mathbf{H}(\mathbf{x}) = [\mathbf{x} \otimes \boldsymbol{\kappa}^{-1} \otimes \mathbf{x}]_{sym}$, $\boldsymbol{\kappa} = \mathbf{x}.\bar{\boldsymbol{L}}.\mathbf{x}$ and ζ characterizing the ellipsoidal geometry (on the unit sphere $\|\mathbf{x}\| = 1$). Let us note the anisotropic character of the polarisation tensor $\boldsymbol{P}$, due to its determination in terms of the reference stiffness (the overall tangent stiffness in the self-consistent scheme), which is anisotropic, even for an isotropic elasto-plastic material. Therefore it has to be determined numerically at each step of an incremental simulation.

In this approach, the overall tangent behaviour can be written as:

$$\dot{\boldsymbol{\Sigma}} = \bar{\boldsymbol{L}}(\mathbf{E}) : \dot{\mathbf{E}}. \tag{66}$$

The elasto-plastic nature of the instantaneous moduli leads to more realistic estimates (less stiff) than those given by the Kröner or Taylor model. The model of Hill was extended by Hutchinson [99] in 1976 to visco-plasticity by using tangent creep compliances instead of elasto-plastic ones. He noticed that, for power law creep, Hill's formulation may be integrated into a 'total' one making use of the secant creep compliances.

4.3 The Secant, Tangent and Affine Formulations

Following the work of Hill, several authors quickly realised that there are several possible ways to linearize the constitutive laws and that the incremental formulation of Hill is not unique. Thus, a few years later, several papers (Berveiller and Zaoui [11], Tandon and Weng [168]) were published, in the field of the non-linear homogenisation based on a secant linearization of the constitutive law. In the model of Berveiller and Zaoui, the secant linearization consists in replacing the local constitutive law $\boldsymbol{\sigma}(\mathbf{x}) = \mathbf{L}(\mathbf{x}) : (\boldsymbol{\varepsilon}(\mathbf{x}) - \boldsymbol{\varepsilon}^p(\mathbf{x}))$ by $\boldsymbol{\sigma}(\mathbf{x}) = \boldsymbol{L}^{sec}(\boldsymbol{\varepsilon}) : \boldsymbol{\varepsilon}(\mathbf{x})$ where $\boldsymbol{L}^{sec}(\boldsymbol{\varepsilon})$ is the secant module. In the particular case of a spherical inclusion with an isotropic behaviour, these authors have shown that the obtained localisation rule is formally identical to the model of Kröner, but with a reduction of the elastic moduli of the reference homogeneous medium by a factor characterising the evolution of the secant moduli of the effective medium. Moreover, this factor decreases very quickly as the plastic deformation grows.

Molinari et al. [129] proposed in 1987 a new method for estimating the visco-plastic behaviour of polycrystals which

is based on a tangent linearization of the local constitutive laws:

$$\boldsymbol{\sigma}(\mathbf{x}) = \boldsymbol{L}(\mathbf{x}) : \dot{\boldsymbol{\varepsilon}}(\mathbf{x}) + \boldsymbol{\tau}(\mathbf{x}), \tag{67}$$

where $\boldsymbol{L}$ is the tangent modulus of the phase medium subjected to a pre-stress $\boldsymbol{\tau}$. For the homogenisation, like their predecessors, these authors used the self-consistent scheme. Initially, in order to lighten the calculations, Molinari et al. [129] assumed that the polarisation tensor is isotropic.

Later, a development was proposed by Lebensohn and Tomé [108] without using this assumption. In these two formulations, the definition of the effective characteristics $\bar{\boldsymbol{L}}$ and $\bar{\boldsymbol{\tau}}$ which define the overall response of the material is nevertheless given only in the case of a power-law constitutive equation (with the same exponent for all the phases and all the slip systems). These authors thus thought to guarantee the property $\bar{\boldsymbol{L}} = d\Sigma/d\dot{\mathbf{E}}$ for the overall relation, itself a power law with the same exponent. It has been shown recently by Masson [119] and Masson et al. [120] that the effective moduli and compliances using the tangent local quantities are in general not any more tangent. Moreover, they showed that it is not necessary to use a power law only. This observation has motivated the affine formulation proposed by Masson et al. [120]. As Molinari et al. [129], they used a tangent linearization of the local constitutive laws:

$$\begin{aligned} &\boldsymbol{\sigma}(\mathbf{x}) = \boldsymbol{L}(\mathbf{x}) : (\boldsymbol{\varepsilon}(\mathbf{x}) - \boldsymbol{\eta}(\mathbf{x})); \\ &\boldsymbol{\varepsilon}(\mathbf{x}) = \boldsymbol{S}(\mathbf{x}) : \boldsymbol{\sigma}(\mathbf{x}) + \boldsymbol{\tau}(\mathbf{x}), \end{aligned} \tag{68}$$

where $\boldsymbol{\eta}$ is the pre-strain. However the affine formulation is based on a linear thermoelastic reference medium. The tangent effective moduli and the pre-stress are then defined using the following expressions:

$$\begin{aligned} &\bar{\boldsymbol{L}} = \langle \boldsymbol{L} : \boldsymbol{A} \rangle = \sum_r c_r \boldsymbol{L}_r : \boldsymbol{A}_r, \\ &\bar{\boldsymbol{\tau}} = -\bar{\boldsymbol{L}} : \bar{\boldsymbol{\eta}}, \qquad \bar{\boldsymbol{\eta}} = \langle {}^t\boldsymbol{B} : \boldsymbol{\eta} \rangle = \sum_r c_r : \boldsymbol{B}_r^t : \boldsymbol{\eta}_r. \end{aligned} \tag{69}$$

Using the self-consistent scheme in the case of similar and aligned ellipsoidal inclusions, the localisation rule can now be written as:

$$\boldsymbol{\varepsilon}_r = \boldsymbol{A}_r : [\mathbf{E} + \boldsymbol{P} : (\boldsymbol{L}_r : \boldsymbol{\eta} - \bar{\boldsymbol{L}} : \bar{\boldsymbol{\eta}})]. \tag{70}$$

We have also the overall constitutive equation as:

$$\boldsymbol{\Sigma} = \bar{\boldsymbol{L}} : (\mathbf{E} - \bar{\boldsymbol{\eta}}). \tag{71}$$

As mentioned in Masson and Zaoui [120], the operator $\bar{\boldsymbol{L}}$ does not correspond exactly with the current tangent overall stiffness of the overall stress-strain response of the composite. In this model, as in the incremental tangent formulation, the stiffness tensors (anisotropic), the localisation and polarisation tensors have to be evaluated at each step at a given load. Moreover, the eigenstrains and the tangent stiffness are taken as uniform inside each phase, but the stress and strain fields are not necessarily uniform.

The development of variational approaches [165, 181] for a behaviour deriving from a single potential (non-linear elasticity or viscosity) has made possible to compare some of these non-linear estimates to rigorous bounds of Hashin-Shtrikman type. It has been shown by Gilormini [79] that both the incremental and the classical secant formulations lead to estimates which are too stiff and can even violate these bounds in some cases. More recently, Chaboche et al. [37, 40] have used some of these procedures in the context of composite materials, and compared their estimates to unit-cell finite element calculations using periodic boundary conditions. The obtained main results are illustrated in Sect. 5.4.

4.4 The "Beta Rule"

In the same category of the modified Kröner approach by a secant method, we have a slightly different one, useful to describe the transition in local accommodation between phases, from the small inelastic strains to very large ones.

Introduced by Cailletaud [29], this rule replaces $\boldsymbol{\varepsilon}^p$ and $\mathbf{E}^p$ in (60) by an "accommodation" variable called $\boldsymbol{\beta}_s$, and its average $\mathbf{B} = \sum_s c_s \boldsymbol{\beta}_s$. The evolution rule for $\boldsymbol{\beta}_s$ is given by the classical Armstrong-Frederick rule of plasticity:

$$\dot{\boldsymbol{\beta}}_s = \dot{\boldsymbol{\varepsilon}}_s^p - D\boldsymbol{\beta}_s \|\dot{\boldsymbol{\varepsilon}}_s^p\|. \tag{72}$$

It allows to recover Kröner elastic accommodation for small plastic strains, and Sachs for larger ones, when plastic strains are important in most of the phases. Compared to the methods described just above, we may notice the following advantages:

- the correct applicability under any cyclic or multi-axial loading;
- the much lower computational cost than in incremental or affine methods.

Using comparisons with 3D finite element analyses, the $\boldsymbol{\beta}$ rule has been shown by Cailletaud [30] and Cailletaud and Pilvin [31] as having self-consistent overall properties.

4.5 Higher Order Theories

A modified secant theory has been proposed by Suquet [164]. It is based on second-order moments in each individual phase of the linear comparison solid. The use of second-order moments has also been considered by Hu [97] and Buryachenko [28]. It has been shown by Suquet [164] and Ponte Castañeda and Suquet [147] that this secant theory based on second-order moments coincides with the Ponte

Castañeda's [142] variational procedure; this property ensures that the resulting estimates do not lead to the violation of any bound. More recently, the second-order moments have been used by Brenner et al. [22] in the affine formulation to take into account the intra-phase heterogeneity.

On the other hand, new linearizations have been searched for, with the objective of generating softer estimates even when using the classical reference quantities. This is the second order procedure proposed by Ponte Castañeda [143, 144] which makes use of a second-order Taylor development of the strain or stress potentials. The comparison of the second-order method to numerical simulations (Moulinec and Suquet [132]) has shown that quite accurate estimates are obtained even at high values of heterogeneity contrast, including the cases of rigid reinforcements or porous materials.

However, it has been demonstrated recently by Leroy and Ponte Castañeda [112] that the second-order estimates can violate the Hashin and Shtrikman bounds [89] near the percolation limit. Moreover, earlier, Nebozhyn and Ponte Castañeda [135] have pointed out the non convex character of the predictions for the effective yield surface in the case of porous materials with an incompressible matrix phase. Later, Ponte Castañeda [145] has then proposed an improved second order method incorporating field fluctuations. The method delivers then nonlinear estimates that are exact to second order in heterogeneity. The new homogenisation technique is motivated by the fact established by Suquet [164] that the original second order method uses the first moments, or averages of the fields over the phases while second moments of the fields are known to be important when the field fluctuations are significant, as it is the case near percolation.

Several applications of this new second order method which incorporates both first and second-moment information are then presented later for porous and rigidly reinforced composites (Ponte Castañeda [146]). The results show that the new theory satisfies rigorous bonds, even near the percolation limit, where field fluctuations become important, case for which the original second order estimates failed. The case of porous materials with an incompressible matrix is also now well estimated with the new method, and in general the new estimates appear in better agreement with numerical simulations taken from the literature.

5 Semi-analytical Methods

Semi-analytical methods can be defined as direct micro-macro procedures for which the local constitutive equations and criteria are evaluated at the local scale using explicit relations to establish the link between the macroscopic and the microscopic fields. Such method correlates the overall macroscopic behaviour with microstructural responses. The analytical relations are usually based on mean field procedures. One advantage is that the local inelastic constitutive laws are totally free. Contrarily, in most variational methods or higher order theories like discussed in Sect. 4.5, there is the assumption of a unique potential, therefore limiting the application to non linear elasticity or deformation plasticity. The following sections give an overview of some relevant works from the literature applying this type of procedures.

5.1 The Transformation Fields Analysis

Regarding approximate schemes, the Transformation Field Analysis proposed by Dvorak and co-workers can be seen as an elegant way of reducing the number of macroscopic internal variables by assuming the microscopic fields of internal variables to be piecewise uniform. The method has been developed initially for elasto-plastic composites (Dvorak and Rao [52], Dvorak and Bahei-El-Din [50], Dvorak et al. [54], Teply and Dvorak [170]). Its formalisation by Dvorak and Benveniste [51] and Dvorak [49] has provided a theoretical basis for further works.

The Transformation Field analysis is based on the idea of a purely elastic redistribution of the macroscopic stress and strain, and of the local eigenstresses or eigenstrains. TFA is a generalised way of writing explicit scale transitions, based on purely elastic interactions between sub-volumes of the RVE, and it can be shown that many classical approaches (self-consistent, Sachs, Taylor, Kröner, etc.) are special cases. In this method, the plastic strain and the thermal expansion are considered as given eigenstrains. The local stress field is then determined from the fields of eigenstrain by solving linear problems with eigenstrains and the plastic strain field which is updated by the flow rule.

Considering a representative volume V of an heterogeneous material where the size of the inhomogeneities is small compared to that of V, the volume V is subdivided into several local sub-domains V_r, $r = 1, 2, \ldots, N$, such that each contains one phase material. The local constitutive relations in each sub-volume are written in the following form:

$$\begin{aligned} &\boldsymbol{\sigma}_r(\mathbf{x}) = \mathbf{L}_r : \boldsymbol{\varepsilon}_r(\mathbf{x}) + \boldsymbol{\lambda}_r(\mathbf{x}), \\ &\boldsymbol{\varepsilon}_r(\mathbf{x}) = \boldsymbol{\varepsilon}_r^e(\mathbf{x}) + \boldsymbol{\mu}_r(\mathbf{x}), \qquad \boldsymbol{\lambda}_r(\mathbf{x}) = -\mathbf{L}_r : \boldsymbol{\mu}_r(\mathbf{x}), \end{aligned} \tag{73}$$

$\boldsymbol{\mu}_r(\mathbf{x})$ denotes a prescribed distribution of local eigenstrains and $\boldsymbol{\lambda}_r(\mathbf{x})$ is the corresponding eigenstress field. The eigenstrain and eigenstress fields may consist of contributions of distinct physical origin like thermal strains, plastic strains and transformation strains. The relation between the local and overall fields is given by the following localisation rule:

$$\begin{aligned} &\boldsymbol{\varepsilon}_r = \mathbf{A}_r : \mathbf{E} + \sum_s \mathbf{D}_{rs} : \boldsymbol{\mu}_s, \\ &\boldsymbol{\sigma}_r = \mathbf{B}_r : \boldsymbol{\Sigma} - \sum_s \mathbf{F}_{rs} : \boldsymbol{\lambda}_s \end{aligned} \tag{74}$$

$\mathbf{D}_{sr}$ and $\mathbf{F}_{sr}$ are the "transformation influence tensors" (fourth rank tensors). All the tensors $\mathbf{A}_r, \mathbf{B}_r, \mathbf{D}_{rs}, \mathbf{F}_{rs}$ depend on the local and overall elastic moduli, and on the shape and the volume fraction of the phases, and can be derived once, independently of the inelastic process.

Let us note that expressions (74) are simple discretizations of exact expressions involving the non-local elastic Green operator $\boldsymbol{\Gamma}(\mathbf{x}, \mathbf{x}')$ of the homogeneous elastic medium. For instance:

$$\boldsymbol{\varepsilon}(\mathbf{x}) = \mathbf{A}(\mathbf{x}) : \bar{\boldsymbol{\varepsilon}} + \frac{1}{V} \int_V \mathbf{D}(\mathbf{x}, \mathbf{x}') : \boldsymbol{\mu}(\mathbf{x}') d\mathbf{x}', \tag{75}$$

where $\mathbf{D}(\mathbf{x}, \mathbf{x}') = \boldsymbol{\Gamma}(\mathbf{x}, \mathbf{x}') : \mathbf{L}(\mathbf{x}')$ gives the strain at point $\mathbf{x}$ created by a transformation strain $\boldsymbol{\mu}(\mathbf{x}')$ at point $\mathbf{x}'$.

In cases where two phases are considered, with one sub-volume only for each phase, these quantities $\mathbf{A}_r$ and $\mathbf{D}_{rs}$ (respectively $\mathbf{B}_r$ and $\mathbf{F}_{rs}$) can be expressed in closed form by means of Eshelby tensor. Contrarily, when using a decomposition into several sub-domains for each phase, these tensors can be determined by solving a set of linear problems (6 for the concentration tensors and $6N$ for the influence tensors), by a finite element method (Dvorak, [55], Carrère et al., [36]).

This formalism has been used in different works with more complex behaviour (thermo-visco-plasticity, damage, interface debonding) by Dvorak et al. ([53, 55]) and by other groups namely Kattan and Voyiadjis [100], Chaboche et al. [39], Fish et al. [70], Fish and Yu [69].

In the paper of Chaboche et al. [39] the transformation field analysis has been extended to take into account the non-linearities due to changing local behaviour induced by temperature or damage. A generalised eigenstrain which takes into account thermal and damage effects on the elastic behaviour is defined such as at the local scale the local constitutive equation

$$\boldsymbol{\sigma}_r = \hat{\mathbf{L}}_r : (\boldsymbol{\varepsilon}_r - \boldsymbol{\varepsilon}_r^{\theta} - \boldsymbol{\varepsilon}_r^{p}) \tag{76}$$

is replaced by:

$$\boldsymbol{\sigma}_r = \mathbf{L}_r : (\boldsymbol{\varepsilon}_r - \boldsymbol{\varepsilon}_r^{GE}), \tag{77}$$

where $\hat{\mathbf{L}}_r$ is the average damaged stiffness in the sub-volume and the thermal strain. The generalised eigenstrain is considered as an eigenstrain of the same nature as the plastic and thermal ones:

$$\boldsymbol{\varepsilon}_r^{GE} = (\boldsymbol{\varepsilon}_r^{th} + \boldsymbol{\varepsilon}_r^{p} + \boldsymbol{\varepsilon}_r^{d}), \tag{78}$$

where the damage strain $\boldsymbol{\varepsilon}_r^{d} = (\mathbf{I} - \mathbf{L}_s^{-1} : \hat{\mathbf{L}}_s)(\boldsymbol{\varepsilon}_s - \boldsymbol{\varepsilon}_s^{p} - \boldsymbol{\varepsilon}_s^{\theta})$.

Then the localisation rule is written as follows:

$$\boldsymbol{\varepsilon}_r = \mathbf{A}_r : \boldsymbol{\Sigma} + \sum_s \mathbf{D}_{rs} : \mathbf{L}_s : \boldsymbol{\varepsilon}_s^{GE}. \tag{79}$$

It is also demonstrated in [35] that by considering a large number sub-volumes the method captures the local stress and inelastic strain fields with good accuracy in comparison to finite-element simulations.

Interface decohesion effects in composites were introduced later by Dvorak and Zhang [53]. The authors represent stress changes due to local debonding under increasing overall loads by damage equivalent eigenstrains which adjust local stresses in the affected volumes to values implied by the selected decohesion models. Interaction between the still bonded and partially debonded phases at any damage state is described by transformation influence functions using TFA.

The TFA has been used by Fish et al. [70] to analyse a composite structure by the finite element method. These authors found a good agreement between the two-point averaging scheme (plane TFA with uniform plane strain in the matrix) and a more refined computation (multi-point incremental homogenisation).

However, it has long been recognised by Dvorak himself (Teply and Dvorak [170] and confirmed by others (Suquet [162]; Chaboche et al. [39]; Michel et al. [123]) that the application of the TFA to two-phase systems may require, for non-linear heterogeneous materials, a sub-division of each individual phase into several sub-domains to obtain a satisfactory description of the effective behaviour. As a consequence, the number of internals variables needed in the effective constitutive relations, although finite, can be prohibitively high. The need for a finer sub-division of the phase results from the intrinsic non-uniformity of the plastic strain field which can be highly heterogeneous even within a single material phase.

5.2 Non Uniform TFA

In order to better take into account the non-linear redistributions induced by plasticity, the TFA method uses a subdivision of each individual phase into several sub-domains, in which are assumed uniform transformation strains (or eigenstrains, or plastic strains). With the aim of reducing the number of such sub-volumes, the NTFA (Non-Uniform Transformation Field Analysis) was proposed by Michel and Suquet ([123, 124]). The plastic strain is decomposed on a finite set of plastic modes which can present large deviations from uniformity:

$$\boldsymbol{\varepsilon}^{an}(\mathbf{x}) = \sum_k \varepsilon_k^{an} \boldsymbol{\mu}^k(\mathbf{x}). \tag{80}$$

The ε_k^{an} are now coefficients of the decomposition (that may depend on time) and the $\boldsymbol{\mu}^k(\mathbf{x})$ are the non-uniform transformation fields, defined independently on each phase. These modes $\boldsymbol{\mu}^k$ are non uniform (not even piecewise uniform) and are meant to capture the salient features of the plastic

flow modes. They are determined once (most often by solving specific numerical problems on given unit cells) and are normalised with $\langle \boldsymbol{\mu}^k_{eq} \rangle = 1$ in order for ε^{an}_k to be homogeneous to a plastic strain.

The constitutive relations are expressed in terms of scalar projections on the modes (there is a direct analogy with crystal plasticity):

$$\tau_k = \langle \boldsymbol{\sigma} : \boldsymbol{\mu}^k \rangle, \qquad e_k = \langle \boldsymbol{\varepsilon} : \boldsymbol{\mu}^k \rangle, \qquad e^{an}_k = \langle \boldsymbol{\varepsilon}^{an} : \boldsymbol{\mu}^k \rangle. \quad (81)$$

The NTFA localisation rule becomes then:

$$\boldsymbol{\varepsilon}(\mathbf{x}) = \mathbf{A}(\mathbf{x}) : \bar{\boldsymbol{\varepsilon}} + \sum_l \langle \mathbf{D} * \boldsymbol{\mu}^k \rangle (\mathbf{x}) \varepsilon^{an}_l \quad (82)$$

that can be rewritten, after multiplication by $\boldsymbol{\mu}^k$ and averaging over V:

$$e_k = \mathbf{a}_k : \bar{\boldsymbol{\varepsilon}} + \sum_l D_{kl} \varepsilon^{an}_l, \quad (83)$$

where the second order tensor $\mathbf{a}_k$ and the influence factor D_{kl} are defined as:

$$\mathbf{a}_k = \langle \mathbf{A}^T : \boldsymbol{\mu}^k \rangle, \qquad \mathbf{D}_{kl} = \langle \boldsymbol{\mu}^k : (\mathbf{D} * \boldsymbol{\mu}^l) \rangle. \quad (84)$$

Having assumed that all phases are elastically isotropic, characterised by a bulk modulus κ_k and a shear modulus G_k, the "resolved shear stress" is given by:

$$\tau_k = 2G_k(e_k - e^{an}_k). \quad (85)$$

As we will see in Sect. 6.2 one interest of the TFA procedure is to contain a general writing for macroscopic constitutive equations based on the micromechanical evolution laws. This property is partly retained with NTFA method. In [123] there are two versions proposed:

- the uncoupled model: the reduced macroscopic state variables of the model are the overall strain $\bar{\varepsilon}$, the set of all the ε^{an}_k and a set of tensorial variables β_k associated with each mode (and representing the field of internal variables at the local scale).
- the coupled model: in order to reduce the number of internal variables, this version attaches an internal variable β_r to each phase, and not to each mode. It also couples the different modes supported by the same phase, by a quadratic average like:

$$A^{an}_r = \left(\sum_{k=1}^{M(r)} |A^{an}_k|^2 \right)^{1/2}, \quad (86)$$

where the A^{an}_k are thermodynamic forces associated with the β_r, and $M(r)$ is the number of modes in phase r.

The explicit forms of the two corresponding macroscopic models are not indicated here. They assume a restriction of inelastic local constitutive equations of the phases to a Generalised Standard Material format (Halphen and Nguyen [86]), and to a linear kinematic hardening. The interested reader is invited to report to Michel and Suquet ([123, 124]) for additional information.

An example is given here, taken from (Michel and Suquet [124]), for a plane strain unit cell (square periodicity), with a cylindrical elastic fibre ($E_f = 400$ GPa, $\nu_f = 0.2$) and an elasto-plastic matrix with non-linear isotropic hardening ($E_m = 75$ GPa, $\nu_m = 0.3, \sigma_0 = 75$ MPa, $h = 416.5$ MPa, $m = 0.3895$), such that $\sigma_{eq} \leq R(p) = \sigma_0 + hp^m$. There are 3 modes introduced, corresponding to 3 independent monotonous inelastic analyses with the same constitutive behaviour (made by FFT or by FE), uniaxial tension in directions 1 and 2, as well as pure shear.

Figure 2 shows the plastic mode $\boldsymbol{\mu}^1$, with its 4 components $\mu^1_{11}, \mu^1_{22}, \mu^1_{12}, \mu^1_{33}$. Figure 3a indicates the results for uniaxial (1) and shear (2) loadings for the reference calculations (very fine mesh), for TFA (with 1 sub-volume by phase), for NTFA with the coupled version (with the 3 modes). Very clearly TFA delivers a much too stiff macroscopic response, though NTFA correlates very well with the reference solution. In Fig. 3b there are comparisons for 3 other loading conditions.

The advantage of NTFA over classical TFA is evident, from the above example and others. However, there are still some limitations, like:

- the need for a number of initial numerical elasto-plastic solutions and the corresponding selection of the relevant modes for a given situation. Moreover, only the coupled version seems to work well for combined loadings, not corresponding to the reference modes (see examples in [123]);

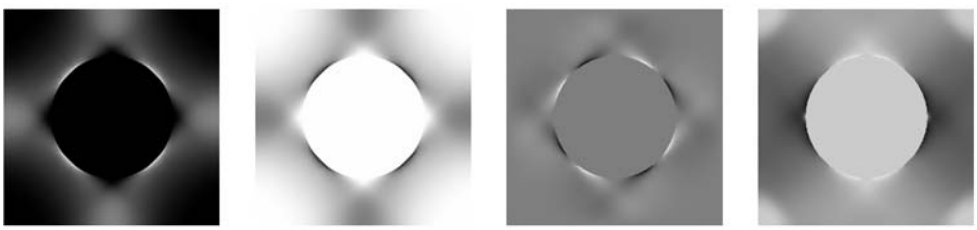

Fig. 2 Plastic mode $\boldsymbol{\mu}^1$, with its 4 components (with permission of P. Suquet)

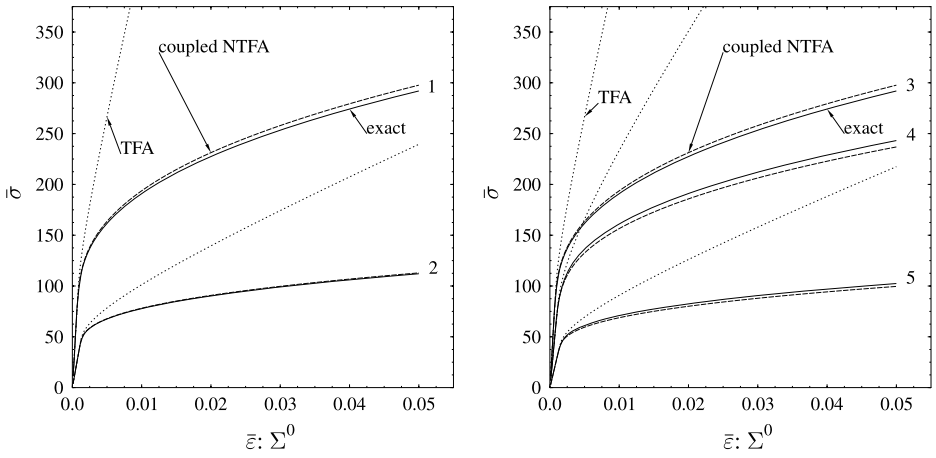

Fig. 3 Comparisons between TFA, NTFA and the reference computation for 5 loading conditions (with permission of P. Suquet)

– the situations where cyclic conditions or non proportional loading conditions are taking place, or non-isothermal ones, which was not the case in the shown example;
– the GSM format that is needed, which limits the possible flexibility of the local constitutive behaviour (non-linear kinematic hardening, visco-plasticity…).

Another advantage of the NTFA method is its ability to easily recover the local fields, in a natural way, after the solution of the overall structural boundary value problem. Such a capability is illustrated by examples given in Michel and Suquet [124]. See also Sect. 8 that is devoted to the localisation methods.

5.3 The Methods of Cells or Generalised Methods of Cells

Another quite popular method in the literature is the Methods of Cells of Aboudi ([1, 2]). As in the Transformation Field Analysis all the inelastic strains (thermal expansion, plasticity, visco-plasticity) are considered as eigenstrains, assumed to be known before applying the micro-macro transition rule. The method consists of a discretization of the (periodic) unit cell as rectangular (in 2D) or parallelepiped (in 3D) sub-domains.

In his first works, the representative cell consists of four sub-cells; one is occupied by the fibrous material whereas the other three are occupied by the matrix. The generalised cell method (Paley and Aboudi [139]) is the generalisation to any number of sub-cells. In these methods local equilibrium/compatibility equations are solved in an average sense for uniform eigenstrains in each sub-cell. Continuity of traction and displacement rate on an average basis are imposed at the interfaces between the constituents. The local equilibrium is guaranteed by the assumption that the velocity factor is linearly expanded in terms of the local coordinates of the sub-cell. This forms the relation between the microscopic and the macroscopic strains, through the relevant concentration factors. The overall behaviour is finally expressed as a constitutive relation between the average stress, strain and plastic strain in the conjunction of the elastic stiffness tensor of the composite.

The method looks as an approximation of an hybrid formulation of the finite element method. In the context of unidirectional composites, the generalised cell method allows accurate and efficient analysis of the impact of fibre shape and arrangement on the inelastic macroscopic response of the composite as demonstrated by Arnold et al. [7]. The predictive capability of the method in various applications has been summarised by Aboudi [4].

Damage effects also have been incorporated in the model by Aboudi [2] to treat interface debonding or by Voyiadjis and Deliktas [177], using the local incremental damage model of Voyiadjis and Park [178].

However, despite the accuracy of the method in modelling the inelastic macroscopic response of periodic composites, the accuracy with which local stress and strain fields are captured is not as good, not allowing the possibility of following precisely the evolution of damage at the local scale. Aboudi et al. [5] have recently proposed a new method for periodic multiphase materials to correct these effects. As previously, the approximate solution for the displacement field within each sub-cell is constructed based on volumetric averaging of the equilibrium equations together with the imposition of periodic boundary conditions, on both the displacement and traction continuity conditions in an average sense between the cells and sub-cells used to characterize the microstructure of the material.

The particularity of this new approach is to approximate the displacement field within each sub-cell, by quadratic functions expressed in local coordinates. The capability of the method to capture both the macroscopic response and the local stress and inelastic strain fields is shown on a unidirectional gr/al composite by comparisons to finite element analyses and analytical models.

5.4 Corrected TFA

As it has been recalled in the Sect. 5.1, the original TFA method does not lead to satisfactory estimates of the global and local behaviour of the composite when it is applied to two-phase medium using plastic strains uniform over each of the two phases. One way to reduce the excessive stiffness of the TFA localization rule, is to take into account the intrinsic non-uniformity of the plastic strain as it is done by Suquet and Michel (see Sect. 5.2). Another approach, based on the use of an asymptotic stiffness tensor, is proposed in 1998 by Pottier [148] and Chaboche et al. [39]. The proposed corrected method consists of writing the total elastic localisation rule with corrected values for the eigenstrains.

Consider a composite made of elasto-plastic phases with $\boldsymbol{\varepsilon}_s^p$ as the plastic deformation in the phase s. The correction consists of writing the total elastic localisation rule with corrected values for the eigenstrains as follows:

$$\boldsymbol{\varepsilon}_r = \mathbf{A}_r : \mathbf{E} + \sum_s \mathbf{D}_{rs} : \mathbf{K}_s : \boldsymbol{\varepsilon}_s^p. \tag{87}$$

Moreover, we assume the asymptotic tangent stiffness of the local constitutive equation to be known, such as $\dot{\boldsymbol{\varepsilon}}_r^p = (\boldsymbol{L}_r^p)^{-1} : \dot{\boldsymbol{\sigma}}_r$. In practice, it is obtained from the knowledge of the hardening rules in each phase. For instance, in the case of rate dependent plasticity, its modulus is the kinematic hardening parameter (that plays a role in the large strain domain).

The corrected tensors $\mathbf{K}_s$ are then determined by the rate forms of the localisation rule:

$$\dot{\boldsymbol{\varepsilon}}_r = \mathbf{A}_r : \dot{\mathbf{E}} + \sum_s \mathbf{D}_{rs} : \mathbf{K}_s : \dot{\boldsymbol{\varepsilon}}_s^p \tag{88}$$

with the corresponding elastic tangent one:

$$\dot{\boldsymbol{\varepsilon}}_r = \boldsymbol{A}_r : \dot{\mathbf{E}}, \tag{89}$$

where the asymptotic tangent concentration tensor $\boldsymbol{A}_r$ is defined by the following expression:

$$\boldsymbol{A}_r = [\mathbf{I} + \boldsymbol{P} : (\boldsymbol{L}_r - \bar{\boldsymbol{L}})]^{-1} \tag{90}$$

and the elasto-plastic tangent stiffness by $\boldsymbol{L}_r^{-1} = (\boldsymbol{L}_r^p)^{-1} + \mathbf{L}_r^{-1}$.

It is then shown that the following expression can be obtained:

$$\sum_s \mathbf{D}_{rs} : \mathbf{K}_s : (\boldsymbol{L}_s^{-1} - \mathbf{L}_s^{-1}) : \mathbf{L}_s : \boldsymbol{A}_s = \boldsymbol{A}_r - \mathbf{A}_r. \tag{91}$$

In this equation, the operators $\mathbf{A}_s$, $\mathbf{D}_{rs}$ are constant and evaluated once from the elastic properties of the constituents. The tensors $\mathbf{K}_s$, $\boldsymbol{L}_s$, $\boldsymbol{A}_s$, are also constant and delivered from the knowledge of the asymptotic tangent stiffness.

Moreover, the system in $\mathbf{K}_s$ in (91) is indeterminate. But choosing $\mathbf{K}_s = \mathbf{I}$ for the system with the smallest plastic strain, its solution can be easily obtained.

We have to notice that the asymptotic tangent stiffness is known only in its isotropic part, because the direction of plastic flow is not known in advance. Therefore, the tensor $\mathbf{K}_s$ is determined once, as an isotropic tangent corrector. Despite the standard TFA formalism, the proposed modification does not follow exactly the Levin-Mandel equation.

5.5 Methods Comparisons

In order to compare some of the different methods listed here, we have performed a numerical study on composite materials in the context of asymptotic homogenisation. Assuming a periodic structure for the composite made up of many repetitive unit cells, reference solutions for the overall and the local constitutive behaviour of the composite are obtained. The exact responses can then be used to evaluate the accuracy of different homogenisation methods.

The results presented here are focussed on a two-phase particle composite.

The inclusion volume fraction is taken as 0.3 and the spherical inclusion is elastic isotropic with $E_f = 400$ GPa, $\nu_f = 0.2$ and the matrix isotropic elasticity is given by $E_f = 75$ GPa, $\nu_f = 0.3$ exactly the same conditions considered by Michel and Suquet [122]. The constitutive behaviour of the matrix is described by a Von Mises elasto-plasticity with a power law for isotropic hardening:

$$\sigma_{eq} - Hp^{\alpha} - \sigma_0 \leq 0 \tag{92}$$

with $H = 416$ MPa, $\alpha = 0.3895$ and $\sigma_0 = 75$ MPa. In (92) p is the accumulated plastic strain defined by $\dot{p} = \sqrt{\frac{2}{3}\dot{\boldsymbol{\varepsilon}}_p : \dot{\boldsymbol{\varepsilon}}_p}$. This case corresponds to a configuration considered by some others authors (Michel and Suquet [122]; Gonzales and Llorca, [80]; Doghri and Ouaar [47]). The particle repartition is assumed regularly distributed. For all the simulations, the interface between the particle and the matrix is considered as perfect.

The composite has a square/hexagonal arrangement of particles leading to an isotropic spatial repartition. The corresponding 3D unit cell can be nevertheless correctly approximated by an axisymmetric unit cell (Chaboche et al. [40]).

The composite behaviour with a random distribution is obtained through the finite element analysis of a periodic cubic unit cell containing a random dispersion of 38 non-overlapping identical spheres. A compromise between the accuracy of the solution and the computer time to solve the problem (in the context of a sequential computation) has lead to this choice. The final particle arrangement is statically isotropic (all the directions in the unit cell are macroscopically equivalent). Figure 4 shows the local accumulated

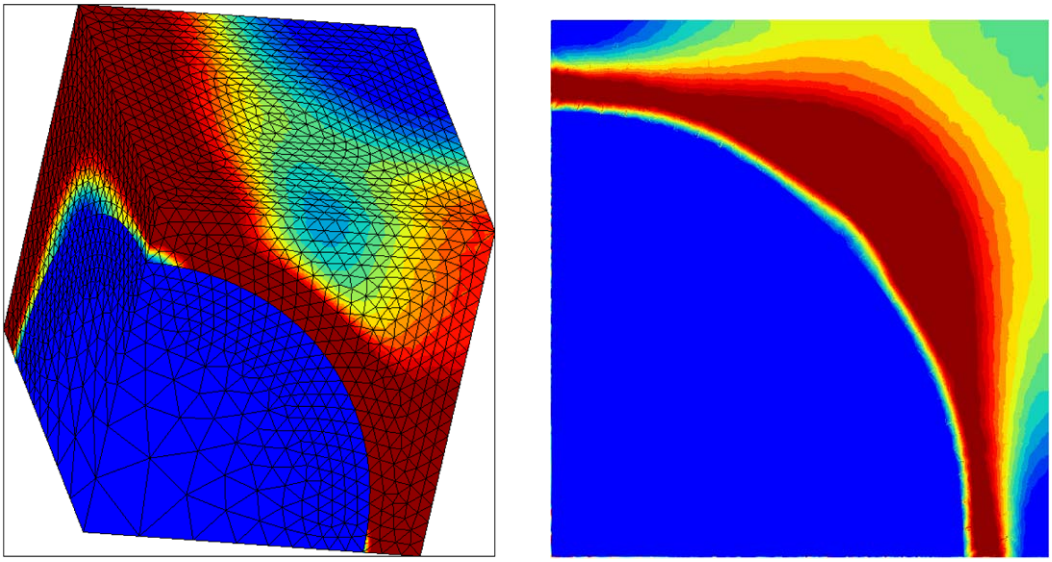

Fig. 4 Iso-values of the plastic strain in the RVE of the composite with a regular microstructure

plastic strains obtained in the composite with a regular microstructure.

The global stress/strain responses obtained with various mean-field methods (the analytical TFA, the Hill's incremental, the Affine and finally the corrected TFA approaches) have been then compared to the reference overall stress/strain responses delivered by the finite element simulation on the unit cells. In each application of the mean field methods that will be presented here, the homogenisation rule of Mori-Tanaka (Mori and Tanaka [131]) has been chosen.

We have to remind that in the incremental and affine methods, the tangent polarisation tensor $\boldsymbol{P}$ is anisotropic because of the anisotropic character of $\boldsymbol{L}$. It has then to be evaluated numerically, at each time step of an incremental or affine simulation. However, the anisotropic stiffness can be replaced by an isotropic approximation (Chaboche and Kanouté [37]):

$$\boldsymbol{L}_s^* = 3k_s\mathbf{J} + 2\gamma_s\mathbf{K} \tag{93}$$

with $\mathbf{J} = \frac{1}{3}(\mathbf{1}\otimes\mathbf{1})$, $\mathbf{K} = \mathbf{I} - \mathbf{J}$. Assuming an isotropic Von Mises plastic flow, we have $2\gamma_s = 2\mu_s h_s^p/h$ where $h = 3\mu_s + h_s^p$, with the current plastic modulus h_s^p defined as $h_s^p = \partial\sigma_{eq}/\partial p$. The incremental and the affine method have been evaluated using the complete anisotropic polarisation tensor and this isotropic approximation.

Other isotropic approximations can be also considered namely the following isotropic form based on the general projection method (Bornert, [17]; Doghri and Ouaar, [47]):

$$\mathbf{L}_s^{iso} = 3k_s\mathbf{J} + 2\boldsymbol{\mu}_s^t\mathbf{K} \quad \text{with } \mu_s^t/\mu_s = (4 + h_s^p/h_s)/5.$$

The results presented in Fig. 5 show the comparisons between the reference FE solution assuming a regular microstructure of the composite and several mean field methods.

Regarding the Fig. 5, the following remarks can be done:

- The affine, the incremental and the TFA procedures give an extremely stiff response. The affine delivers a slightly softer response than the TFA and the incremental methods.
- The isotropic approximations of the affine and incremental procedure, deliver much softer responses, much more in accordance with the finite element reference solution, but slightly softer. The same results has been obtained for the incremental method (Gonzales and Llorca, [80]; Doghri and Ouaar, [47] for randomly distributed particle).
- The best approximations of the global behaviour of the composite are given by the corrected TFA approach and the incremental method based on an isotropic approximation of the polarisation tensor.

6 Sequential Multiscale Procedures

When dealing with the inelastic analysis of a structural component, when the overall behaviour explicitly takes into account information and processes present at the lower scale, there are currently two main approaches. In what follows we will call them:

– *the sequential multiscale procedures*, in which the multiscale analysis, or the micro-to-macro homogenisation process, is made separately from the structural analysis. Prior treatments then define a set of overall constitutive equations which format could be guided by the scale change method. Material parameters in these equations

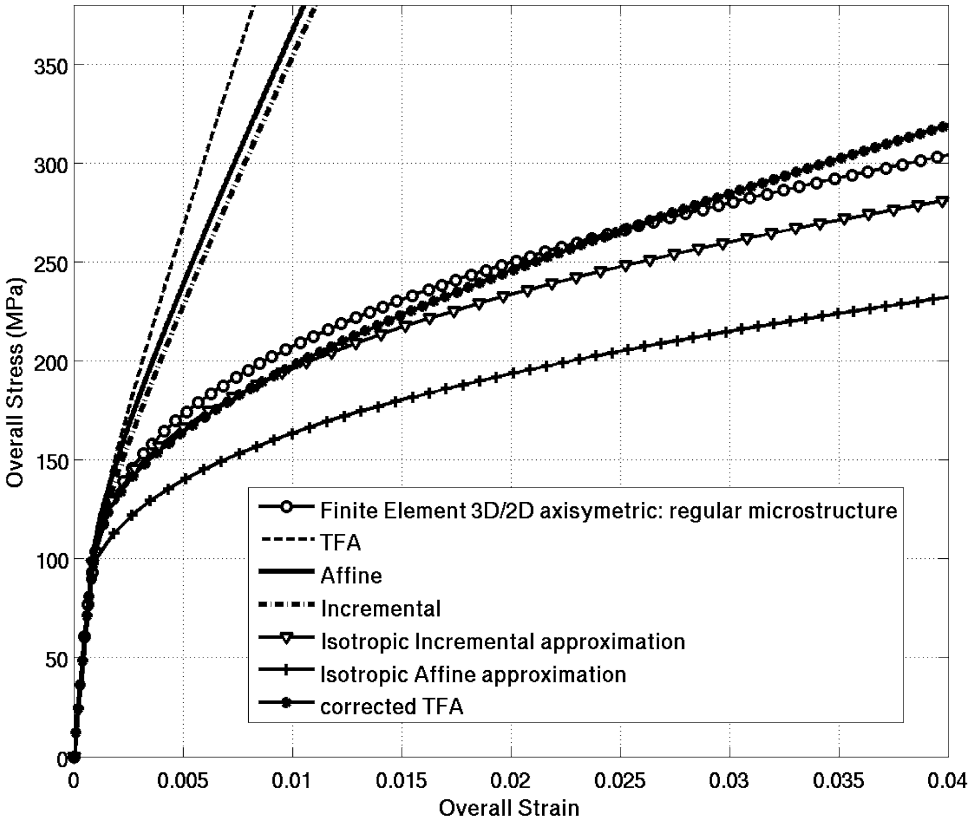

Fig. 5 Comparison between the reference FE solution and various mean field methods. Case of a power law matrix composite

are subsequently identified with microscopic or macroscopic results, either true experiments or virtual experiments performed through systematic applications of the multiscale method. Such an approach is currently the one used when we define the effective properties of a composite or multiphase material from the knowledge of the corresponding local properties and the phase arrangement;

– *the integrated multiscale procedures*, in which all the complexity of the local microstructure (at least its finest representation) is present during all the analysis of the structural component, without summarising it in some overall constitutive framework. In such cases, at each step of the non-linear boundary value problem, the actual overall response of each material point "asks" for the microscale response, through the localisation/homogenisation process. To some extent, through an averaging scheme, the internal variables in the overall boundary value problem are those of the microscale unit cells used in this integrated multiscale numerical procedure.

In what follows, we summarise a narrow selection of works done along the lines of the so-called sequential procedure. We consider also as a sequential approach the ones in which the macroscopic constitutive model are expressed more or less analytically through the local constitutive equations, provided the scale change method (localisation/homogenisation rule) is taken in its simplest form. Applications of TFA methodologies in Sect. 5.4 appear of this kind, as there are some approximations, eventually some overall correction factors identified from numerical experiments. More sophisticated local representations, like TFA with many sub-domains, the NTFA method, the HFGMC, the use of FFT techniques or multilevel finite elements, are considered as integrated multiscale procedures. They are illustrated in Sect. 6.2.

6.1 Unit Cell Methods

The class of so-called unit cell methods can be classified in the category of sequential multiscale procedures. In these methods, numerical computations involving a detailed representative volume element (RVE) are used to induce macroscopic model.

These approaches have been used by many authors. We can quote the works of Christman et al. [44] who have studied the deformation characteristics of ceramic whisker and particulate reinforced metal matrix composites using unit cell formulations to deliver the overall constitutive response of the composite. Brockenbrough et al. [23] presented in 1991 numerical results on the effects of fibre distribution and fibre cross-section geometry on the deformation of metal-matrix composite reinforced with continuous fibres. Nakamura and Suresh [134] studied the combined effects of thermal residual stresses and fibre packing on deformation of

metal matrix composites using unit cell finite element calculations. Tvergaard [173] uses the same technique to analyse the tensile properties for whiskers-reinforced metal matrix composites. More recently, the works of Van der Sluis [174] lie within this framework.

In the same period a lot of works have been carried out in metal matrix composites to determine the thermally-induced residual stresses at the interface fibre/matrix and to evaluate their influence on the behaviour of this interface debonding capability namely, Böhm [14], Mital et al. [128], Gunawardena [84], Allen et al. [6], Arnold and Wilt [8]. Sorensen and Talreja [160] analyse the influence of the fibre distribution on the initiation of matrix cracks.

More recently, different works have been carried out with more complex unit cells. We can quote for instance Böhm et al. [15] who use a multi-inclusion unit cell approach to study the elastic and elasto-plastic behaviour of metal matrix composites reinforced by randomly oriented short fibres. Comparisons between three-dimensional and two-dimensional multi-particle unit cell models were also performed (Böhm and Han [16]) for particle reinforced metal matrix composites. The recent works of Gonzales et al. [83] lie within this context.

6.2 Macroscopic Constitutive Equations Obtained from Analytical Homogenisation Techniques

Many homogenisation techniques are nowadays available, generating a microscopically based stress-strain relation. Most of this techniques consider only small elastic or elasto-plastic deformations on both micro-macro levels. They provide adequate predictions of the overall behaviour of composites or polycrystalline polymers. They are mainly based on mean-field approaches (see Sect. 4) or on semi-analytical methods (see Sect. 5). The focus here is on purely macroscopic constitutive equations which are inferred from other analytical homogenisation techniques. Such models contain some microscopic features although they are written as purely phenomenological equations at the global scale.

Chaboche et al. [38] proposed a thermo-elastic-visco-plastic constitutive equation for metal matrix composites with short fibres built up from a simplified micromechanical analysis. The paper considers the undamaged state of composite with small strains. Using the Transformation Field Analysis (TFA) developed a few years ago by Dvorak and Benveniste (see Sect. 5.1) a completely macroscopic constitutive model is derived. TFA is a very general manner of writing explicit scale transitions, based on purely elastic interactions between sub volumes of the RVE. Considering an elastic elasto-visco-plastic matrix and an elastic fibre, the yield surface is defined by the Von Mises criterion and the visco-plasticity by the normality rule and a power law:

$$f_r = \|\boldsymbol{\sigma}_r - \mathbf{X}_r\| - \sigma_y, \qquad \|\mathbf{a}\| = \left(\frac{3}{2}\mathbf{a} : \mathbf{I}^d : \mathbf{a}\right)^{1/2}, \tag{94}$$

$$\dot{\boldsymbol{\varepsilon}}_r^p = \left\langle \frac{f_r}{K} \right\rangle^n \frac{\partial f_r}{\partial \boldsymbol{\sigma}_r}. \tag{95}$$

Moreover, a multi-kinematic non linear hardening rule is considered:

$$\mathbf{X}_r = \sum_q \mathbf{X}_r^q, \qquad \dot{\mathbf{X}}_r^q = \mathbf{C}^q : \dot{\boldsymbol{\varepsilon}}_r^p - \boldsymbol{\Gamma}^q : \mathbf{X}_r^q \|\dot{\boldsymbol{\varepsilon}}_r^p\|, \tag{96}$$

σ_y, n, K are material coefficients, possibly depending on temperature. $\mathbf{C}^q$ and $\boldsymbol{\Gamma}^q, q = 1, 2$, etc., are hardening and dynamic recovery tensors. The macroscopic constitutive equation set is derived by substituting the local stress of the matrix in its local plasticity criteria by its expression given by the TFA localisation rule. The formulation obtained leads to a well established model in the thermodynamic framework. The model has been used to simulate the visco-plastic response of a short fibre SIC/Al composite. The fairly good correlation with numerical results, obtained with the periodic homogenisation method, has led to apply this formulation in the analysis of structural components.

Later on, Pottier [148] has used the same methodology for long fibre composites and has introduced an anisotropic macroscopic damage. To have a damage directly at the heterogeneities scale, Carrère et al. ([34, 36]) proposed an extended formulation. To that end the extension of TFA proposed by Chaboche et al. [34] is used to take into account the non-linearities due to changing elastic local behaviour (temperature or damage induced). Let us consider the following localisation rule:

$$\boldsymbol{\varepsilon}_r = \mathbf{A}_r : \boldsymbol{\Sigma} + \sum_s \mathbf{D}_{rs} : \mathbf{L}_s : \boldsymbol{\varepsilon}_s^{GE} \tag{97}$$

with $\boldsymbol{\varepsilon}_r^{GE} = (\boldsymbol{\varepsilon}_r^{th} + \boldsymbol{\varepsilon}_r^p + \boldsymbol{\varepsilon}_r^d)$ (see Sect. 5.1).

This leads to a system linking $\boldsymbol{\sigma}$ and $\boldsymbol{\varepsilon}$. By regrouping the terms in $\boldsymbol{\sigma}$, we obtain a simple matrix system:

$$\begin{aligned} &\boldsymbol{\sigma}_r = \bar{\mathbf{B}}_r : \boldsymbol{\Sigma} - \bar{\mathbf{A}}_r (T - T_0) - \sum_k \bar{\mathbf{H}}_{kr} : \boldsymbol{\varepsilon}_k^p \\ &\text{with } \bar{\mathbf{B}}_r = \{\mathbf{K}^{-1}\mathbf{B}\}_r, \bar{\mathbf{A}}_r = \{\mathbf{K}^{-1}\mathbf{A}\}_r, \bar{\mathbf{H}}_{kr} = \{\mathbf{K}^{-1}\mathbf{H}_k\}_r. \end{aligned} \tag{98}$$

$\mathbf{K}$ is a square matrix (2×2), $\mathbf{B}$, $\mathbf{A}$, and $\mathbf{H}_r$ are (1×2) matrices. Each term of these matrices is a fourth order tensor depending on the spatial distribution of the inclusions and on the elastic properties of the fibres and the matrix.

Finally, the macroscopic constitutive equations are written as follows:

$$\begin{cases} \boldsymbol{\Sigma} = \tilde{\mathbf{L}}(T, D) : (\mathbf{E} - \mathbf{E}^p - \mathbf{E}^{th}), \\ \mathbf{E}^p = \sum_r \left\{ c_r \mathbf{B}_r^T : \boldsymbol{\varepsilon}_r^p - c_r \mathbf{B}_r^T : \Delta\mathbf{S}_r : \sum_k \bar{\mathbf{H}}_{kr} : \boldsymbol{\varepsilon}_k^p \right\}, \\ \tilde{\boldsymbol{\alpha}} = \sum_r \{c_r \mathbf{B}_r^T : \boldsymbol{\alpha}_r\} - \sum_r \{c_r \mathbf{B}_r^T : \Delta\mathbf{S}_r : \bar{\mathbf{A}}_r\} \end{cases} \tag{99}$$

with $\tilde{\mathbf{L}}(T, D) = (\mathbf{S}_0 + \Delta\tilde{\mathbf{S}})^{-1}$ where $\mathbf{S}_0$ is the initial macroscopic compliance tensor, and $\Delta\tilde{\mathbf{S}}$ the modification of compliance by temperature T and damage D. The $\boldsymbol{\alpha}_r$ and $\tilde{\boldsymbol{\alpha}}$ are respectively the thermal expansion tensor of the phase and the macroscopic one.

Among the existing models, we can also quote the works of Voyiadjis and Kattan [176] and Kattan and Voyiadjis [100] who use micromechanical considerations to correlate overall and local damage effect of fibre reinforced composite materials. An overall fourth-rank damage effect tensor is introduced using the assumption of elastic energy equivalence to account for the overall damage of the composite system. In addition, two local fourth-rank damage effect tensors are also considered to convey the damage effects in the composite phases. Both scales are correlated together using analytical scale transitions. The effective stress concept is then used to describe the evolution of the internal parameters.

In the context of granular materials, this type of approaches has usually been used. Some examples of recent studies are given in references ([32, 41, 104, 121]).

7 Multiscale Computational Techniques

Finite element analysis of simple heterogeneous periodic or quasi-periodic materials is nowadays a routine exercise that can be easily handled at the level of the representative volume element (RVE). In the last few years, in the context of structural inelastic analysis, a variety of direct micro-macro methods has been developed. These approaches estimate the relevant stress-strain relationship at a macroscopic point by performing separate calculations on the RVE, assigned to that macroscopic point. The analysis on the RVE is performed using the finite element method, in Smit [158], Smit et al., [159], Feyel [61–65], Miehe et al. [126], Terada and Kikuchi [171], the Voronoï cell method in Ghosh et al. [78] or the fast Fourier transforms in Moulinec and Suquet [132].

Although these methods are computationally expensive, they offer the possibility of computing the macro-structural response of heterogeneous materials with an arbitrary microscopic geometry and constitutive behaviour. The following sections give an overview of the most relevant works from the literature applying this type of procedures.

7.1 Multiscale FE Models

In most of the direct micro-macro methods in literature, the analysis on the RVE, assigned to the macroscopic point, is made by finite elements. The idea of using directly a finite element discretization of the microstructure, linked to the macroscopic scale, using homogenisation rules, was first proposed by Renard et al. [150] in 1987. Its complete generalisation and implementation in a general purpose finite element code was done in 1998 by Feyel, in the context of cyclic visco-plastic and damage analysis of components made in a metal matrix composite. Later on numerous authors will use it.

Terada and Kikuchi [171] generalized the two-scale modelling scheme for the analysis of heterogeneous media with fine periodic microstructures by using variational statements. By means of the generalized variational principle of Hu-Washizu [98] applied in the framework of non-linear elasticity, they have shown that the global-local type computational schemes can be unified in association with the homogenisation procedure for general non-linear problems.

The two-scale derived variational problem is then solved using the Newton-Raphson iterative scheme. In spite of the successful computations for a heterogeneous elasto-plastic body, the numerical analysis leads to underlying difficulties in performing general class of non-linear multiscale analyses. One of these is that, since the microscopic problems are solved at each Gauss point of the FE mesh of the overall structure, the deformation histories at time t_n must be stored until the equilibrium state at current time t_{n+1} is obtained. The non-linearities require large computational resources in practical applications.

Miehe et al. [127] present a theoretical and computational framework for the treatment of a homogenised macro-continuum with locally attached microstructure. The proposed concept is applied to the simulation of texture evolution in polycrystalline metals, where the micro-structure consists of a representative assembly of single crystal grains. The deformation of this micro-structure is then coupled with the local deformation at a typical material point of the macro-continuum. In a process driven by the deformation of the macro-continuum, this coupling can be defined by three alternative constraints of the micro-structure deformation: zero fluctuation in the domain (Taylor-type assumption); zero fluctuation on the boundary; or periodic fluctuations on the boundary. These boundary conditions induce, in combination with a given constitutive model for the materials constituents, a static equilibrium state of the microstructure at a certain stage of the deformation process.

The macroscopic extensive variables such as stresses and dissipation are then defined as volume averages of their microscopic counterparts defined by the equilibrium state of the micro-structure. In the proposed procedure, these averages are evaluated in a straightforward manner. This covers the set-up and the solution of two locally coupled boundary value problems for the finite deformations of the micro-continuum and the pointwise associated micro-structure, respectively.

In the same period, a general method called FE^2 was introduced by Feyel [61–65], which consists in describing the behaviour of heterogeneous structures by using a multiscale finite element model. To each integration point at the macroscopic scale a representative volume element is assigned and

a separate finite element computation is performed simultaneously. This procedure does not require to specify the macroscopic constitutive behaviour which is deduced from the non-linearities in the behaviour of the associated microstructure. Once the relevant mechanical scales are chosen, the model is built up using three main ingredients:

1) A modelling of the mechanical behaviour at the lower scale (the RVE)
2) A localisation rule which determines the local solutions inside the unit cell, for any given overall strain
3) A homogenisation rule giving the macroscopic stress tensor, knowing the micromechanical stress state.

In principle any localization/homogenisation rule can be used for points 1–3, but the most common method is the periodic homogenisation of Sect. 3, which is considered here. Two F.E. meshes are needed: one for the cell of periodicity and the other one for the macroscopic structure. The computation is carried out simultaneously on both scales.

In the cell of periodicity located in each Gauss point of the macroscopic structure the method allows to compute the stress tensor at time t, knowing the strain and strain rate at that time and the mechanical history since the beginning on. In classical phenomenological models at macroscopic scale the mechanical history is taken into account through a set of internal variables. Here the internal variable set is constructed by assembling all microscopic data required by the FE computation at lower level. This includes of course microscopic internal variables needed to describe dissipative phenomena.

The local analysis yields the macroscopic (average) stresses and strains, defined as

$$\begin{aligned} \mathbf{\Sigma}_{ij} &= \bar{\boldsymbol{\sigma}}_{ij} = \frac{1}{V}\int_V \boldsymbol{\sigma}_{ij} dV, \\ E_{ij} &= \bar{e}_{ij} = \frac{1}{V}\int_V e_{ij} dV \end{aligned} \tag{100}$$

also known as Bishop-Hill relations [12].

The integrated approach can be easily implemented in classical finite element codes, based upon a Newton-Raphson algorithm to handle all non-linearities. It consists in fact of a sequence of Newton algorithms at global and local level.

For its optimum performances, the tangent stiffness matrix at macroscopic level has to be computed. For this calculation we need the macroscopic (algorithmic) tangent matrix in the Gauss points which can be computed from the variation of the average strains and stresses of (100) as

$$\mathbf{D}^{macro} = \frac{\boldsymbol{\delta}\Delta\mathbf{\Sigma}}{\boldsymbol{\delta}\Delta\mathbf{E}} \tag{101}$$

where Δ denotes the increment of the quantity between time t and time $t + \Delta t$. This computation depends of course on the homogenisation theory used, and on its finite element implementation.

In the case of the periodic homogenisation theory it is convenient to add at local level (mesh of the cell of periodicity) some degrees of freedom to the elements corresponding to average or macroscopic strain $\mathbf{E}$. It is recalled that at local level the unknown displacements are the periodic part $\mathbf{u}^1$ of the total displacement $\mathbf{u}$ on the cell. $\mathbf{u}^1$ is obtained through (54) and (39). These, together with the first of (100) are contained in the condensation procedure outlined below, proposed in [62].

The deformation tensor is computed by (34) and may be written as

$$\underset{\sim}{\mathbf{e}}^0(x, y) = \underset{\sim}{\mathbf{e}}_{(x)}(\mathbf{u}^0) + \underset{\sim}{\mathbf{e}}_{(y)}(\mathbf{u}^1) = \underset{\sim}{\mathbf{E}} + \underset{\sim}{\mathbf{e}}_{(y)}(\mathbf{u}^1). \tag{102}$$

The $\mathbf{B}$ matrix needed in this case, called $\hat{\mathbf{B}}$, is similar to the usual one, except that a new part comes from degrees of freedom associated with $\mathbf{E}$ (these degrees of freedom are put at the end of the whole degrees of freedom list)

$$\hat{\mathbf{B}} = (\mathbf{B}\ \mathbf{1}), \tag{103}$$

where $\mathbf{B}$ denotes as usual the standard symmetric gradient of the shape functions. According to our choice, $\mathbf{E}$ has associated degrees of freedom and hence the associated reactions give the mean stress $\mathbf{\Sigma}$, to be multiplied by the volume of the cell.

The assembled tangent stiffness matrix at the cell scale can be written as

$$\mathbf{K} = \int_{cell} \hat{\mathbf{B}}^T \mathbf{D} \hat{\mathbf{B}} d\Omega. \tag{104}$$

Taking into account (103) leads to

$$\mathbf{K} = \int_{\Omega_e} \begin{bmatrix} \mathbf{B}^T\mathbf{D}\mathbf{B} & \mathbf{B}^T\mathbf{D} \\ \mathbf{D}\mathbf{B} & \mathbf{D} \end{bmatrix} d\Omega = \begin{bmatrix} \mathbf{k} & \mathbf{G}^T \\ \mathbf{G} & \mathbf{H} \end{bmatrix}, \tag{105}$$

where $\mathbf{D}$ represents the tangent matrix given by all microscopic phenomenological constitutive equations.

Recalling the meaning of the additional d.o.f. and the associated reactions, the macroscopic tangent matrix $\mathbf{D}^{macro}$ is then nothing but a condensation of the previous matrix onto the degrees of freedom associated to $\mathbf{E}$ (at most 6 degrees of freedom shared across the whole microscopic mesh) inserted at the end of the list. That is

$$\mathbf{D}^{macro} = \frac{1}{volume}(\mathbf{H} - \mathbf{G}\mathbf{k}^{-1}\mathbf{G}^T), \tag{106}$$

$$\begin{aligned} \mathbf{k} &= \int_{cell} \mathbf{B}^{\mathbf{T}}\mathbf{D}\mathbf{B} d\Omega, \qquad \mathbf{G} = \int_{cell} \mathbf{D}\mathbf{B} d\Omega, \\ \mathbf{H} &= \int_{cell} \mathbf{D} d\Omega. \end{aligned} \tag{107}$$

This condensed matrix is then very easy to compute. Then, depending on the complexity of the macroscopic structure,

this model may lead to large computations. Parallel computing is proposed to overcome this difficulty and has been applied to the analysis of a reinforced "bling" (bladed ring), by Feyel and Chaboche [62].

The method has been used in generalised continua [64] to treat the cases for which the classical periodic media theory cannot be applied, for instance where the size of the RVE is not very small compared to the size of the structure itself and also compared to the size of the mechanical gradients. However, the present FE^2 framework does not treat specifically edge effects and may not deliver good solutions near edges.

A similar multi-level finite element modelling has been developed by Smit [158], Smit et al. [159] and applied more recently in the large strain context. The method has also been extended to higher-order continua, by Kouznetsova et al. [101].

Another multi scale computational strategy which makes use of the homogenisation theory is proposed by Ladevèze and co-workers [105–107]. In that case the structure is considered as an assembly of substructures and interfaces. The junction between the macro and micro scales takes place only at the interfaces. Namely, in the recent works of Markovic and Ibrahimbegovic [118], a multi-level finite element procedure is applied for modelling the inelastic behaviour of heterogeneous materials. In the paper strongly coupled scales are considered, where the finite element method is used at both scales. Yet, the micro-scale is not infinitively smaller than the macro scale. The coupling of the scales is obtained trough the framework of localised Lagrangian multipliers. The macro mesh plays the role of a frame which is connected to the micro mesh through the Lagrangian multipliers.

The works of Fish [66] may also be classified in this category of models. The multiscale computational procedure proposed by Fish is a superposition based method. A hierarchical decomposition of the solution space u is made into global u^G and local u^L effects, $u = u^L + u^G$. Enforcement of solution compatibility is obtained by prescribing homogeneous boundary conditions on u^L at the global interface Γ_{GL}. A multilevel solution scheme, termed as the s-version of the finite element method has then been developed where each level is discretized using a finite element mesh of arbitrary element size and polynomial order. Selection of the interface Γ_{GL} is one of the critical issues in this superposition based method. A mathematical analysis aimed at quantifying pollution effects on localized phenomena on the global structural behaviour and identifying the optimal location of the interface has also been carried out by Babuska [9] and Fish [67].

7.2 The Voronoï Cell Method

One of the first simultaneous global-local computational procedures has been carried out by Ghosh and co-workers [78] with the *Voronoï cell finite element method* (VCFEM). In this method, the finite element mesh evolves naturally by Dirichlet Tessellation of a representative structure. This is a process of subdivision of space, determined by set of points, in such a way that each point has associated with it a region that is closer to it than to any other. The subdivided regions are called Voronoi cells. The cells may be identified with basic structural elements in a heterogeneous microstructure. They represent regions of immediate influence for each heterogeneity and also define neighbour regions by the cell facets. The germinating points are then replaced by heterogeneities with shape, size and orientation. The discretization should account for these features and avoid intersection of the Voronoï cell edges with the heterogeneities.

A mesh generator accounting for arbitrariness in shape, size and spatial distribution of inclusions has also been introduced by Ghosh and Mulkopadhyay [77]. Tessellation of a microstructural representative material element discretizes the domain into a network of multi-sided convex 'Voronoi' polygons or cells. Each Voronoï cell contains at most one second phase inclusion.

Formulations have been developed to directly treat multiple phase polygons as elements in a finite element model by Ghosh and Mulkhopadhyay [77] for linear elasticity and by Ghosh and Liu [75] for micro-polar thermo-elasticity and for elastic-plastic problems in Moorthy at al. [130] and Gosh and Moorthy [76]. Several applications of the method to account for non-linear composite materials have been presented in recent papers. The main drawback of this method is its time and memory consuming.

7.3 Models Based on Fast Fourier Transform

Walker et al. [179] used in 1994 the periodic microstructure assumption together with Fourier series approximation to analyse the non-linear visco-plastic behaviour of fibrous composites. The unit cell is discretized into triangular subvolumes. In each step of the loading history the total strain at any point is governed by an integral equation. The strain and stress fields within the repeating unit cell are obtained using Fourier series approximations. The non-linearity arising from the visco-plastic behaviour of the material constituents is treated as a fictitious body force in the governing integral. The authors have also shown that the problem can be written using Green's function approaches, a more general method because it doesn't need the periodic assumption, and for which the numerical resolution converges more rapidly.

Fotiu and Nemat-Nasser [72] have also used Fourier series approximation to estimate the overall properties of

elasto-visco-plastic periodic composites in the context of the periodic distribution of inclusions assumption. The formulation is presented in three dimensions as well as for plane-stress and plane-strain problems. The two methods have the particularity to employ quite accurate field representation within the repeating cell but can be computational time consuming

To avoid the difficulty due to meshing in case of complex microstructure, when solving the local problem by FEM methods, and to make direct use of microstructure images of heterogeneous materials, Moulinec and Suquet [132] proposed in 1998 an alternative method based on Fast Fourier Transforms. FFT algorithms require data sampled in a grid of regular spacing, allowing the direct use of digital images of the microstructure. A specificity of the formulation is the use of an iterative method not requiring the formation of a stiffness matrix. Introducing an homogeneous reference material with elastic stiffness $\mathbf{c}^0$, they have shown that the local problem to be solved on a typical volume element can be re-written as an implicit integral equation (the so-called Lippman-Schwinger equation). It takes the form:

$$\boldsymbol{\varepsilon}(\mathbf{u}(\mathbf{x})) = -\boldsymbol{\Gamma}^0 * (\mathbf{c}(\mathbf{x}) - \mathbf{c}^0) : \boldsymbol{\varepsilon}(\mathbf{u}(\mathbf{x})) + \mathbf{E}, \tag{108}$$

where $\boldsymbol{\varepsilon}$ and $\mathbf{E}$ are respectively the local and the overall strain tensors. This expression becomes in the Fourier space:

$$\begin{aligned} &\hat{\boldsymbol{\varepsilon}}(u)(\xi) = -\hat{\boldsymbol{\Gamma}}^0(\xi) : (\mathbf{c}(\mathbf{x}) - \mathbf{c}^0) : \boldsymbol{\varepsilon}(u)(\xi), \quad \forall \xi \neq 0, \\ &\hat{\boldsymbol{\varepsilon}}(0) = \mathbf{E}, \end{aligned} \tag{109}$$

where $*$ denotes the convolution product and where $\boldsymbol{\Gamma}^0$ is the Green operator associated with $\mathbf{c}^0$ which is explicitly known in Fourier space. An iterative scheme is then derived from the previous equation:

$$\boldsymbol{\varepsilon}(\mathbf{u}^{i+1}) = -\boldsymbol{\Gamma}^0 * ((\mathbf{c} - \mathbf{c}^0) : \boldsymbol{\varepsilon}(\mathbf{u}^i)) + \mathbf{E}. \tag{110}$$

Noting that a convolution product in real space becomes a mere product in Fourier space:

$$\begin{aligned} &\hat{\boldsymbol{\varepsilon}}^{i+1}(\xi) = \hat{\boldsymbol{\varepsilon}}^i(\xi) - \hat{\boldsymbol{\Gamma}}^0(\xi) : (\hat{\mathbf{c}} : \hat{\boldsymbol{\varepsilon}}^i)(\xi), \quad \forall \xi \neq 0, \\ &\hat{\boldsymbol{\varepsilon}}^{i+1}(0) = \mathbf{E}. \end{aligned} \tag{111}$$

This method requires a number of iterations roughly proportional to the contrast between the mechanical properties of the phases and thus is inadequate for highly contrasted or infinitely contrasted composites. The advantages of the method are the following:

- Images of microstructures can be directly used in the analysis, which avoids meshing the microstructure.
- The iterative procedure does not require the formation or inversion of a stiffness matrix.
- The convergence is fast.

The method present the following limitations:

- The convergence is not ensured for materials containing voids or rigid inclusions.
- The number of degrees of freedom is high in comparison with the FEM. The method can be applied only on computers with high memory capabilities.

To allow the application of this method for contrasted materials, Eyre and Milton [59] improved the procedure by introducing an accelerated scheme. The rate of convergence obtained is then proportional to the square root of the contrast but still cannot be applied to composites with infinite contrast (like porous materials). An alternative scheme based on augmented Lagrangians and Fourier Transforms has later been proposed in the paper of Michel et al. [125] for highly contrasted or even infinitely contrasted materials. These direct micro-macro methods have essentially been developed and applied in the small strain format.

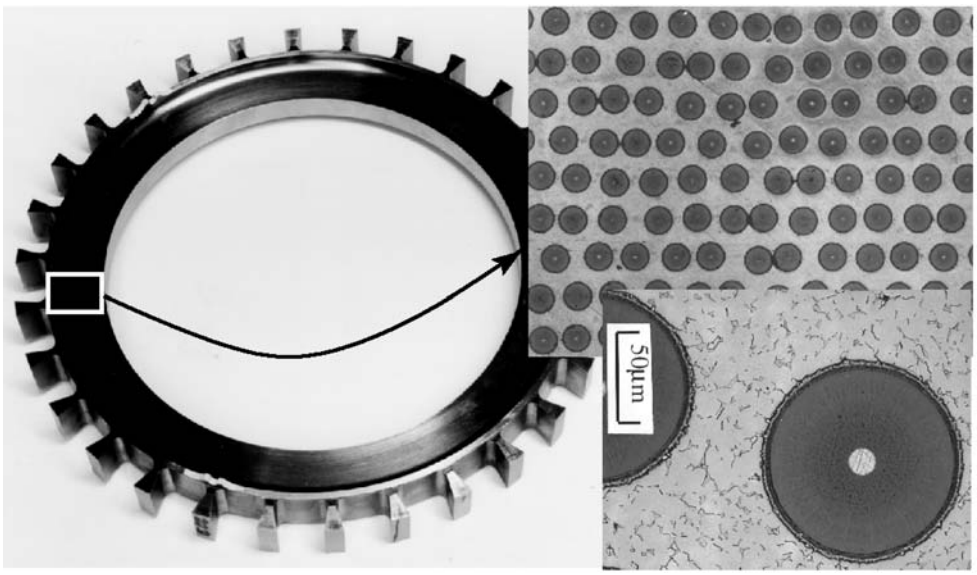

Fig. 6 The principle of the bladed ring with a SiC-Ti composite insert, as considered for future engine design

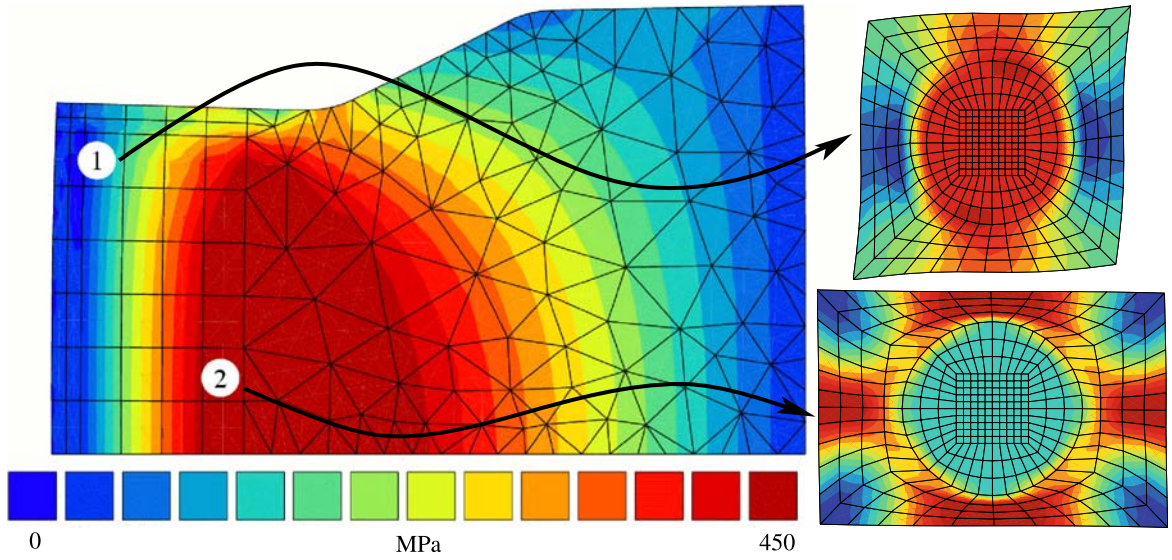

Fig. 7 Results obtained at the two scales at the maximum rotation speed. The constitutive equation of the matrix is a classical elasto-visco-plastic model with two back-stresses. *Left*: radial stress at the macroscale; *right*: radial strain in two local cells (the amplification factor for displacements is 10)

7.4 Example 1: FE^2 Method Applied to a SiC/Ti Composite Bling Component

This example illustrates the application of the so-called FE^2 version of the multilevel finite element procedures (Feyel [60]), in a non-linear incremental plasticity context. The method is a totally integrated one, as implemented in a general purpose finite element code (ZéBuLoN, the finite element solver of Z-Set platform^{TM}).

The lower level FE scale is solved as a periodic boundary value problem, in which the average strain increment is given by the overall FE solver, exactly as for any other macroscopic constitutive equation in the code. After solving the lower scale, the average stress increment, as well as the consistent tangent matrix (algorithmic), are returned to the overall problem. The tangent matrix is obtained by the condensation procedure detailed in Sect. 7.1 ((104) to (107)).

The model component is a simplified version of a "bling" (or "bladed ring"), currently considered for possible replacement of compressor or turbine discs in aeronautical turbo-engines. The component, considered here as axisymmetric, is made of a Titanium alloy (Fig. 6). It contains a circumferentially reinforced part made in a SiC/Titanium composite (long fibres, circumferential, large diameter, 100 to 140 µm, Fig. 6b). The Titanium matrix inside the composite part is assumed the same as in the homogeneous part. The boundary $r = R_{int}$ on the left is free, though the one at $z = 0$ takes into account a symmetry condition.

At each Gauss point of the overall FE mesh and at each iteration of the overall implicit incremental analysis of the component, the localisation/homogenisation procedure is made through an associated FE unit cell (mesh shown on Fig. 7a). It delivers the local current inelastic response, using the elasto-visco-plastic constitutive equations of the Titanium matrix inside the composite (the fibre is considered as elastic).

After the analysis, the available results are both macroscopic stress and strain fields (Fig. 7a) and local fields at every unit cell, as shown on Fig. 7b for two typical points in the composite part, including a point where shearing effects were predominant.

Still in the context of the bling component analysis, this FE^2 method has been extended further (Carrère [33]) by using for the Titanium matrix inelastic constitutive equation a scale change based on a self-consistent methodology (the "beta rule" mentioned in Sect. 4.4). The polycrystalline matrix is described using 48 grain orientations, crystal visco-plasticity in each grain, with basal, prismatic and pyramidal slip systems, as well as twinning pseudo-slip. The method, called FE$^{2.5}$, was useful to determine the impact of various possible textures in the polycrystalline matrix on the overall response of the component.

7.5 Example 2: Application of the Asymptotic Theory of Homogenisation to a Nonlinear Problem with Three Scales

If applied iteratively, asymptotic theory of homogenization may also be used for non-linear situations. Furthermore, it can obviously be used to bridge several scales. Here the example deals with the thermo-mechanical analysis of a Nb_3Sn based strand used to wind the superconducting coils

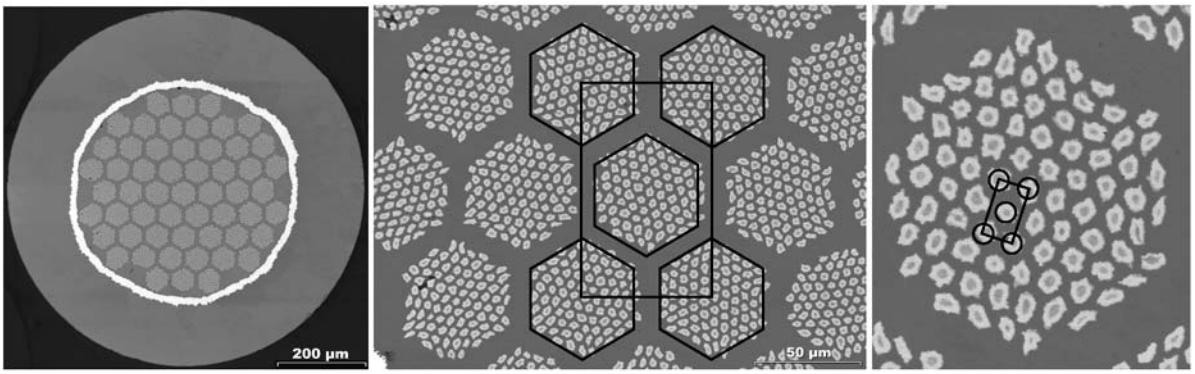

Fig. 8 Three level hierarchy in the strand made by European Advanced Superconductors Co. The central part of the strand (*left*) consists of 55 groups of 85 filaments (about 4 micrometers diameter), embedded in tin rich bronze matrix, while the outer region is made of high conductivity copper. The strand diameter is 0.81 mm. Images: courtesy of P.J. Lee, University of Wisconsin-Madison Applied Superconductivity Center

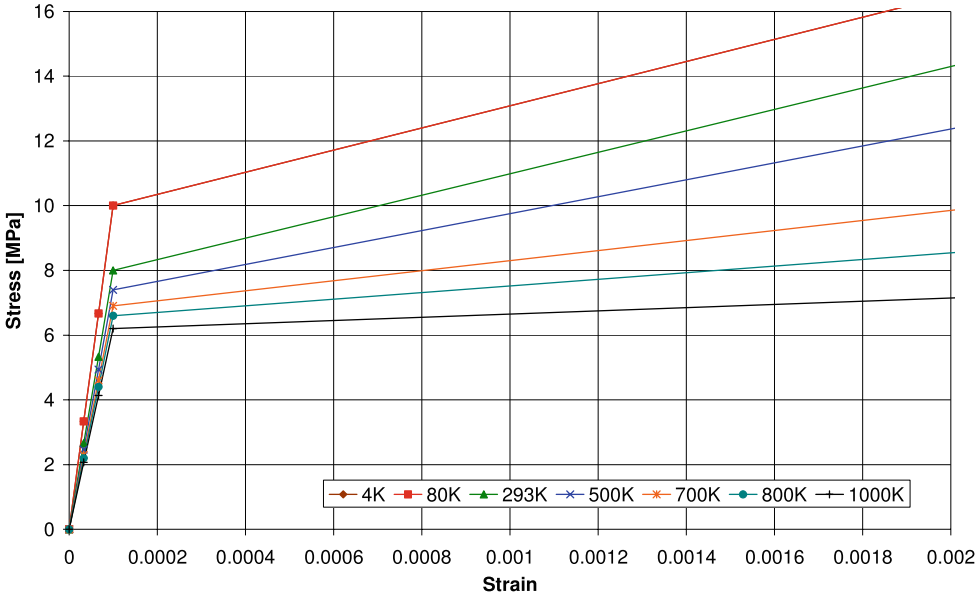

Fig. 9 Copper stress-strain curve for some reference temperatures. Piecewise linear behaviour is assumed

of the next thermo-nuclear experimental reactor (ITER). In the strand (Fig. 8) a three-level hierarchy can be identified [18, 19]. Asymptotic theory of homogenisation is adopted for the non linear situation and the three scales are bridged by applying it in concurrent manner. The example shows the cool down of the strand from Nb_3Sn reaction temperature (923 K) to the coil working condition (4 K).

We have to deal with non-linear, temperature-dependent material characteristics. In the cross section of the strand (Fig. 8) we can distinguish two main areas: an external ring made of Oxygen-Free Electronic (OFE) copper separated by a thin tantalum barrier from an internal circle composed of periodically repeated hexagonal cells in a tin rich bronze matrix. Each of the hexagons is constructed by the repetition of another unit cell: the cross section of a single superconducting Nb_3Sn filament embedded in a bronze matrix. We assume that the strand components are in equilibrium at 923 K without eigenstresses or strains, which are relaxed since the strand remains for several hours at high temperature where Nb_3Sn is formed. Strains develop during the cool down to 4 K because of the different thermal contraction coefficients of Nb_3Sn, bronze, tantalum and copper. Material characteristics are not easy to find over the whole temperature range needed, for Nb_3Sn it is even more difficult owing to the complexity of the experimental tests. Most of the values used are taken from the conductor database [46]. The Nb_3Sn intermetallic has a low thermal contraction but a relatively high elastic modulus and a very high yield strength, so that it remains in its elastic state all over the cooling treatment. Bronze, tantalum and copper are elasto-plastic materials, copper and bronze having a quite low yielding limit, therefore they are plastically flowing for most of the process. Copper and bronze stress-strain behaviour for some reference

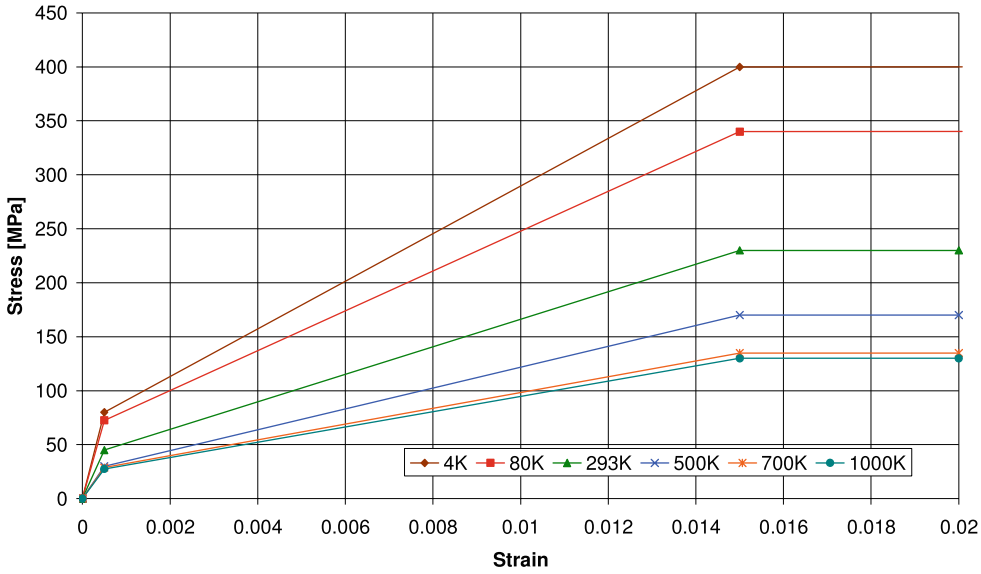

Fig. 10 Bronze stress-strain curve for some reference temperatures. Piecewise linear behaviour is assumed

temperatures is presented in Fig. 9 and Fig. 10 respectively.

Because of the assumed behaviour of material properties we deal with a sequence of problems of linear elasticity written for a non-homogeneous material domain and with coefficients that are functions of both temperature and stress level. At meso (filament hexagonal group) and micro level (single filament) we must make sure that the yield conditions of the single component materials are not violated. This is carried out by an elastic-plastic analysis of the cells of periodicity. If yielding occurs the cell of periodicity will be modified and new, effective properties calculated for the next step.

The usual procedure starts with the composite cell of periodicity with given elastic components. As the strain increases step by step, effective material coefficients are constant until the stress reaches the yield surface at some points of the cell. The yield surface in the space of stresses is different for each material component, being thus a function of position. The region, where the material yields, is of finite volume at the end of the step, thus it is easy to replace the material with the yielded one, with the elastic modulus equal to the hardening modulus of the elastic-plastic material and with the Poisson ratio tending to 0.5.

The cell of periodicity is hence transformed into another one with one more material and the usual analysis procedure is restarted again with a uniform strain, a new homogenization function and a new stress map over the cell. We identify each new region where further local yielding occurs, then redefine the cell and perform the analysis. The loop is repeated as many times as needed. Also the recovery procedure of stress and heat flux have to be applied at each level taking into account the temperature dependence of the material characteristics [18]. The algorithm is summarized in Box 1.

It is to note, that for solving "the kinematical problem" mentioned in points 6 and 8 of Box 1, it is not always necessary to use the true finite element solution. If the cell of periodicity has not been changed before, this solution can be composed according to (39), (40) suitably rewritten.

The analysed structure and the three scales are shown in Fig. 8, where the single filament (micro scale), groups of filaments (meso scale) and the superconducting strand (macro scale) can be seen.

On the meso level we have the repetitive pattern of the superconducting filament in the bronze matrix (micro scale RVE), filling the hexagonal region as illustrated on the right hand side of Fig. 8 and Fig. 11. The second translational structure is the net of the hexagonal filament groups (meso scale RVE) in the body of the single strand shown in the centre of Fig. 8 and Fig. 11. The homogenization splits thus into two steps, each one dealing with rather similar geometry and a comparable scale separation factor.

After the homogenization procedure, the resulting equivalent material has an orthotropic behaviour, depending upon the material characteristics and the geometrical configuration of the unit cell. The main diagonal terms are shown in Fig. 12.

The particular nature of the thermo-elastic-plastic process has allowed the use of a tangent stiffness procedure of Box 1, which avoids costly equilibrium iterations of a Newton-Raphson procedure at macroscopic level. In the adopted procedure the updating of the cell (step 9 of Box 1) is compulsory to avoid to drift away from equilibrium path. The results are remarkably accurate as shown in Fig. 13, where the computed and measured residual strains after the cool down process are compared.

1. Compute effective coefficients at micro level;
2. Compute effective coefficients at meso level;
3. Apply increment of forces and/or temperature at the macro level, solve global homogeneous problem;
4. Compute global strain $E_{ij} : E_{ij} = e_{ij}(\mathbf{u}^0)$ reminding that $E_{ij} = \tilde{e}^{\varepsilon}(\mathbf{x})$ (see (100))
5. Apply E_{ij} to meso level cell by equivalent kinematical loading (displacement on the border);
6. Solve the kinematical problem at the meso level for $\mathbf{w}^1(\mathbf{y})$, compute stress (unsmearing for meso level) and strain E_{ij}; now $E_{ij} = e_{ij}(\mathbf{w}^0)$ and $E_{ij} = \tilde{e}^{\varepsilon}(\mathbf{y})$
7. Apply E_{ij} from meso to micro level cell by equivalent kinematical loading (displacements on the border);
8. Solve the kinematical problem at the micro level for $\mathbf{w}^1(\mathbf{z})$, compute stress (unsmearing for micro level);
9. Verify yielding of the material **in the physically true situation at micro level**. If yes change mechanical parameter of the material and go to 1, else if exit.

Box 1 Three-scale bridging within a tangential stiffness procedure. $\mathbf{w}^1(\mathbf{z})$ of point 8 is the first order term of the displacement expansion $\mathbf{w}$ at micro level

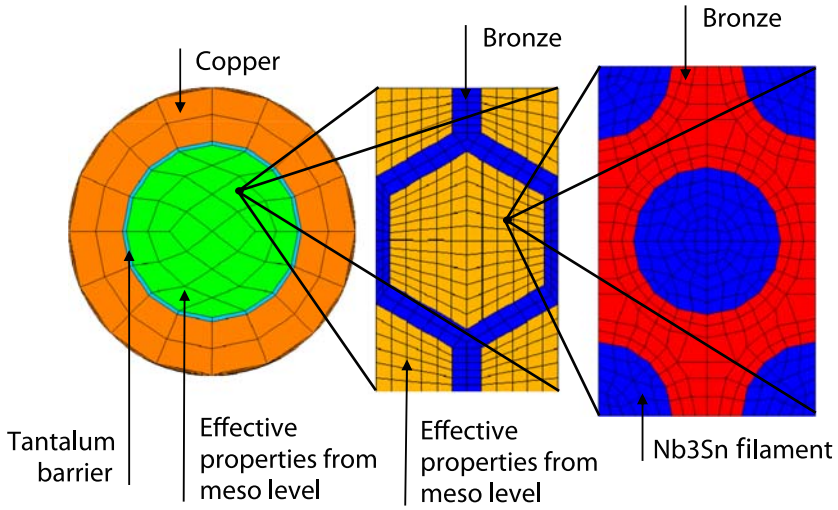

Fig. 11 Finite element mesh of micro- (on the *right*) and meso- (in the *middle*) scale unit cell

7.6 Example 3: Application of a Self Consistent Like Method to a Thermo-Elastic Problem

As mentioned, in the generalised self consistent method the inclusion is encased in a shell of matrix material outside of which the effective medium is considered. In this case the investigation is extended to the coupled thermo-mechanical field, for a composite with linear, temperature dependent material characteristics.

As an example we show the application of the method to a thermo-mechanical problem involving the superconducting strand shown in Fig. 14. Similar to the previous one, it is composed of an outer ring of OFE copper separated by a tantalum barrier from a inner bronze matrix where superconducting filaments are embedded. The strand is here modelled according to the scheme of Fig. 15, where the radii $r = a, b$ are given by the area ratios of the cross section. The material characteristics are the same as in the previous example, but copper and bronze are considered elastic. The goal of this work is to find the values of the effective Young modulus E^{eff}, Poisson ratio v^{eff} and thermal expansion coefficient α^{eff} [19, 20].

We consider a problem of thermo-elasticity defined in a heterogeneous body such as that depicted in Fig. 15 subjected to a variation of temperature. Stress $\boldsymbol{\sigma}$, strain $\boldsymbol{\varepsilon}$ and displacements $\mathbf{u}$ (which are the elements of the solution of the boundary value problem over the heterogeneous domain) are defined piecewise with respect to the radius r as follows (Fig. 15):

$$\mathbf{u} = \begin{cases} \mathbf{u}^a, & r < a, \\ \mathbf{u}^b, & a < r < b, \\ \mathbf{u}^c, & r > b, \end{cases} \qquad \boldsymbol{\varepsilon} = \begin{cases} \boldsymbol{\varepsilon}^a, & r < a, \\ \boldsymbol{\varepsilon}^b, & a < r < b, \\ \boldsymbol{\varepsilon}^c, & r > b, \end{cases}$$
$$\boldsymbol{\sigma} = \begin{cases} \boldsymbol{\sigma}^a, & r < a, \\ \boldsymbol{\sigma}^b, & a < r < b, \\ \boldsymbol{\sigma}^c, & r > b. \end{cases} \tag{112}$$

The problem is defined by the usual equilibrium equations which, referred to a cylindrical system of coordinates (r radial component, θ circumferential component and z longitudinal component) and taking into account the axial sym-

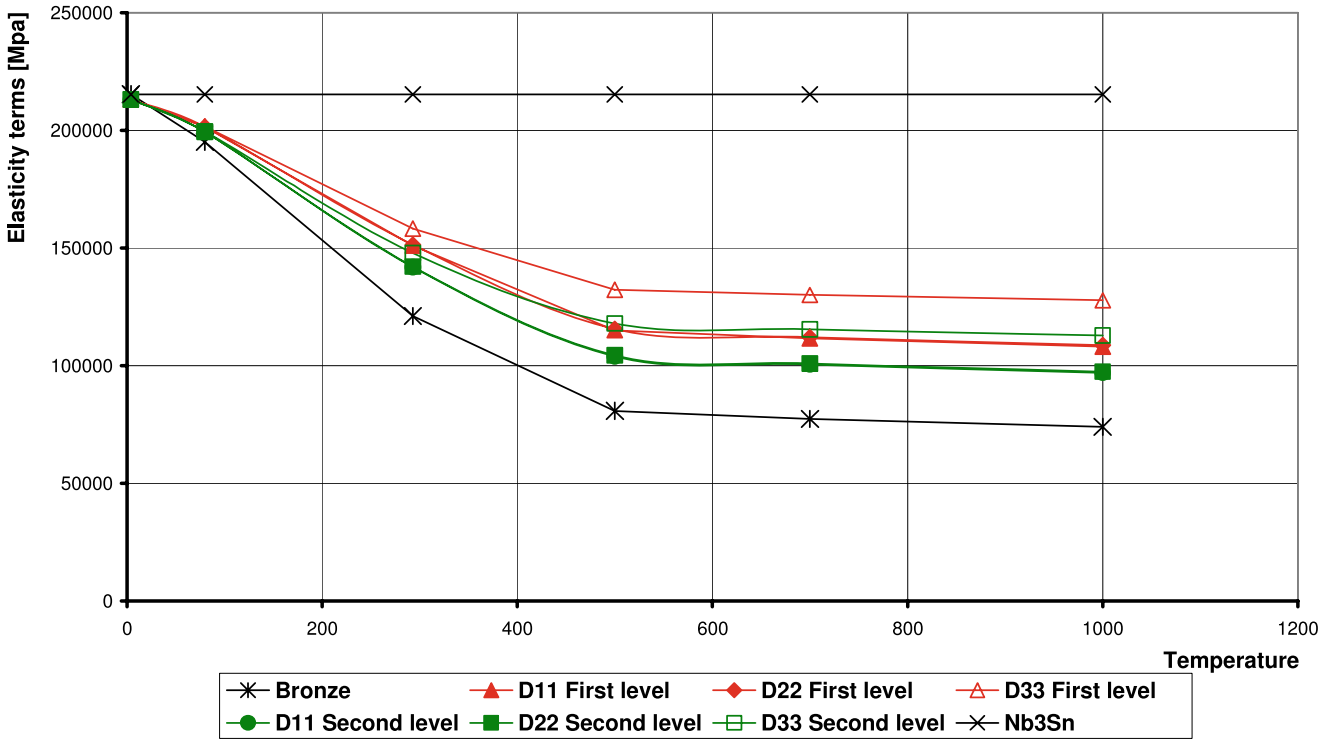

Fig. 12 Main diagonal elasticity terms for bronze (*stars*), Nb3Sn (*crosses*), meso and macro level homogenization results

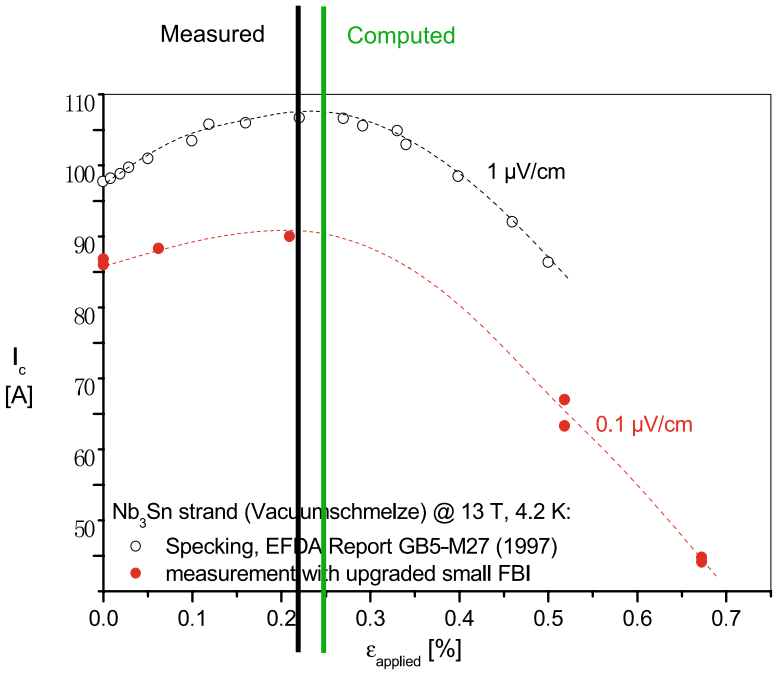

Fig. 13 Validation: measured [180] and computed residual strains in the strand of Fig. 8, after the cool down process from 923 K to 4.2 K

metry of the problem (shear stress component and angular strain component are zero) can be written as

$$\frac{\mathrm{d}\sigma_r^i}{\mathrm{d}r} + \frac{\sigma_r^i - \sigma_\theta^i}{r} = 0, \quad i = a, b, c \tag{113}$$

with the following continuity and boundary conditions

$$\begin{cases} \sigma_r^a = \sigma_r^b & \text{for } r = a, \\ \sigma_r^b = \sigma_r^c & \text{for } r = b, \\ \lim\limits_{r \to +\infty} \sigma_r^c = 0. \end{cases} \tag{114}$$

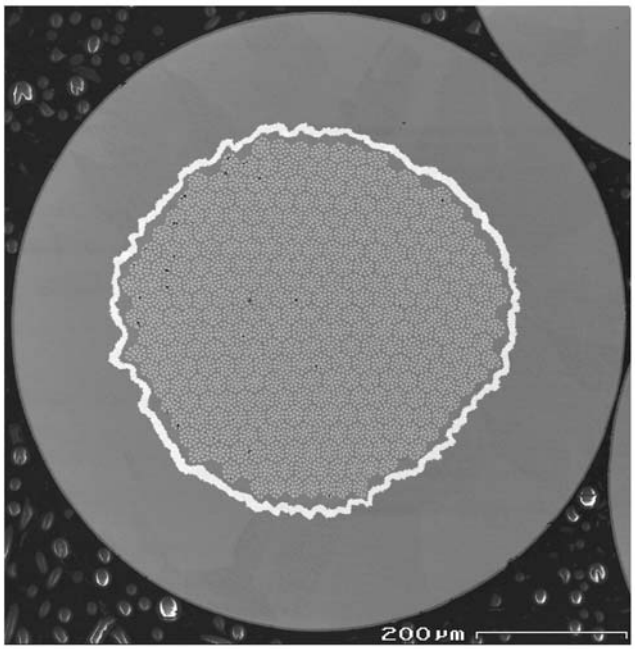

Fig. 14 Strand from Furukawa Co. Courtesy of P. Lee, University of Wisconsin-Madison Applied Superconductivity Center

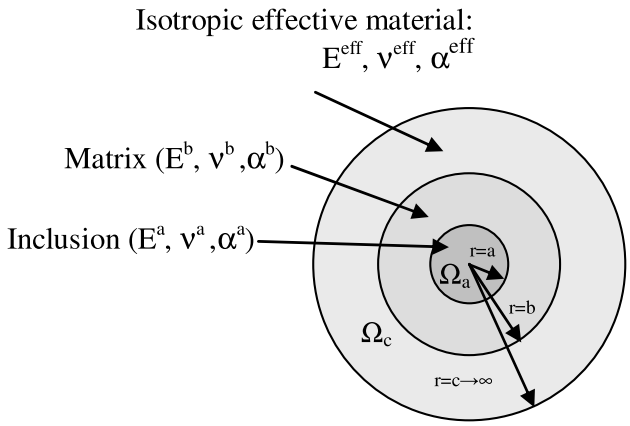

Fig. 15 Domain and sub-domains. In region c the effective material is considered

Finally the kinematical admissibility requires

$$\begin{cases} u_r^a = u_r^b & \text{for } r = a, \\ u_r^b = u_r^c & \text{for } r = b. \end{cases} \tag{115}$$

Taking into account the axial symmetry, the only non zero components are

$$\boldsymbol{\sigma} = \begin{pmatrix} \sigma_r \\ \sigma_\theta \\ \sigma_z \end{pmatrix}, \qquad \boldsymbol{\varepsilon} = \begin{pmatrix} \varepsilon_r \\ \varepsilon_\theta \\ \varepsilon_z \end{pmatrix} \tag{116}$$

related by the following tensor of elasticity

$$C = \frac{E}{(1+\upsilon)(1-2\upsilon)} \begin{pmatrix} 1-\upsilon & \upsilon & \upsilon \\ \upsilon & 1-\upsilon & \upsilon \\ \upsilon & \upsilon & 1-\upsilon \end{pmatrix}. \tag{117}$$

As for the determination of the effective properties, we are looking for an equivalent, homogeneous and isotropic material that can replace the composite at the macro scale. The unknown effective Young modulus E^{eff}, Poisson ratio υ^{eff} and thermal expansion coefficient α^{eff} may vary during the loading process due to the temperature dependency of material characteristics. The equivalent behaviour is described by the displacement, strain and stress fields that verify the equilibrium conditions in the infinite domain filled with the homogeneous material and subjected to the same loading condition as the composite.

Let us consider a field of displacements defined by:

$$\begin{cases} u_r^a = A^a r, \\ u_r^b = A^b r + \dfrac{B^b}{r}, \\ u_r^c = A^c r + \dfrac{B^c}{r}, \end{cases} \quad \begin{cases} u_\theta^a = 0, \\ u_\theta^b = 0, \\ u_\theta^c = 0, \end{cases} \quad \begin{cases} u_z^a = e_z z, \\ u_z^b = e_z z, \\ u_z^c = e_z z, \end{cases} \tag{118}$$

where the value of e_z for the displacement component in z direction is given (we assume that the cross section of the strand remains plane). It is easy to check that the displacement field defined in (118) implies a stress field which verifies the balance conditions inside each sub-domain.

The thermo-elastic problem is solved with MAPLE symbolic code, which gives formal relations for displacement, strain and stress fields in each sub-domain. The five constants of integration A^i and B^i in (118) are defined by the continuity and boundary conditions (114) and kinematical conditions (115). At this point the problem is formally solved: displacement, strain and stress fields are expressed as a function of the known material characteristics $E^a, \nu^a, \alpha^a, E^b, \nu^b, \alpha^b$ and the unknown effective properties $E^{eff}, \nu^{eff}, \alpha^{eff}$.

To obtain the homogenised material characteristics we define the following functionals, expressing (in terms of strain or stress components) the difference between the solution of problem written for the infinite homogenised domain and the solution computed for the composite material

$$\Pi(E^{eff}, \upsilon^{eff}, \alpha^{eff}) = \int_0^\infty ((\varepsilon_r^{eff} - \varepsilon_r)^2 + (\varepsilon_\theta^{eff} - \varepsilon_\theta)^2 + (\varepsilon_z^{eff} - \varepsilon_z)^2) dr, \tag{119}$$

$$\Gamma(E^{eff}, \upsilon^{eff}, \alpha^{eff}) = \int_0^\infty ((\sigma_r^{eff} - \sigma_r)^2 + (\sigma_\theta^{eff} - \sigma_\theta)^2 + (\sigma_z^{eff} - \sigma_z)^2) dr \tag{120}$$

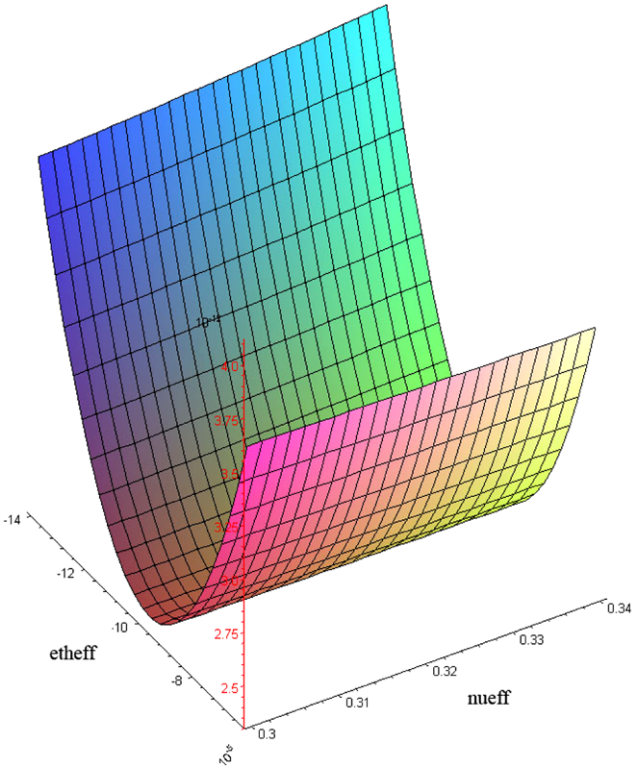

Fig. 16 Functional Π by arbitrarily fixing the value of $E^{eff} = 110$ GPa

These functionals are related to the energy difference between the homogenised and composite solution. In the above equations the dependence of functionals Γ and Π on $E^{eff}, v^{eff}, \alpha^{eff}$ is explicitly marked. It is worth to underline that these characteristics depend upon temperature, so the effective values are computed for a certain number of reference temperatures. By minimizing the two functionals we would get two sets for the values of the effective material characteristics, which could be considered as a sort of bounds. In this way, from the physical point of view, the research of the best material properties for the homogenised body would be performed always over the statically and kinematically admissible fields of stress and strain. However a direct minimization of the two functionals above, with three unknowns, is not straightforward.

On the other hand, by arbitrarily fixing for instance the value of E^{eff} equal to a certain value and plotting the functional Π as a function of v^{eff}, α^{eff}, it appears that it exhibits a minimum (Fig. 16). In an analogous way, by arbitrarily fixing for instance the value of α^{eff} equal to a certain value and plotting the functional Γ as a function of E^{eff}, v^{eff}, it shows again to admit a minimum (Fig. 17). As a consequence the procedure can be automated and speeded up: the triplet $(E^{eff}, v^{eff}, \alpha^{eff})$ can be computed using two 2D Newton-type algorithms, according to the following scheme:

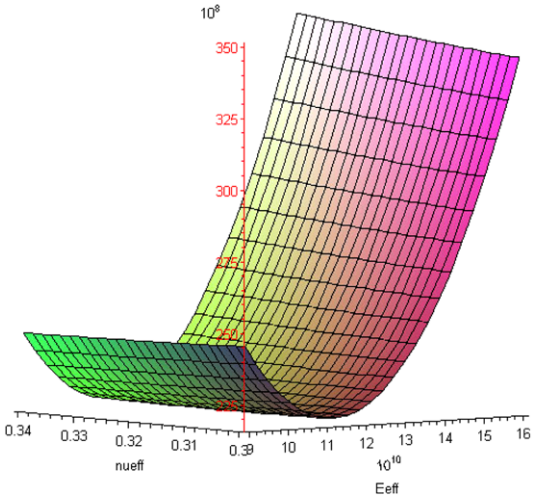

Fig. 17 Functional Γ by arbitrarily fixing the value of $\alpha^{eff} = 0.98\ 10^{-5}\ \mathrm{K}^{-1}$

1. Initialization: $E^{eff} = (E^a + E^b)/2$
   $v^{eff} = (v^a + v^b)/2$
   $\alpha^{eff} = (\alpha^a + \alpha^b)/2$
2. Keeping $(\alpha^{eff})^{\Pi}_{i+1} = (\alpha^{eff})^{\Pi}_{i}$, minimize Γ to get $(E^{eff}, v^{eff})^{\Gamma}_{i+1}$
3. Update: $(E^{eff}, v^{eff})^{\Gamma}_{i} = (E^{eff}, v^{eff})^{\Gamma}_{i+1}$
4. Keeping $(E^{eff})^{\Pi}_{i+1} = (E^{eff})^{\Gamma}_{i+1}$, minimize Π to get $(\alpha^{eff}, v^{eff})^{\Pi}_{i+1}$
5. Update α^{eff} : $(\alpha^{eff})^{\Pi}_{i} = (\alpha^{eff})^{\Pi}_{i+1}$ ignore $(v^{eff})^{\Pi}_{i+1}$
6. Go to 2 with new α^{eff}.

The procedure stops when the difference between two successive values of the set $(E^{eff}, v^{eff})^{\Gamma}$ or of $(\alpha^{eff})^{\Pi}$ is less than a pre-defined tolerance.

8 Recovery Methods After the Component Analysis

Recovery methods after the component analysis have partly already been addresses when presenting the different procedures (Sects. 3.4 and 7) but will be dealt with again here in some detail because of their importance in many situations. An important part of multi-scale modelling is the recovery of stress and heat flux as well as strain, temperature and displacements at the level of the microstructure.

When the size of the microstructure on which we want to recover local stresses is very small (scales well separated), it is sufficient to apply the localisation rule by considering, on the volume occupied by the local unit cell, that the overall macroscopic stress field is uniform. Additional problems arise when the microstructure is quite large compared with the component size and with the wavelength of the macroscopic stress field. The present section summarises and illustrates some techniques that could be used in this context.

8.1 Stress Recovery through Least Square Fit and Projection

A simple procedure for stress recovery which does not depend on the particular way the macroscopic displacement field has been obtained is presented by projection [182]. It is applicable to any kind of solid continuum as long as the displacement field is known with sufficient accuracy. However it finds its natural application in the study of composite materials. It stems from a least square fit [96]

$$\chi = \int_\Omega (\boldsymbol{\sigma} - \boldsymbol{\sigma}^*)^2 d\Omega$$

with smoothing function substituted by $\boldsymbol{\sigma}^* = \mathbf{N}\overline{\boldsymbol{\sigma}}$, (121)

where $\boldsymbol{\sigma}$ denotes the unsmoothed stresses, coming e.g. from a finite element calculation, $\boldsymbol{\sigma}^*$ the stresses obtained by interpolation through shape functions $\mathbf{N}$ from the yet unknown nodal values of the stresses $\overline{\boldsymbol{\sigma}}$, which are sought for. The condition of minimum of χ with respect to $\overline{\boldsymbol{\sigma}}$ yields

$$\int_\Omega \mathbf{N}^T \mathbf{N} \boldsymbol{\sigma}^* d\Omega = \int_\Omega \mathbf{N} \boldsymbol{\sigma} d\Omega. \tag{122}$$

This procedure is called *functional smoothing* and is applicable in general.

In the following we will use a local discrete smoothing, where we limit ourselves to one element or a patch of elements at a time and to stresses given in a limited number of points, i.e. in the Gauss points. The procedure is explained for the more general 3-D case (allowing e.g. to handle beam bending and torsion at the same time) [74] and the smoothing matrix is then given also for a plane situation.

First a local finite element discretization is constructed in the region under investigation with at least one element per material component. The displacements of the macrosolution, obtained by other means, are sampled at the nodes of this local mesh to compute the Gauss point stresses and their nodal projection. Attention is now restricted to a single element of the local discretization e.g. a prismatic 3-D Lagrangian element with 27 nodes. The above sampled displacements are imposed on these 27 nodes. In this way a quadratic distribution of each displacement component can be obtained in the element and therefore a linear distribution of their derivatives. In a linear elastic problem, by means of the usual differential rules, strains are obtained in the Gauss points located in the known positions and finally the constitutive law gives the stresses in the same points. Stresses at these points are of good accuracy [96, 184].

In the elastic-plastic case a local equilibrium problem has to be solved with the imposed displacements in the nodes using the microscopic constitutive laws and enforcing the yield condition. This again yields stresses in the Gauss points.

At this point stresses should be extrapolated to the nodes by means of the discrete local smoothing procedure. Considering eight Gauss points in the above element, if σ_i $(i = 1, 2, \ldots, 8)$ are the unsmoothed stresses in these points, the extrapolated stress values at the corner nodes of the three-dimensional solid element are obtained by minimising the functional

$$\chi = \sum_{i=1}^{8} (\sigma_i - g(x_i, y_i, z_i))^2,$$

$$\text{where } g(x_i, y_i, z_i) = \sum_{j=1}^{8} \tilde{N}_j(x_i, y_i, z_i)\tilde{\sigma}_j \tag{123}$$

with $\tilde{N}_j$ linear smoothing functions and σ_i as above the unknown smoothed nodal stresses. Note that the smoothing shape function is an order lower than the shape functions for the above displacement interpolation and in the stress calculation in the elasto-plastic case. The minimization of the above functional yields the following equation [74]

$$\tilde{\mathbf{N}}^T \tilde{\mathbf{N}} \tilde{\boldsymbol{\sigma}} = \tilde{\mathbf{N}}^T \boldsymbol{\sigma}, \tag{124}$$

where $\tilde{\mathbf{N}}$ is an (8×8) matrix collecting the smoothing shape functions, evaluated in the Gauss points. By inverting the matrix $\tilde{\mathbf{N}}$ a direct relation between the smoothed stresses at the corner nodes of a three-dimensional solid element and the unsmoothed stresses at the $2 \times 2 \times 2$ Gauss points of the same element is obtained.

$$\tilde{\boldsymbol{\sigma}} = \tilde{\mathbf{N}}^{-1} \boldsymbol{\sigma}. \tag{125}$$

For prismatic elements in which the Jacobian determinant is constant, the matrix $\tilde{\mathbf{N}}^{-1}$ is given by

$$\tilde{\mathbf{N}}^{-1} = \begin{bmatrix} a & b & c & b & b & c & d & c \\ b & a & b & c & c & b & c & d \\ c & b & a & b & d & c & b & c \\ b & c & b & a & c & d & c & b \\ b & c & d & c & a & b & c & b \\ c & b & c & d & b & a & b & c \\ d & c & b & c & c & b & a & b \\ c & d & c & b & b & c & b & a \end{bmatrix} \tag{126}$$

where

$$a = \frac{5 + 3\sqrt{3}}{4}, \qquad b = \frac{-\left(\sqrt{3} + 1\right)}{4},$$

$$c = \frac{\sqrt{3} - 1}{4}, \qquad d = \frac{5 - 3\sqrt{3}}{4}.$$

It has to be observed that in (125) the vector $\tilde{\boldsymbol{\sigma}}$ indicates the eight stress components σ_{ij} (with the same indices) acting on the nodes as function of the relevant components at

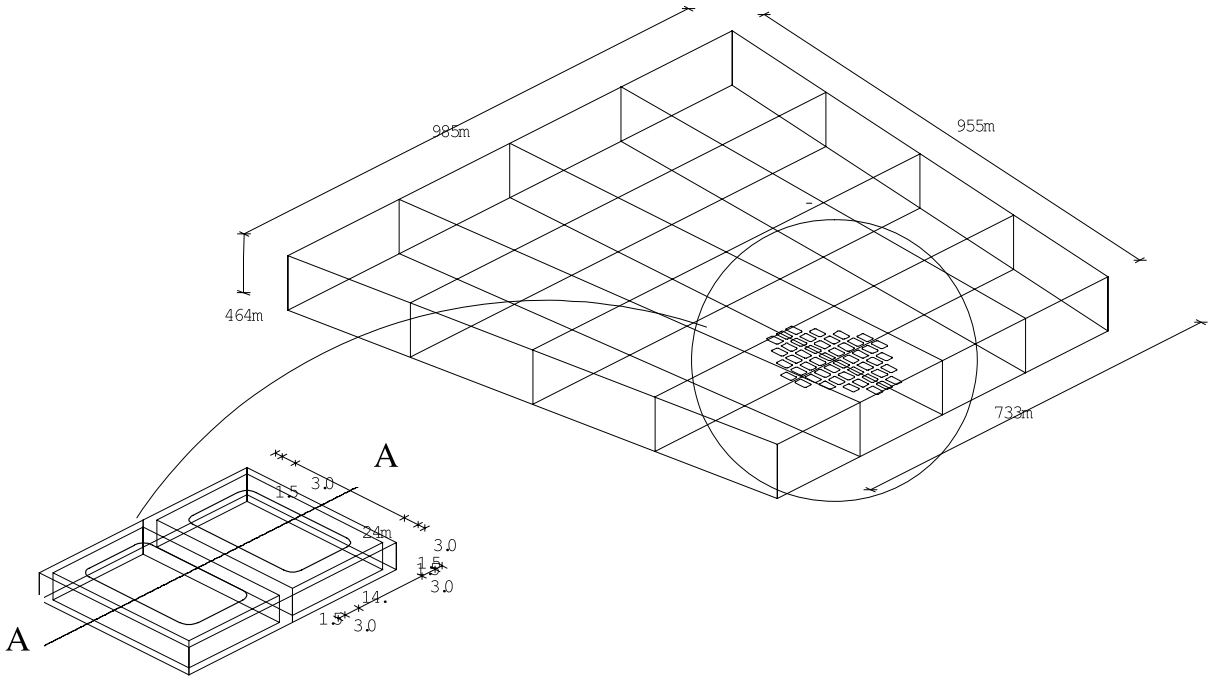

Fig. 18 Cells of periodicity (visible in both images) and one layer of the macroscopic mesh in the cross section of the coil on the right hand side (the coil is about 13 meters high)

the Gauss points. Therefore the knowledge of the full three-dimensional stress state in the eight nodes requires the application of (125) to the six stress components. The so obtained nodal stress values of neighbouring elements can be averaged to eliminate stress discontinuities within material boundaries (layers). Smoothing is not performed across layers. This procedure has been applied with success in [74], especially what through-thickness shear stresses are concerned. For plane problems the procedure is the same, only that now 9-node quadrilateral elements are used for the interpolation of the displacements, with at least one element per each material component (layer).

For each of the 9-node elements stresses are calculated with the real material properties at the four Gauss points located at element co-ordinates $[\xi = \pm 1/\sqrt{3}, \zeta = \pm 1/\sqrt{3}]$.

For projection linear shape functions are used, yielding for the corner node stresses

$$\begin{Bmatrix} \overline{\sigma}_1 \\ \overline{\sigma}_2 \\ \overline{\sigma}_3 \\ \overline{\sigma}_4 \end{Bmatrix} = \begin{bmatrix} a & c & b & c \\ c & a & c & b \\ b & c & a & c \\ c & b & c & a \end{bmatrix} \begin{Bmatrix} \sigma_{\mathrm{I}} \\ \sigma_{\mathrm{II}} \\ \sigma_{\mathrm{III}} \\ \sigma_{\mathrm{IV}} \end{Bmatrix} \tag{127}$$

where $a = 1 + \sqrt{3}/2$, $b = 1 - \sqrt{3}/2$ and $c = -1/2$. Superscripts 1–4 indicate corner nodes, while subscripts I–IV refer to Gauss points. It is recalled that linear distribution of stresses are exactly represented by this method whereas more complex stress fields are approximated by means of a least squares fit.

Projection can also be applied to carry out the stress recovery in case of asymptotic homogenization: the strains of the macroscopic solution are transferred to the finite element mesh of the single cell used to obtain numerically the effective coefficients, see Sect. 3.5. These macroscopic strains are treated as input data for the local (microscopic) problem. This yields the stresses in the Gauss points. The minimization is carried out as above, usually over a patch of elements. If needed, a previous least square minimization of the macroscopic strains can be carried out over an array of neighbouring cells [155].

As an example we refer to a D shaped superconducting coil with cable in conduit superconductors [109]. A cross section of the coil, and two cells of periodicity are shown in Fig. 18. Each cell is made up of an outer layer of epoxy and an adjacent layer of stainless steel. The central void part is in reality filled by a bundle of superconductors similar to those treated in Sect. 7.5 and 7.6. They do not contribute to the overall load bearing capacity of the coil and are hence here neglected. The mechanical analysis of the coil has been carried out on a rather rough finite element mesh using the material properties obtained through asymptotic theory homogenization of Sect. 3, giving the displacements at the nodes. Two adjacent cells of Fig. 18 are discretized locally by 27-node elements and the above displacements are sampled at these nodes. The six components of the stresses in the nodes are obtained with the above procedure. The distribution of the normal stress σ_{11} and of the three shear stresses τ_{12}, τ_{13}

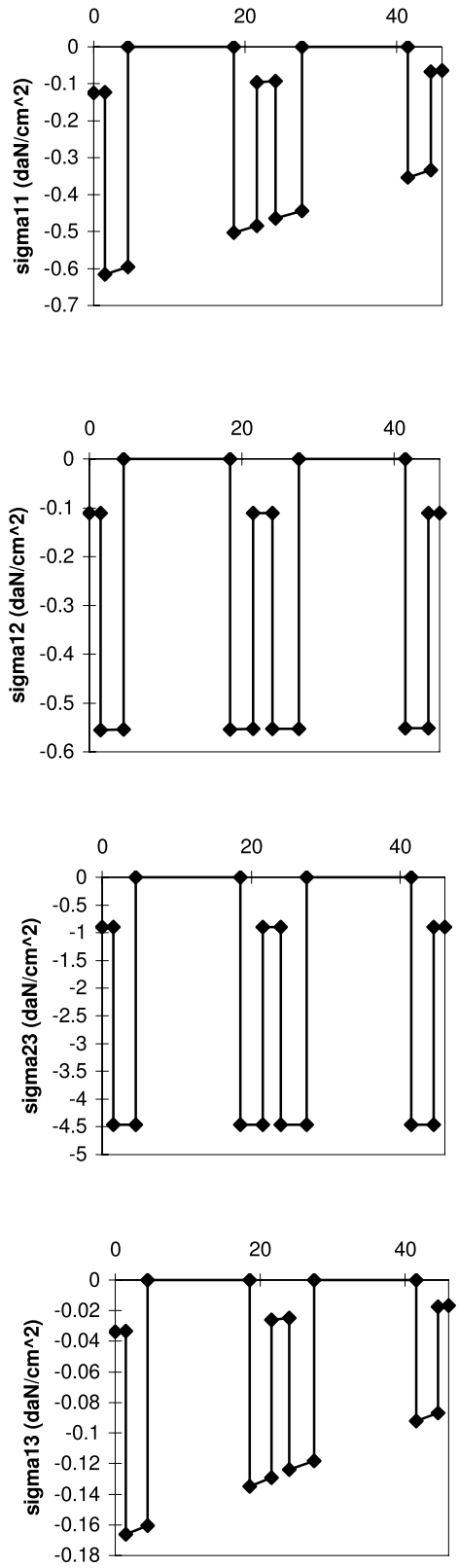

Fig. 19 Distribution of (*from top to bottom*): the normal stress σ_{zz}; tangential stress τ_{xy}; tangential stress τ_{yz}; tangential stress τ_{xz}; along two adjacent cells of Fig. 18

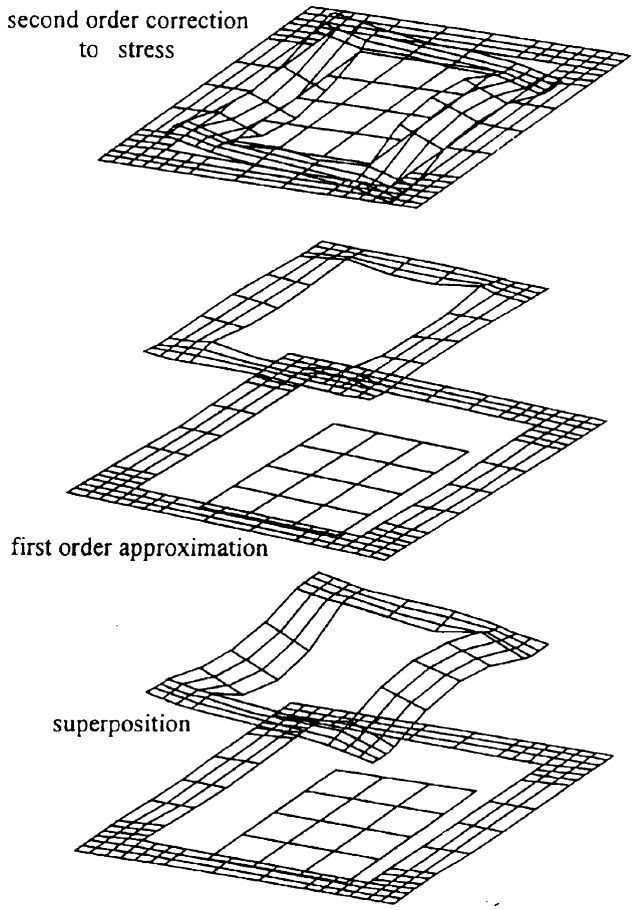

Fig. 20 Graph of normal stresses over a cell of periodicity: influence of second order correctors. *Top*: second order correction to stress; *middle*: first order approximation; *bottom*: the final stress field obtained through superposition. The undeformed grid is the reference position

and τ_{23} along two adjacent cells (line AA of Fig. 18) are shown in Fig. 19. These values compare well with those obtained through the procedure described in the next section [155], hence there is a choice available for the most appropriate procedure.

8.2 Asymptotic Correctors

The local approximation of stresses in case of asymptotic theory of homogenization was already dealt with in Sect. 3.4. This yields constant stresses over a particular material in the unit cell (zero order approximation of the stress field). However, if the separation of scales between local and global phenomena is not so sharp i.e. the micro-structural parameter ε of (14) is larger than e.g. 0.1, or for instance bending phenomena are of importance, it is advisable to take into account the second-order term in the expansion of the displacements (22). This gives the possibility of computing first-order terms in the stress description [48, 155].

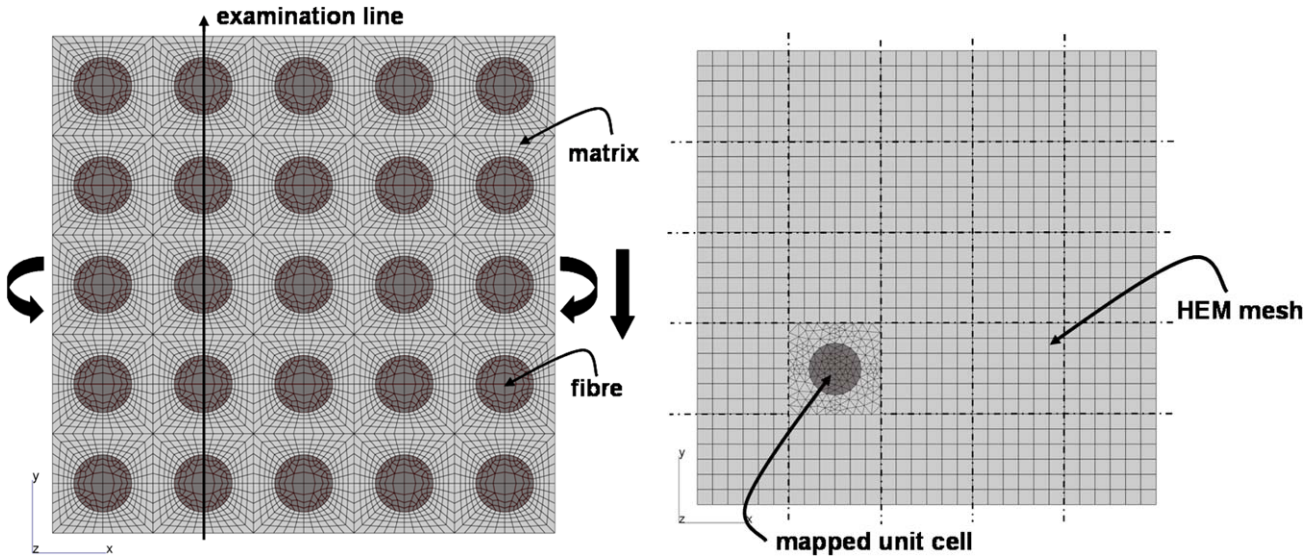

Fig. 21 (**a**) FE meshes for the reference calculation; (**b**) the macroscopic calculation with the mapped local unit cell mesh that serves for the local stress recovery step

Similar to (39) we have

$$u_i^2(\mathbf{x},\mathbf{y}) = \kappa_i^{pqr}(\mathbf{y}) e^0_{pq,r}(\mathbf{x}) + C_i^2(\mathbf{x}), \tag{128}$$

where a new homogenization function $\kappa_i^{pqr}(y)$, also called corrector, appears together with the gradients of global strains. These correctors are obtained by solving a variational problem

$$\text{Find} \quad \kappa_i^{pqr} \in V_Y \quad \text{such that}: \quad \forall v_i \in V_Y$$

$$\int_Y a_{ijkl}(\mathbf{y})(\kappa^{pqr}_{k,l(y)}(\mathbf{y}) - \delta_{kr}\chi_l^{pq}(\mathbf{y}))v_{i,j(y)}(\mathbf{y})dY \tag{129}$$
$$= \int_Y a^v_{irpq}(\mathbf{y}) v_i(\mathbf{y}) dY$$

and the enhanced stresses are obtained via

$$\sigma^{\varepsilon}_{ij}(\mathbf{x},\mathbf{y}) = a_{ijkl}(\mathbf{y})[(\delta_{pk}\delta_{ql} - \chi^{pq}_{k,l})e^0_{pq} + \varepsilon(\kappa^{pqr}_{k,l(y)}(\mathbf{y}) - \delta_{kr}\chi_l^{pq}(\mathbf{y}))e^0_{pq,r}]. \tag{130}$$

The numerical implementation is described in [155] and results in an equation of the type of (54). It is just recalled that instead of 6 components in the strain vector we have to handle 18 components of the strain gradient vector. The size of the matrices in the final equation increases accordingly. As an example the graph of normal stresses of a square cell of periodicity is shown in Fig. 20. This cell is again made up of an outer layer of epoxy and an adjacent layer of stainless steel. The central part is void. It represents the jacket of a cable in conduit superconductor. The structural problem solved is that of a D-shaped coil [155] subjected to Lorentz forces. In Fig. 20 clearly the non-uniform stress distribution

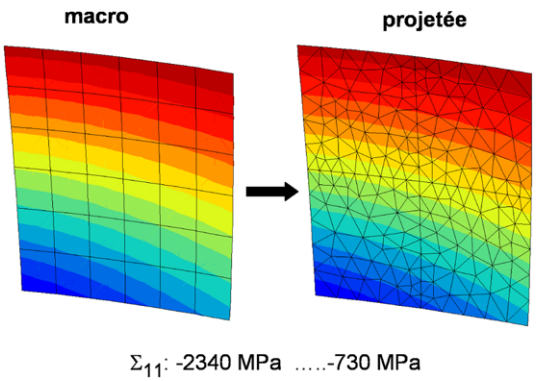

Fig. 22 Macroscopic stress projection on the unit cell before the local stress recovery

over a single material is shown which has been obtained by means of the second order stress correction.

8.3 Example of Stress Recovery After an Overall Finite Element Analysis Made with a Macroscopic Constitutive Law

In many applications, we will have to use sufficiently simple macroscopic constitutive equations for the inelastic analysis of the structural component. Such constitutive equations may be defined from prior-micro-to-macro analyses. This is the so-called "sequential multiscale" approach, see Sect. 6. The TFA is one of these approaches. In its multi-subvolumes version (Dvorak [55], Carrère et al. [35]) it considers a unit cell finite element analysis to determine the various localisation and influence tensors. The same unit cell will be used below to treat the local stress recovery step.

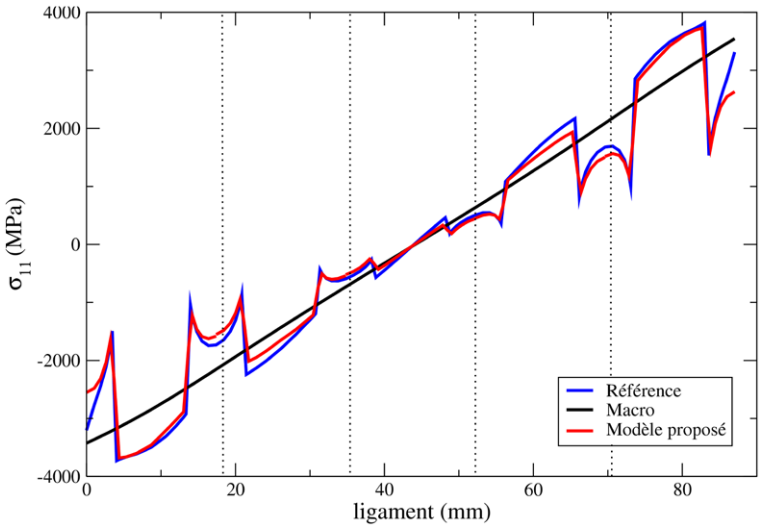

Fig. 23 Comparison of the calculated elasticity solutions for stress component σ_{11}, without taking into account edge effect

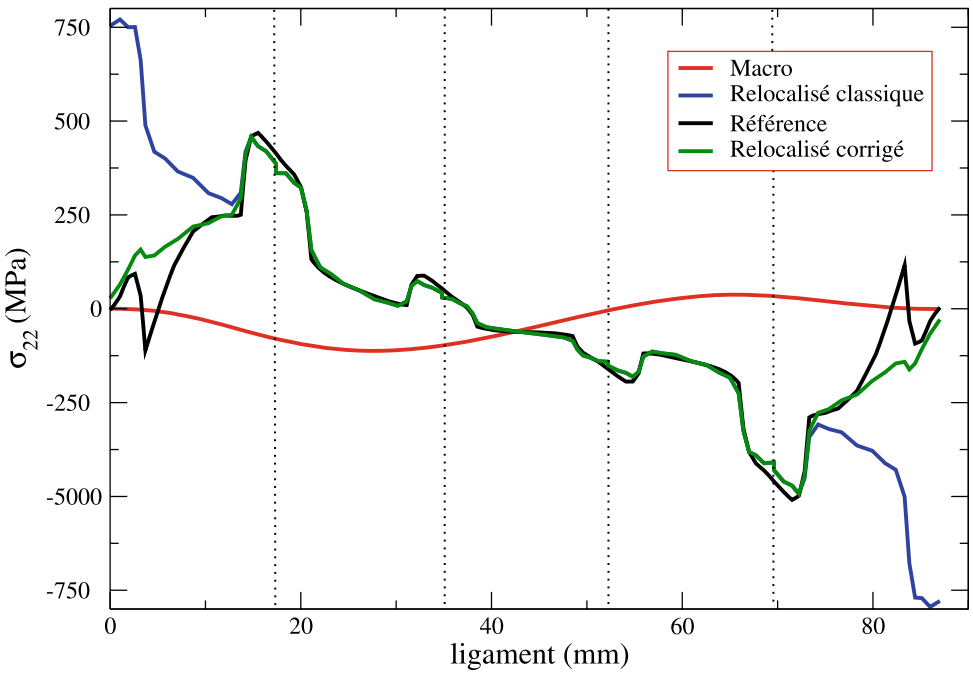

Fig. 24 Comparison of the calculated elasticity solutions for stress component σ_{22}, taking into account edge effects or not the edge effect

Let us assume an overall component analysis made with a constitutive equation built by the TFA approach. In a post-processing of this analysis, we intend to recover the local fields (stress, strain, plastic strain) on the true microstructure (supposed to be known locally). The method presented here is an application of classical periodic homogenisation, within the same kind of approximations than in Sect. 8.1 above.

It is shown that it may deliver quite good local results, even for a coarse microstructure relative to the component size and wavelength of the overall fields (large overall stress gradients).

The test example taken here is given on Fig. 21a, in an unidirectional composite part (long fibres) submitted to combined transverse loads, bending and shear. It is treated in 2D, first for elastic constituents. The reference solution is obtained with mesh in Fig. 21a. The macroscopic solution is given with a coarse mesh like in Fig. 21b, and a constitutive equation deduced from a single unit cell (mesh shown on Fig. 21b) by TFA method (reduced here to elasticity):

$$\mathbf{\Sigma} = \mathbf{L} : \mathbf{E} \tag{131}$$

in which $\mathbf{L} = \sum_r c_r \mathbf{L}_r : \mathbf{A}_r$, with $\mathbf{A}_r$ being the strain localisation tensor such that

$$\boldsymbol{\varepsilon}_r = \mathbf{A}_r : \mathbf{E}. \tag{132}$$

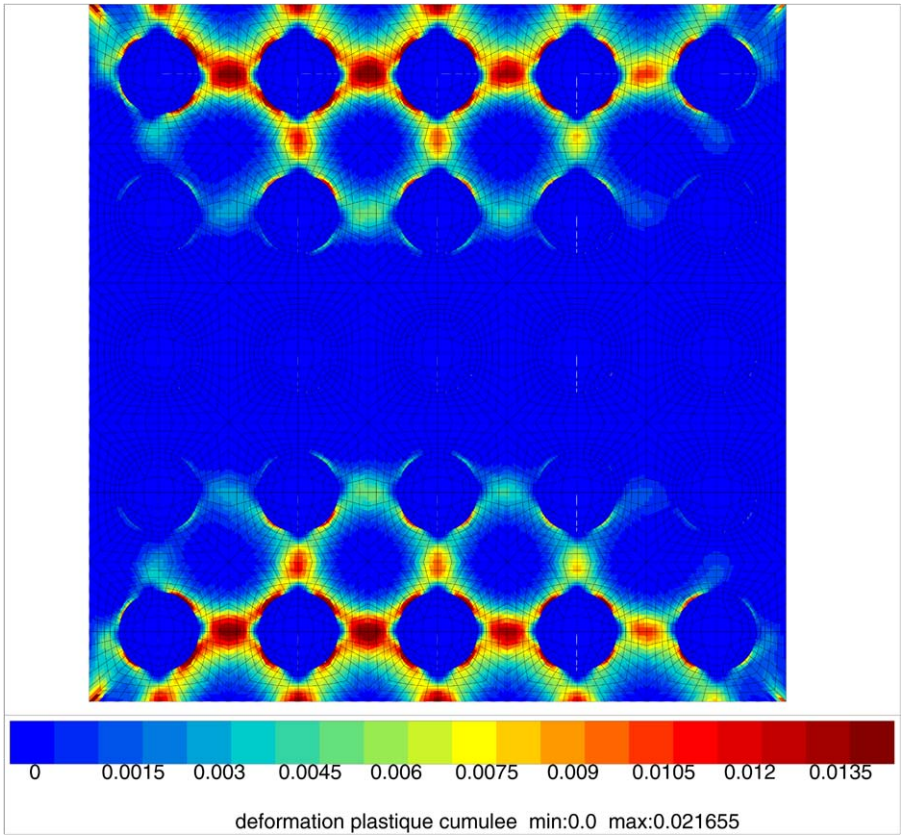

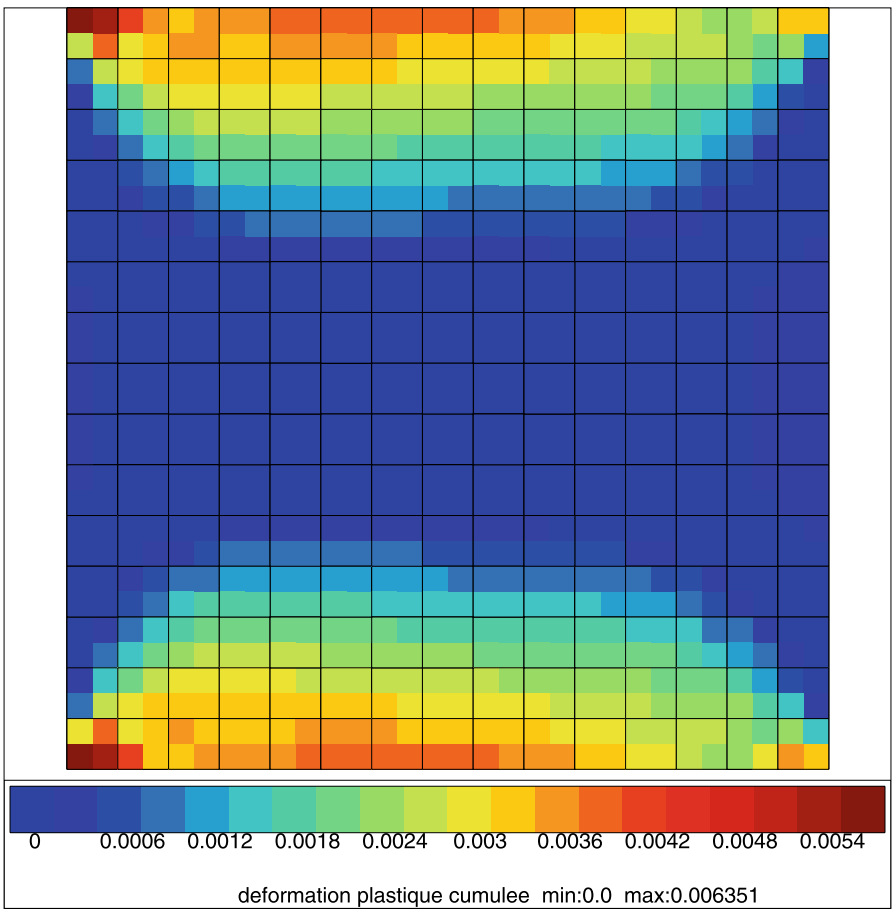

Fig. 25 Cumulated Plastic strain, (**a**) for the reference calculation and (**b**) for the macroscopic calculation

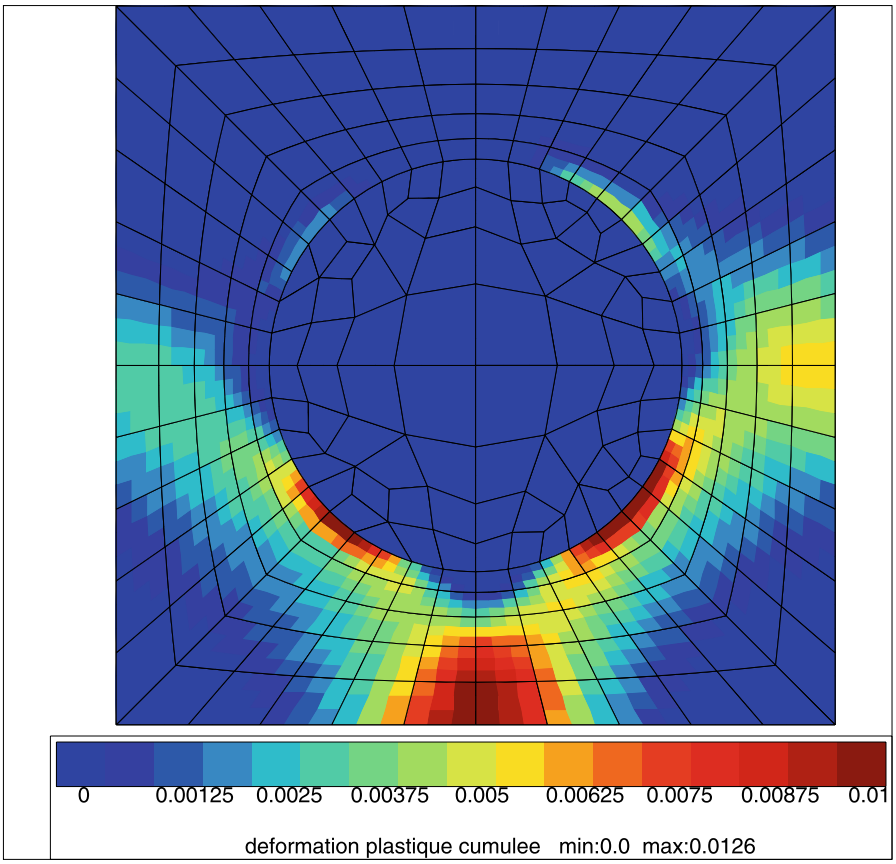

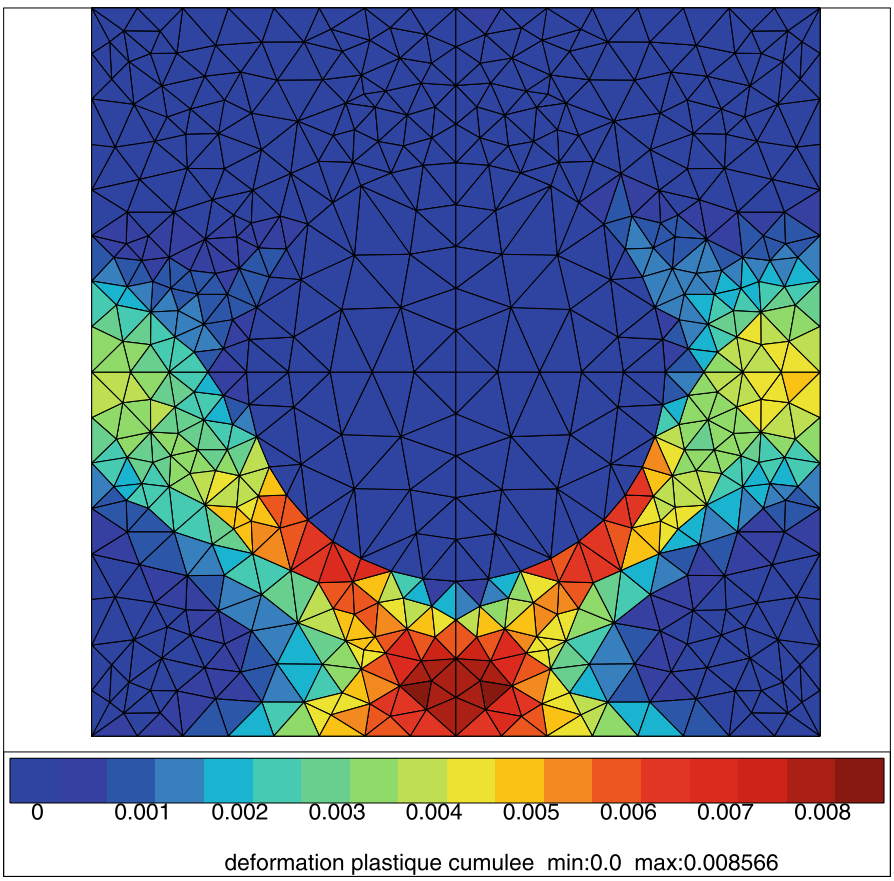

Fig. 26 (**a**) Reference calculation on one cell of Fig. 25a and (**b**) Recovery plastic field

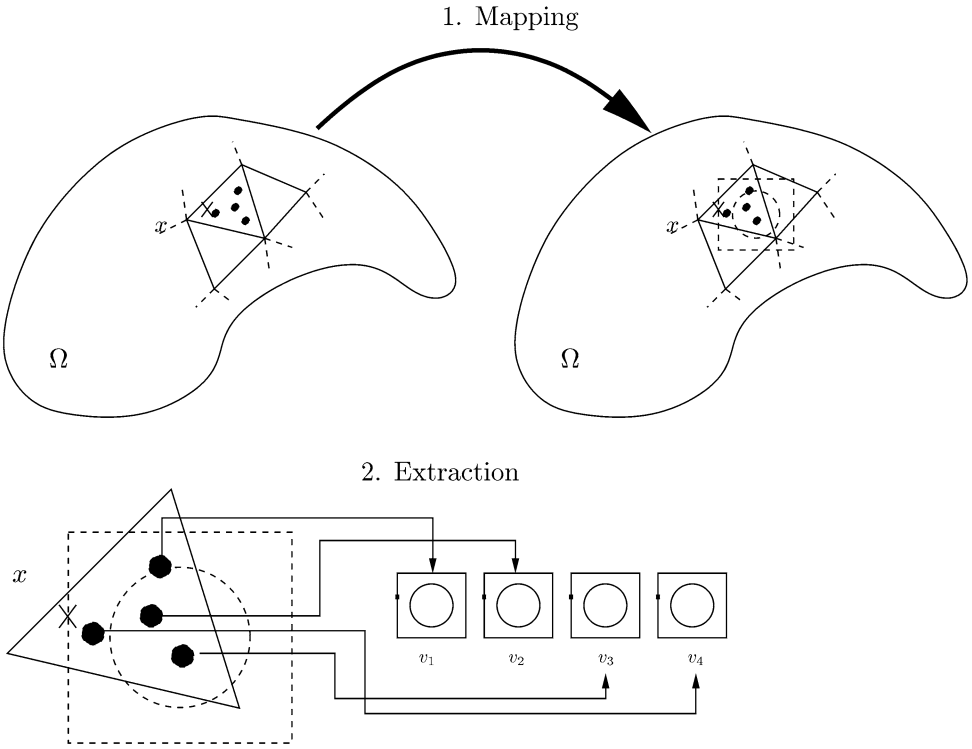

Fig. 27 Principle of the recovery by an "interpolated mapping"

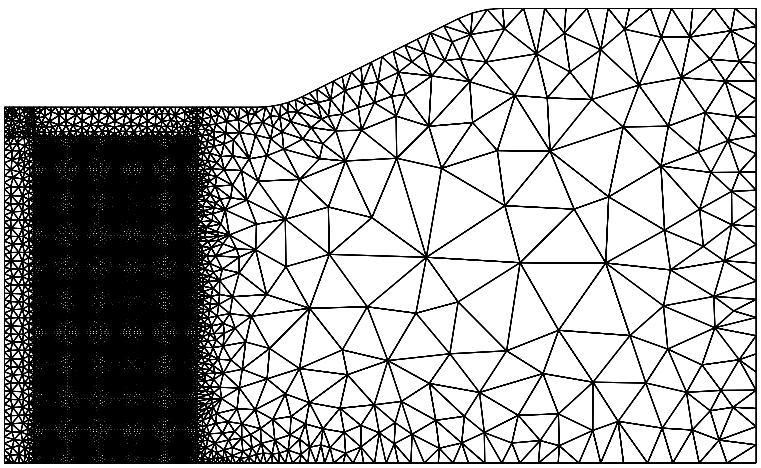

Fig. 28 Complete mesh of the actual structure for the reference computation

The obtained macroscopic solution is then mapped (interpolated and projected) on the TFA unit cell, as shown on Fig. 22, for the cell positioned at (2, 2) as shown in Fig. 21a. This is done everywhere in the part, or in the region of interest at which we need a local stress field. In the elastic case, it is made by applying the stress localisation tensor (of the microscale) to the overall solution $\boldsymbol{\Sigma}(\mathbf{x})$, that is non-uniform (as in previous sections, $\mathbf{y}$ denotes the local scale, $\mathbf{x}$, the overall one). We then write:

$$\boldsymbol{\sigma}_s = \boldsymbol{\sigma}(\mathbf{x}, \mathbf{y}) = \mathbf{B}_s(\mathbf{y}) : \boldsymbol{\Sigma}(\mathbf{x}). \tag{133}$$

The obtained solution by this first order recovery method (in fact the classical one in periodic homogenisation) compares very well with the reference solution, Fig. 23, except at the edges (see below).

In Fig. 24 for a lower valued stress component, we see also a good comparison on the three central cells, though the macroscopic solution is even not the average of the local one.

Still within the same first order scheme, the local recovery can also be made in the non linear inelastic case. In the shown example, still the one of Fig. 21a, the macroscopic solution is obtained through a TFA based constitutive model (Sect. 6.2). Figure 25a shows the reference solution (all fibres meshed) for the accumulated plastic strain. The corresponding macroscopic solution is indicated on Fig. 25b.

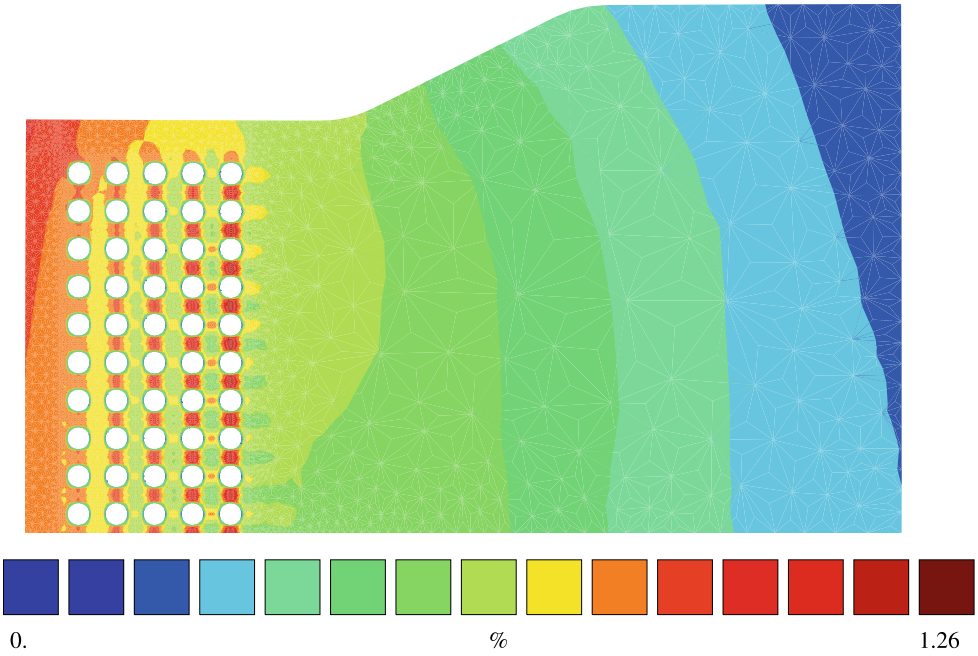

Fig. 29 Accumulated visco-plastic strain in the reference computation at time $t = 7.5$ s

The local recovery after the coarse macroscopic solution is made using TFA. In the present case it has been rewritten in a rate form, as:

$$\dot{\boldsymbol{\sigma}}_s = \dot{\boldsymbol{\sigma}}(\mathbf{x},\mathbf{y}) = \mathbf{B}_s(\mathbf{y}) : \dot{\boldsymbol{\Sigma}}(\mathbf{x}) - \sum_r \mathbf{F}_{sr}(\mathbf{y}) : \mathbf{L}_r : \dot{\boldsymbol{\varepsilon}}_r^p, \quad (134)$$

$$\dot{\boldsymbol{\varepsilon}}_r^p = \dot{\lambda}_r \frac{\partial f_r}{\partial \boldsymbol{\sigma}_r} = \boldsymbol{L}_r^p : \dot{\boldsymbol{\sigma}}_r. \quad (135)$$

Formally, through the TFA discretization, the $\dot{\boldsymbol{\sigma}}_r$, as well as $\dot{\boldsymbol{\varepsilon}}_r^p$, are depending also on the local position of the sub-volume "r". $\boldsymbol{L}_r^p$ is the instantaneous local plastic tangent operator in the same sub-volume.

Knowing the overall stress rate solution $\dot{\boldsymbol{\Sigma}}(\mathbf{x})$, the solution of the above system leads to the local stress rate then to the local plastic strain rate and, by time integration, to the local plastic strain field.

Figure 26b illustrates the obtained local results on the cell indicated Fig. 21b, compared with the reference solution on Fig. 26a. Though different discretizations are used (recall that TFA recovery is not a finite element procedure), the comparison is quite acceptable.

Let us note that improvements of the above techniques are now available "naturally" in the context of NTFA (Non-uniform Transformation Field Analysis) method, as shown for instance by Michel and Suquet [124].

As shown for instance in Fig. 24, the only incorrect results are in the region where take place "edge effects", in the first and last rows of fibres in the present composite example (free edges or transition zones with a pure matrix region). The problem is clearly related with a loss of periodicity. Solving such situations need to rewrite local boundary value problems in these regions, which boundary conditions should be taken from the previously re-localized fields (tractions and/or displacements).

Other solutions were proposed, for instance by Dumontet [48], introducing a boundary layer field, or by Buannic and Cartraud [25] who proposed additional specific boundary conditions. This problem has been dealt with also in Sect. 3.6, where infinite elements have been used [110]. A very simple heuristic way is to introduce spatially decaying stress localisation functions $\mathbf{B}^*(\mathbf{y})$ near the edge, using exponentials or others, like done in Kruch [103]. Figure 24 illustrates the improvement by such a simple interpolation rule, with the local stress that now correctly vanishes at the free edge.

8.4 A Practical Example of Local Field Recovery when Using FE^2 Integrated Multiscale Methods

The method presented here is typically adapted for the case using an integrated multiscale method based on imbricated FE techniques (like FE^2). As will be shown, the method can be applied as a post-processing interpolation technique, without having to reformulate the localisation problem.

The goal is to compute $\boldsymbol{\varepsilon}(\mathbf{x})$, for any $\mathbf{x}$, without any reference to $\mathbf{y}$ (cell coordinate) because all cells have to be mapped at their real locations.

An "interpolated-mapping" of the results obtained by FE^2 methods is used to compute actual fields Fig. 27. Let us suppose that all heterogeneities remain elastic and that the surrounding medium is also elastic. For each macroscopic integration point whose spatial coordinate is $\mathbf{x}_i$, and for each

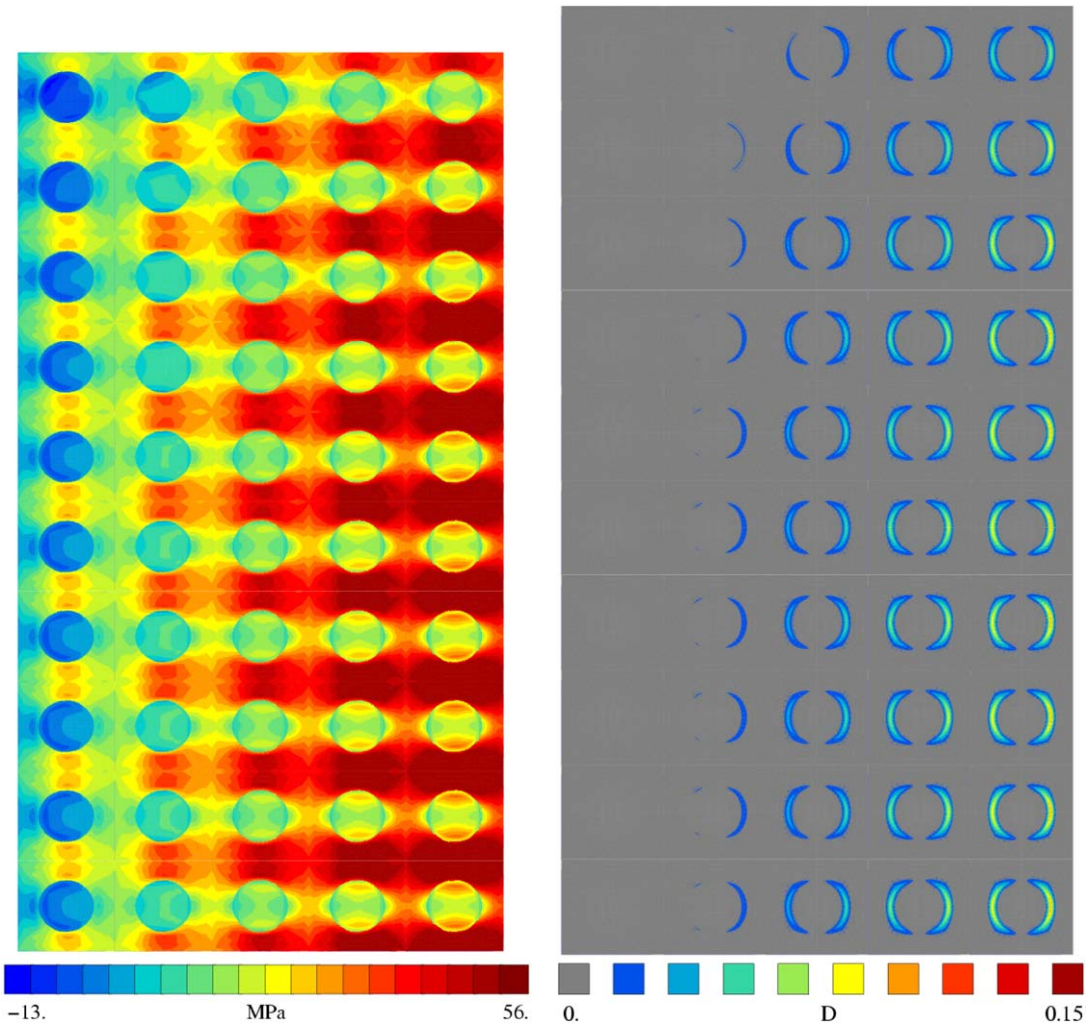

Fig. 30 Results obtained by the recovery technique made after the FE^2 overall analysis, when taking into account damage at the fibre/matrix interface (time $t = 6.76$ s). *Left*: radial stress; *right*: damage at the interface

position inside the underlying unit cell, the instantaneous strain tensor (for instance) is equal to

$$\boldsymbol{\varepsilon}(\mathbf{x}_i, \mathbf{y}) = \mathbf{A}(\mathbf{y}) : \mathbf{E}(\mathbf{x}_i). \tag{136}$$

The recovery technique by an "interpolated-mapping" is nothing but a macroscopic interpolation of results coming from all microscopic computations. Let $\gamma(\mathbf{x})$ be a mechanical component to be interpolated inside a macroscopic element; $\gamma(\mathbf{x})$ can be computed using the shape functions of the finite element containing $\mathbf{x} \sim$:

$$\gamma(\mathbf{x}) = \sum_i \gamma(\mathbf{x}_i) N_i(\mathbf{x}). \tag{137}$$

$N_i(\mathbf{x})$ are the shape function of the current macroscopic element, $\gamma(\mathbf{x}_i)$ are the values of γ at the nodes surrounding the point $\mathbf{x}$. This relation can also be applied to microscopic quantities as soon as the unit cell, resized and translated to its real location and size, is mapped onto the macroscopic mesh. For instance:

$$\begin{aligned}\boldsymbol{\varepsilon}(\mathbf{x}, \mathbf{y}) = \boldsymbol{\varepsilon}(\mathbf{x}, \mathbf{x}/\eta) &= \sum_i \boldsymbol{\varepsilon}(\mathbf{x}_i, \mathbf{x}/\eta) N_i(\mathbf{x}) \\ &= \sum_i \mathbf{A}(\mathbf{x}/\eta) : \mathbf{E}(\mathbf{x}_i) N_i(\mathbf{x}) = \mathbf{A}(\mathbf{x}/\eta) : \mathbf{E}(\mathbf{x}).\end{aligned} \tag{138}$$

This kind of relations can be generalized and extended in non-linear cases like in plasticity or visco-plasticity.

One major advantages of using FE^2 techniques is that the required estimations of $\mathbf{A}$ (that are very difficult to estimate in non-linear cases) have already been implicitly computed during the FE^2 analysis. Another advantage is that the computation of re-localized values can be made a posteriori in a post-processor, since it only requires already computed information. It is then possible to restrict this extra-computation to critical zones of the structure.

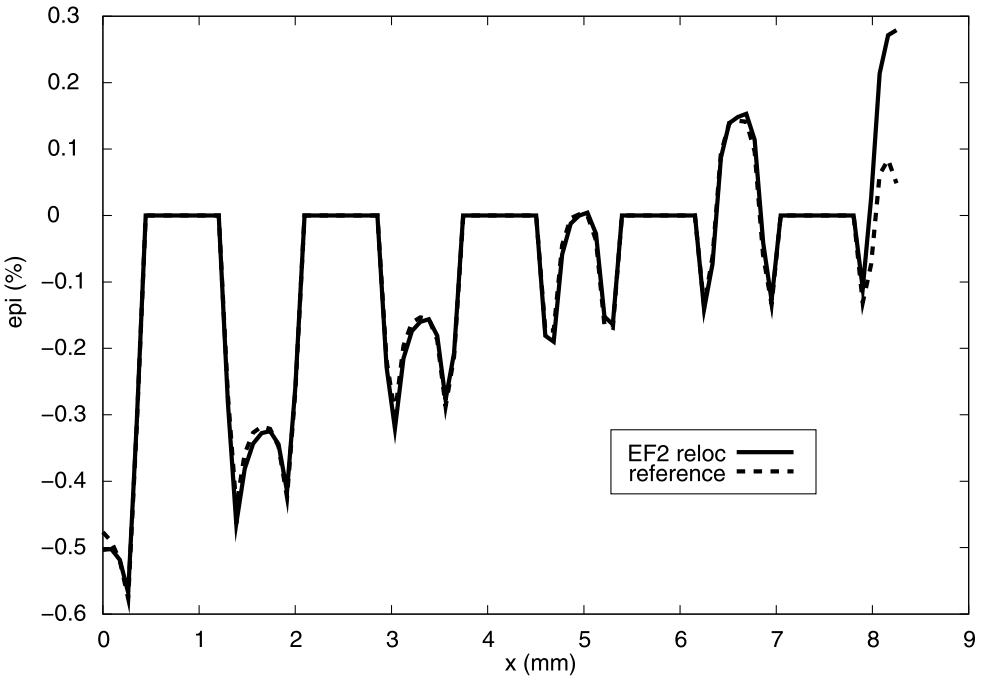

Fig. 31 Comparison between the reference radial inelastic strain in the reference *calculation* and in the re-localization after the FE^2 analysis

From a practical and programming point of view, the re-localization is performed by three steps∼:

1 - map the unit cell onto the global mesh at its real location,
2 - extract the microstructural information from all integration points near **x**, compute nodal values,
3 - compute the re-localized component using (138).

In Feyel [61], it was shown how continuity of the final local fields is automatically enforced when changing the position from a unit cell to the neighbouring one.

Figure 28 to Fig. 31 show some application results to the example of a compressor bling treated in Sect. 7.4. The same macroscopic mesh and mesh of the FE unit cell are used (Fig. 7). However, in the present case, in order to render more difficult the local stress recovery process, we consider much larger fibre sizes (of the order of 2 millimeters). Figure 28 presents the mesh of the complete structure (all fibres meshed) that serve for the reference computation and the subsequent comparisons. Figure 29 illustrates an example of obtained fields, the accumulated visco-plastic strain in Titanium (fibres are still elastic).

Figure 30 shows the σ_{11} (radial) stress field in the composite region of the component after using the FE^2 technique (only the overall coarse mesh and the unit cell shown in Fig. 7) and the recovery by the post-processing described just above. It indicates the perfect continuity of the field between the various cells of the recovery.

One may observe that stresses are relaxed in fibres, due to the partial failure of some fibre/matrix interfaces. This is due to the completely coupled damage analysis performed in that example, in which the interface damage behaviour is modelled by cohesive elements. Figure 30b shows the corresponding localised damage state, still obtained by the same interpolation technique.

The comparison between the re-localized fields and the ones obtained in the reference solution has been made along the radial line drawn in Fig. 28 (third line of fibres). Figure 31 shows the comparison for the component ε^p_{11} of the visco-plastic strain. One may observe a very good comparison, except for the extreme positions (right and left) at which are present edge effects, discussed in the section just above.

9 Conclusions

There exist many methods for the multiscale analysis of composites. They range from analytical methods, semi-analytical ones to purely numerical ones. These methods have been reviewed in this paper. In particular asymptotic analysis, mean field approaches, transformation field analysis and different variants of it, sequential multiscale procedures, especially multiscale FE methods, have been addressed in detail. Examples are shown, and some comparisons which may help the reader to choose the most appropriate method for his purpose. Recovery methods after the component analysis have also been addressed and several examples have been shown. This aspect, essential in a multiscale procedure, is often neglected.

Acknowledgements Support for this work was partially provided by PRIN 2006091542-003: *Thermo-mechanical multiscale modelling of ITER superconducting magnets*, and KMM-NoE—*Knowledge-based multicomponent materials for durable and safe performance—Network of Excellence*. This support is gratefully acknowledged.

We thank Krysinski Yann from Ecole Polytechnique (F) for his contribution to this work.

References

1. Aboudi J (1982) A continuum theory for fiber-reinforced elastoviscoplastic compoites. Int J Eng Sci 20:605–621
2. Aboudi J (1988) Constitutive equations for elastoplastic composites with imperfect bonding. Int J Plast 4:103–125
3. Aboudi J (1992) Mechanics of composite materials—a unified micromechanical approach. Elsevier, Amsterdam
4. Aboudi J (1996) Micromechanical analysis of composites by the method of cells-update. Appl Mech Rev 49(10):S83–S91
5. Aboudi J, Pindera M-J, Arnold SM (2003) Higher-order theory for periodic multiphase materials with inelastic phases. Int J Plast 19:805–847
6. Allen D, Jones R, Boyd J (1994) Micromechanical analysis of a continuous fiber metal matrix composite including the effects of matrix viscoplasticity and evolving damage. J Mech Phys Solids 42(3):505–529
7. Arnold SM, Pindera M-J, Wilt TE (1996) Influence of fiber architecture on the inelastic response of metal matrix composites. Int J Plast 12(4):507–545
8. Arnold S, Wilt T (1992) Influence of engineered interfaces on residual stresses and mechanical response in metal matrix composites. NASA Technical Memorandum 105438, Cleveland, Ohio
9. Babuska I, Strouboulis S, Upadhyay CS, Gangaraj SK (1995) A posteriori estimation and adpatative control of the pollution error in the h-version of the finite element method. Technical Note BN 1175, Institute for Physical Science and Technology, University of Maryland, College Park, MD
10. Bensoussan A, Lions JL, Papanicolau G (1976) Asymptotic analysis for periodic structures. North-Holland, Amsterdam
11. Berveiller M, Zaoui A (1979) An extension of the self-consistent scheme to plastically flowing polycristals. J Mech Phys Solids 26:325–344
12. Bishop JFW, Hill R (1951) A theory of the plastic distortion of a polycrystalline aggregate under combined stresses. Philos Mag 42:414–427
13. Bishop JFW, Hill R (1951) A theoretical derivation of the plastic properties of a polycrystalline face-center metal. Philos Mag 42:1298–1307
14. Böhm H (1993) Numerical investigation of microplasticity effects in unidirectional long-fiber reinforced metal matrix composites. Modell Simul Mater Sci Eng 1:649–671
15. Böhm HJ, Eckschlager A, Han W (2002) Multi-inclusion unit cell models for metal matrix composites with randomly oriented discontinuous reinforcements. Comput Mater Sci 25(1):42–53
16. Böhm HJ, Han W (2001) Comparisons between three-dimensional and two-dimensional multi-particle unit cell models for particle reinforced metal matrix composites. Model Simul Mater Sci Eng 9:47–65
17. Bornert M (2001) Homogénéisation des milieux aléatoires; bornes et estimations. In: Bornert M, Bretheau T, Gilormini P (eds) Homogénéisation en mécanique des matériaux, vol 1. Hermès, Paris, pp 133–221
18. Boso DP, Lefik M, Schrefler BA (2005) A multilevel homogenised model for superconducting strands thermomechanics. Cryogenics 45(4):259–271
19. Boso DP, Lefik M, Schrefler BA (2006) Homogenisation methods for the thermo-mechanical analysis of Nb3Sn strand. Cryogenics 46(7–8):569–580
20. Boso DP, Lefik M, Schrefler BA (2006) Thermal and bending strain on Nb3Sn strands. IEEE Trans Appl Supercond 16(2):1823–1827
21. Boutin C (1995) Heat conduction with microstructural effects. In: Dembicki E, Auriault J-L, Sikora Z (eds) Homogenization, theory of migration and granular bodies. University of Gdansk, Gdansk, pp 53–63
22. Brenner R, Castelnau O, Gilormini P (2001) A modified affine theory for the overall properties of nonlinear composites. C R Acad Sci, Paris, Sér IIB 329(9):649–654
23. Brockenbrough J-R, Suresh S, Wienecke H-A (1991) Deformation of metal-matrix composites with continuous fibers: geometrical effect of fiber distribution and shape. Acta Metall Mater 39(5):735–752
24. Bruggeman DAG (1935) Berechnung verschiedener physikalischer Konstanten von heterogenen Substanzen. I. Dielektrizitätskonstanten und Leitfähigkeitn der Mischkörper aus isotropen Substanzen. Ann Phys 24:636–679
25. Buannic N, Cartraud P (2001) Higher-order effective modeling pf periodic heterogeneous beams. Part II: Derivation of the proper boundary conditions for the interior asymptotic solution. Int J Solids Struct 38:7163–7180
26. Budiansky B (1965) On the elastic moduli of some heterogeneous materials. J Mech Phys Solids 13:223–227
27. Budiansky B, Hashin Z, Sanders JL (1960) The stress field of a slipped crystal and the early plastic behavior of polycrystalline materials. In: Plasticity, proc 2nd symp naval struct mech. Pergamon, Oxford, p 239
28. Buryachenko V (1996) The overall elastoplastic behavior of multiphase materials with isotropic components. Acta Mech 119:93–117
29. Cailletaud G (1987) Une approche micromécanique phénoménologique du comportement inélastique des métaux. PhD, Université Pierre et Marie Curie, Paris 6
30. Cailletaud G (1992) Micromechanical approach to inelastic behaviour of metals. Int J Plast 8:55–73
31. Cailletaud G, Pilvin P (1994) Utilisation de modèles polycristallins pour le calcul par éléments finis. Rev Eur Elém Finis 3(4):515–541
32. Cambou B, Dubujet P, Emeriault F, Sidoroff F (1995) Homogenisation of granular materials. Eur J Mech A/Solids 14:255–276
33. Carrère N (2001) Sur l'analyse multiéchelle des matériaux composites à matrice métallique: application au calcul de structure. PhD, Ecole Polytechnique, Palaiseau
34. Carrère N, Kruch S, Vassel A, Chaboche J-L (2002) Damage mechanisms in unidirectional SiC/Ti composites under transverse creep loading: experiments and modelling. Int J Damage Mech 11:41–63
35. Carrère N, Féyel F, Kanoute P (2004) A comparison between and embedded FE2 approach and a TFA-like model. Int J Multi Comput Eng 2–4:20–38
36. Carrère N, Maire J-F, Kruch S, Chaboche J-L (2004) Multiscale analysis of SiC/Ti composites. Mater Sci Eng A 365:275–281
37. Chaboche J-L, Kanouté P (2003) Sur les approximations isotrope et anisotrope de l'opérateur tangent pour les méthodes tangentes incrémentale et affine. C R Acad Sci Paris 331:857–854
38. Chaboche J-L, Kruch S, El Mayas N (1994) Lois de comportement thermoelastoviscopastique des composites à matrice métallique. C R Acad Sci Paris Sér II 319:971–977
39. Chaboche J-L, Kruch S, Maire J-F, Pottier T (2001) Towards a micromechanics based inelastic and damage modelling of composites. Int J Plast 17:411–439
40. Chaboche J-L, Kanouté P, Roos A (2005) On the capabilities of mean-field approaches for the description of plasticity in metal matrix composites. Int J Plast 21:1409–1434

41. Chang CS, Liao CL (1990) Constitutive relation for a particulate medium with the effect of particle rotation. Int J Solids Struct 26:437–453
42. Chen W, Fish J (2001) A dispersive model for wave propagation in periodic heterogeneous media based on homogenization with multiple spatial and temporal scales. J Appl Mech (ASME) 68:153–161
43. Christensen R (1990) A critical evaluation for a class of micro-mechanics models. J Mech Phys Solids 38(3):379–404
44. Christman T, Needleman A, Suresh S (1989) Experimental and numerical study of deformation in metal-ceramic composites. Acta Metall Mater 37(11):3029–3050
45. Cioranescu D, Paulin JSJ (1979) Homogenization in open sets with holes. J Math Anal Appl 71:590–607
46. Conductor database, Appendix C, Annex II. Thermal, electrical and mechanical properties of materials at cryogenic temperatures, 24 Aug 2000
47. Doghri I, Ouaar A (2003) Homogenization of two-phase elasto-plastic composite materials and structures study of tangent operators, cyclic plasticity and numerical algorithms. Int J Solids Struct 40:1681–1712
48. Dumontet H (1990) Homogénéisation et effets de bords dans les matériaux composites. Thèse de doctorat d'état, Université Pierre et Marie Curie Paris 6, Paris
49. Dvorak GJ (1992) Transformation field analysis of inelastic composite materials. Proc R Soc Lond A 431:89–110
50. Dvorak G, Bahei-El-Din Y (1987) A bimodal plasticity theory of fibrous composite materials. Acta Mech 69:219–241
51. Dvorak G, Benveniste Y (1992) On transformation strains and uniform fields in multiphase elastic media. Proc R Soc Lond A 437:291–310
52. Dvorak G, Rao M (1976) Axisymmetric plasticity theory of fibrous composites. Int J Eng Sci 14:361–373
53. Dvorak G, Zhang J (2001) Transformation field analysis of damage evolution in composite materials. J Mech Phys Solids 49:2517–2541
54. Dvorak G, Bahei-El-Din Y, Macheret Y, Liu C (1988) An experimental study of elastic-plastic behavior of a fibrous boron-aluminium composite. J Mech Phys Solids 36:655–687
55. Dvorak G, Bahei-El-Din Y, Wafa A (1994) Implementation of the transformation field analysis for inelastic composite materials. Comput Mech 68(5):201–228
56. E W, Engquist B, Li X, Ren W, Vanden-Eijnden E (2007) Heterogeneous multiscale methods: a review. Commun Comput Phys 2:367–450
57. Eshelby JD (1957) The elastic field of an ellipsoidal inclusion and related problems. Proc R Soc A 241:376–396
58. Eshelby JD (1957) The determination of the elastic field of an ellipsoidal inclusion, and related problem. Proc R Soc Lond A 421:376–396
59. Eyre DJ, Milton GW (1999) A fast numerical scheme for computing the response of composites using grid refinement. J Phys III 6:41
60. Feyel F (1998) Application du calcul parallèle aux modèles à grand nombre de variables internes. Thèse de doctorat, Ecole Nationale Supérieure des Mines de Paris
61. Feyel F (1999) Multiscale FE2 elastovisplastic analysis of composite structures. Comput Mater Sci 16:344–354
62. Feyel F, Chaboche JL (2000) FE2 multiscale approach for modelling the elastoviscoplastic behaviour of long fiber SiC/Ti composite materials. Comput Methods Appl Mech Eng 183:309–330
63. Feyel F, Chaboche JL (2001) Multi-scale non linear FE^2 analysis of composite structures: damage and fiber size effects. In: Saanouni, K. (ed) Numerical modelling in damage mechanics—NUMEDAM'00. Revue Europèenne des Elèments Finis, vol 10, pp 449–472
64. Feyel F, Chaboche JL (2003) A multilevel finite element method (FE2) to describe the response of highly non-linear structures using generalized continua. Comput Methods Appl Mech Eng 192:3233–3244
65. Feyel F, Cchaboche JL, Kruch S (1998) Multiscale elastoplastic and damage analysis of composites structures. In: IWCCM8, Stuttgart, October 8–9, 1998
66. Fish J (1992) The s-version of the finite element method: SCOREC report 90-18. Comput Struct 43:539–547
67. Fish J, Markolefas S (1994) Adaptive global-local refinement strategy based on the interior error estimates of the h-method. Int J Numer Methods Eng 37:827–838
68. Fish J, Yu Q (2001) Multiscale damage modelling for composite materials: theory and computational framework. Int J Numer Methods Eng 52:161–191
69. Fish J, Yu Q (2002) Computational mechanics of fatigue and life predictions for composite materials and structures. Comput Methods Appl Mech Eng 191:4827–4849
70. Fish J, Shek K, Pandheeradi M, Shepard M (1997) Computational plasticity for composite structures based on mathematical homogenisation: theory and practice. Comput Methods Appl Mech Eng 148:53–73
71. Fish J, Yu Q, Shek K (1999) Computational damage mechanics for composite materials based on mathematical homogenization. Int J Numer Methods Eng 45:1657–1679
72. Fotiu PA, Nemat-Nasser S (1996) Overall properties of elastic-viscoplastic periodic composites. Int J Plast 12(2):163–190
73. Francfort GA (1984) Homogenisation and fast oscillations in linear thermoelasticity. In: Lewis R, Hinton E, Betess P, Schrefler B (eds) Numerical methods for transient and coupled problems. Pineridge Press, Swansea, pp 382–392
74. Galvanetto U, Pellegrino C, Schrefler BA (1998) Three-dimensional stress recovery procedure for composite materials. Comput Struct 69:567–575
75. Ghosh S, Liu Y (1995) Voronoi cell finite element method for micropolar thermoelastic heterogeneous materials. Int J Numer Methods Eng 38:1361–1398
76. Ghosh S, Moorthy S (1995) Elastic-plastic analysis of arbitrary heterogeneous materials with the Voronoi cell finite element method. Comput Methods Appl Mech Eng 1(1–4):373–409
77. Ghosh S, Mukhopadhyay SN (1991) A two-dimensional automatic mesh generator for finite element analysis of randomly dispersed composites. Comput Struct 41:245–256
78. Ghosh S, Lee K, Moorthy S (1995) Multiple scale analysis of heterogeneous elastic structures using homogenisation theory and Voronoï cell finite element method. Int J Solids Struct 32:27–62
79. Gilormini P (1996) A critical evaluation of various nonlinear extensions of the self-consistent model. In: Pineau A, Zaoui A (eds) Micromechanics of plasticity and damage of multiphase materials. Kluwer Academic, Dordrecht, pp 67–74
80. González C, LLorca J (2000) A self-consistent approach to the elasto-plastic behaviour of two-phase materials including damage. J Mech Phys Solids 48:675–692
81. González C, LLorca J (2001) Micromechanical modelling of deformation and failure in Ti-6Al-4V/SiC composites. Acta Mater 49:3505–3519
82. González C, LLorca J (2003). An analysis of the effect of hydrostatic pressure on the tensile deformation of aluminium-matrix composites. Mater Sci Eng A 341(1–2):256–263
83. Gonzalez C, Segurado J, Llorca J (2004) Numerical simulation of elasto-plastic deformation of composites: evolution of stress microfields and implications for homogenized models. J Mech Phys Solids 52(7):1573–1593
84. Gunawardena S, Jansson S, Leckie F (1993) Modelling of anisotropic behavior of weakly bonded reinforced MMC's. Acta Metall Mater 41(11):3147–3156

85. Hain M, Wriggers P (2008) Numerical homogenization of hardened cement paste. Comput Mech 42:197–212
86. Halphen B, Nguyen QS (1975) Sur les matériaux standard généralisé. J Méc 14(1):39–63
87. Hashin Z (1983) Analysis of composite materials: a survey. ASME J Appl Mech 50:481–505
88. Hashin Z, Shtrikman S (1962) A variational approach to the theory of the elastic behaviour of polycrystals. J Mech Phys Solids 10:343–352
89. Hashin Z, Shtrikman S (1962) On some variational principles in anisotropic and nonhomogeneous elasticity. J Mech Phys Solids 10:335–342
90. Hashin Z, Shtrikman S (1963) A variational approach to the theory of the elastic behaviour of multiphase materials. J Mech Phys Solids 11:127–140
91. Hershey AV (1954) The elasticity of an isotropic aggregate of anisotropic cubic crystals. ASME J Appl Mech 21:236–240
92. Hill R (1952) The elastic behaviour of a crystalline aggregate. Proc Phys Soc A 65:349–354
93. Hill R (1965) A self-consistent mechanics of composite materials. J Mech Phys Solids 13:213–222
94. Hill R (1965) Continuum micromechanics of elastoplastic polycrystals. J Mech Phys Solids 13:89–101
95. Hill R (1967) The essential structure of constitutive laws for metal composites and polycrystals. J Mech Phys Solids 15:79–95
96. Hinton E, Campbell JS (1974) Local and global smoothing of discontinuous finite element functions using a least squares method. Int J Numer Methods Eng 8:461–480
97. Hu G (1996) A method of plasticity for general aligned spherical void of fiber-reinforced composites. Int J Plast 12:439–449
98. Hu-Whashizu K (1982) Variational methods in elasticity and plasticity, 3rd edn. Pergamon, Oxford
99. Hutchinson JW (1976) Bounds and self-consistent estimates for creep and polycrystalline materials. Proc R Soc Lond A 348:101–127
100. Kattan P, Voyiadjiis G (1993) Overall damage and elastoplastic deformation in fibrous metal matrix composites. Int J Plast 9:931–949
101. Kouznetsova VG, Geers MGD, Brekelmans WAM (2004) Multi-scale second order computational homogenisation of multi-phase materials: a nested finite element strategy. Comput Methods Appl Mech Eng 193:5525–5550
102. Kröner E (1958) Berechnung der elastischen Konstanten des Vielkristalls aus den Konstanten des Einkristalls. Z Phys 151:504–518
103. Kruch S (2007) Homogenized and relocalized mechanical fields. J Strain Anal 42:215–226
104. Kruyt NP, Rothenburg L (1997) Statistical theories for the elastic moduli of two-dimensional assemblies of granular materials. Int J Eng Sci 36:1127–1142
105. Lavèdeze P, Nouy A (2003) On a multiscale computational strategy with time and space homogenisation for structural mechanics. Comput Methods Appl Mech Eng 192:3061–3087
106. Lavèdeze P, Loiseau O, Dureisseix D (2001) A micro-macro and parallel computational strategy for highly heterogeneous structures. Int J Numer Methods Eng 52:121–138
107. Lavèdeze P, Nouy A, Loiseau O (2002) A multiscale computational approach for contact problems. Comput Methods Appl Mech Eng 191:4869–4891
108. Lebensohn R, Tomé CN (1993) A self-consistent anisotropic approach for the simulation of plastic deformation and texture development of polycrystals: application to zirconium alloys. Acta Metall Mater 41:2611–2624
109. Lefik M, Schrefler BA (1994) Application of the homogenization method to the analysis of superconducting coils. Fusion Eng Des 24:231–255
110. Lefik M, Schrefler BA (1996) FE modelling of a boundary layer correctors for composites using the homogenisation theory. Eng Comput 13(6):31–42
111. Lefik M, Schrefler BA (2000) Modelling of non-stationary heat conduction problems in micro-periodic composites using homogenisation theory with corrective terms. Arch Mech 52(2):203–223
112. Leroy Y, Ponte Casteñada P (2001) Bounds of the self-consistent approximation for nonlinear media and implications for the second order method. C R Acad Sci Paris IIB 329(8):1203–1227
113. Lin TH (1957) Analysis of elastic and plastic strains of a fcc crystal. J Mech Phys Solids 5:143
114. Llorca J (1994) A numerical study of the mechanism of cyclic strain hardening in metal-ceramic composites. Acta Metall Mater 42:151–162
115. Llorca J (2000) Void formation in metal matrix composites. In: Clyne TW (ed) Comprehensive composite materials. Metal matrix composites, vol 3. Pergamon, Amsterdam, pp 91–115
116. Llorca J, González C (1998) Microstructural factors controlling the strength and ductility of particle-reinforced metal-matrix composites. J Mech Phys Solids 46:1–28
117. Marcellini P (1978) Periodic solutions and homogenisation of nonlinear variational problems. Ann Mat Pura Appl 4:139–152
118. Markovic D, Ibrahimbegovic A (2004) On micro-macro interface conditions for micro scale based FEM for inelastic behavior of heterogeneous materials. Comput Methods Appl Mech Eng 193:5503–5523
119. Masson R (1998) Estimation non linéaires du comportement global de matériaux hétérogènes en formulation affine. Thèse de l'Ecole Polytechnique, Palaiseau
120. Masson R, Bornert M, Suquet P, Zaoui A (2000) An affine formulation for the prediction of the effective properties of nonlinear composites and polycrystals. J Mech Phys Solids 48:1203–1227
121. Mehradi MM, Loret B, Nemat Nasser S (1993) Incremental constitutive relations for granular materials based on micromechanics. Proc R Soc Lond 441:433–463
122. Michel JC, Suquet P (1993) On the strength of composite materials: variational bounds and numerical aspects. In: Bendsoe MP, Mota-Soares C (eds) Topology design of structures. Kluwer Academic, Dordrecht, pp 365–374
123. Michel JC, Suquet P (2003) Nonuniform transformation field analysis. Int J Solids Struct 40:6937–6955
124. Michel JC, Suquet P (2004) Computational analysis of nonlinear composite structures using the nonuniform transformation field analysis. Comput Methods Appl Mech Eng 193:5477–5502
125. Michel JC, Moulinec H, Suquet P (2000) A computational method based on augmented Lagrangians and fast Fourier transforms for composites with high contrast. Comput Model Eng Sci 1(2):79
126. Miehe C, Schröder J, Schotte J (1999) Computational homogenization analysis in finite plasticity. Simulation of texture development in polycrystalline materials. Comput Methods Appl Mech Eng 171:317–418
127. Miehe C, Schotte J, Lambrecht M (2002) Homogenization of inelastic solid materials at finite strains based on incremental minimization principles. Application to the texture analysis of polycrystals. J Mech Solids 50:2123–2167
128. Mital S, Murthy P, Chamis C (1993) Interfacial microfracture in high temperature metal matrix composites, J Compos Mater 27(17):1678–1694
129. Molinari A, Canova GR, Ahzi S (1987) A self-consistent approach of the large deformation polycristal viscoplasticity. Acta Metall 35:2983–2994
130. Moorthy S, Ghosh S, Liu Y (1994) Voronoi cell finite element method for thermo-elastoplastic deformation in random heterogeneous media. Appl Mech Rev 47(1):S207–S220

131. Mori T, Tanaka K (1973) Average stress in matrix and average elastic energy of materials with misfitting inclusions. Acta Metall Mater 21:597–629
132. Moulinec H, Suquet P (1998) A numerical method for computing the overall response of non-linear composites with complex microstructure. Comput Methods Appl Mech Eng 157:69–94
133. Mura T (1993) Micromechanics of defects in solids, 2nd edn. Kluwer Academic, Dordrecht
134. Nakamura T, Suresh S (1993) Effect of thermal residual stress and fiber packing on deformation of metal-matrix composites. Acta Metall Mater 41(6):1665–1681
135. Nebozhyn MV, Ponte Castañeda P (1998) Second order estimates for the effective behavior of nonlinear porous materials. In: Bahei-El-Din Y, Dvorak GJ (eds) IUTAM symposium on transformation problems in composite and active materials. Kluwer Academic, New York, pp 73–88
136. Nemat-Nasser S, Hori M (1999) Micromechanics: overall properties of heterogeneous solids, 2nd edn. Elsevier, Amsterdam
137. Oleinik OA (1984) On homogenisation problems. In: Trends and application of pure mathematics in mechanics. Springer, Berlin
138. Olson T (1994) Improvements on a Taylor's upper bound for rigid-plastic composites. Mater Sci Eng A 175:15–19
139. Paley M, Aboudi J (1992) Micromechanical analysis of composites by the generalized cells model. Mech Mater 14:127–139
140. Paul B (1960) Prediction of elastic constants of multiphase materials. Trans ASME 218:36–41
141. Ponte Castañeda P (1991) The effective mechanical properties of nonlinear isotropic composites. J Mech Phys Solids 39:45–71
142. Ponte Castañeda P (1992) New variational principles in plasticity and their application to composite materials. J Mech Phys Solids 40:1757–1788
143. Ponte Castañeda P (1996) Exact second-order estimates for the effective mechanical properties of non linear composite materials. J Mech Phys Solids 44:827–862
144. Ponte Castañeda P (1997) Non linear composite materials: effective constitutive behaviour and microstructure evolution. In: Suquet P (ed) Continuum micromechanics. CISM courses and lectures, vol 377. Springer, New York, pp 131–195
145. Ponte Castañeda P (2002) Second-order homogenisation estimates for nonlinear composites incorporating field fluctuations: I—theory. J Mech Phys Solids 50(4):737–757 (21)
146. Ponte Castañeda P (2002) Second-order homogenisation estimates for nonlinear composites incorporating field fluctuations: II—applications. J Mech Phys Solids 50(4):759–782 (24)
147. Ponte Castañeda P, Suquet P (1998) Nonlinear composites. Adv Appl Mech 34:171–302
148. Pottier T (1998) Modélisation multiéchelle du comportement et de l'endommagement de composites à matrice métallique. Thèse de Doctorat des Ponts et Chaussées
149. Poza P, Llorca J (1999) Mechanical behaviour of Al-Li/SiC composites. Part III: Micromechanical modelling. Metall Mater Trans A 30:869–878
150. Renard J, Marmonier MF (1987) Etude de l'initiation de l'endommagement dans la matrice d'un matériau composite par une méthode d'homogénisation. Aerosp Sci Technol 6:37–51
151. Reuss A (1929) Berechnung del Fliessgrenze von Mischkristallen auf Grund der Plastizitätbedingung für Einkristalle. Z Angew Math Mech 9:49–58
152. Sachs G (1928) Zur Ableitung einer Fliessdedingung. Z Ver Deu Ing 72:734–736
153. Sanchez-Palencia E (1980) Non-homogeneous media and vibration theory. Springer, Berlin
154. Schrefler BA (2005) Multiscale modelling. In: Zienkiewicz OC, Taylor RL (eds) The finite element method for solid and structural mechanics. Elsevier, Amsterdam
155. Schrefler BA, Lefik M, Galvanetto U (1997) Correctors in a beam model for unidirectional composites. Mech Compos Mater Struct 4:159–190
156. Segurado J, Llorca J (2002) A numerical approximation to the elastic properties of sphere-reinforced composites. J Mech Phys Solids 50
157. Segurado J, Llorca J, González C (2002) On the accuracy of meanfield approaches to simulate the plastic deformation of composites. J Mech Phys Solids 50
158. Smit RJM (1998) Tougness of heterogeneous polymeric systems. PhD thesis, Eindhoven University of Technology, Eindhoven, The Netherlands
159. Smit RJM, Brekelmans WAM, Meijer HEH (1998) Prediction of the mechanical behavior of non-linear heterogeneous systems by multi-level finite element modelling. Comput Methods Appl Mech Eng 155:181–192
160. Sorensen B, Talreja R (1993) Effects of nonuniformity fiber distribution on thermal-induced residual stresses and cracking in ceramic matrix composites. Mech Mater 16:351–363
161. Suquet P (1983) Analyse limite et homogénéisation. C R Acad Sci Paris II 295:1335–1358
162. Suquet P (1987) Elements of homogenisation for inelastic solid mechanics. In: Sanchez-Palencia E, Zaoui A (eds) Homogenization techniques for composite media. Lecture notes in physics, vol 272. Springer, New York, pp 193–278
163. Suquet P (1993) Overall potentials and extremal surfaces of power law or ideally plastic composites. J Mech Phys Solids 41:981–1002
164. Suquet P (1995) Overall properties of nonlinear composites: a modified secant moduli theory and its link with Ponte Castañeda's non linear variational procedure. C R Acad Sci Paris, Sér II 320:563–571
165. Suquet P, Ponte Castañeda P (1993) Small-contrast perturbation expansions for the effective properties of nonlinear composites. C R Acad Sci Paris, Sér II 317:1515–1522
166. Talbot DRS, Willis JR (1985) Variational principles for inhomogeneous non-linear media. J Appl Math 35:39–54
167. Talbot DRS, Willis JR (1992) Some explicit bounds for the overall behaviour of nonlinear composites. Int J Solids Struct 29:1981–1987
168. Tandon GP, Weng GJ (1990) The overall elastoplastic stress-strain relations of dual phase metals. J Mech Phys Solids 38:419–441
169. Taylor GI (1938) Plastic strain in metals. J Inst Metals 62:307–324
170. Teply J, Dvorak G (1988) Bounds on overall instantaneous properties of elastic-plastic composites. J Mech Phys Solids 36:29–58
171. Terada K, Kikuchi N (2001) A class of general algorithms for multi-scale analysis of heterogeneous media. Comput Methods Appl Mech Eng 190:5427–5464
172. Torquato S (2002) Random heterogeneous materials: microstructure and macroscopic properties. Springer, New York
173. Tvergaard V (1990) Analysis of tensile properties for wisker-reinforced metal-matrix composites. Acta Metall Mater 38:185–194
174. Van der Sluis O (2001) Homogenisation of structured elastovisplastic solids. PhD thesis, Eindhoven University of Technology, Eindhoven, The Netherlands
175. Voigt W (1889) Über die Beziehung zwischen den beiden Elastizitätskonstanten isotroper Körper. Wied Ann 38:573–587
176. Voyiadjiis G, Kattan P (1993) Damage of fiber-reinforced composite materials with micromechanical characterization. Int J Solids Struct 30(20):2757–2778
177. Voyiadjis GZ, Deliktas B (1997) Damage in MMCs using the GMC theoretical formulation. Composites B 28:597–611

178. Voyiadjis GZ, Park T (1995) Local and interfacial analysis damage of metal matrix composites. Int J Eng Sci 33:1595–1613
179. Walker KP, Freed AD, Jordan EH (1994) Thermoviscoplastic analysis of fibrous periodic composites by the use of triangular subvolumes. Compos Sci Technol 50(1):71–84
180. Weiss KP (2006) Cryogenic laboratory test for V-I characterisation of subcable samples, Association FZK-Euratom. Karlsruhe, Germany. Progress report 3 (Contract FU06-CT-2003-00335), January 25, 2006
181. Willis JR (1986) Variational estimates for the overall response of an inhomogeneous nonlinear dielectric. In: Ericksen JL et al (eds) Homogeneization and effective moduli of materials and media. Springer, New York, pp 247–263
182. Wisniewski K, Schrefler BA (1993) On recovery of stresses for a multi-layered beam element. Eng Comput 10:563–569
183. Zhang HW, Zhang S, Bi JY, Schrefler BA (2007) Thermomechanical analysis of periodic multiphase materials by a multiscale asymptotic homogenization approach. Int J Numer Methods Eng 69(1):87–113
184. Zienkiewicz OC, Taylor RL (2005) The finite element method for solid and structural mechanics, 6th edn. Elsevier, Amsterdam
185. Zohdi TI (2004) Homogenization methods and multiscale modeling. In: Encyclopedia of computational mechanics. Solids and structures, vol 2. Wiley, New York